University of Sussex

Quantum Black Holes at the LHC

Production and decay mechanisms of non-thermal microscopic black holes in particle collisions

Nina Gausmann

Submitted for the degree of Doctor of Philosophy

University of Sussex

September 2013

Declaration

I hereby declare that this thesis has not been and will not be submitted in whole or in part to another University for the award of any other degree.

Signature:

Nina Gausmann

UNIVERSITY OF SUSSEX

Nina Gausmann, Doctor of Philosophy

Quantum Black Holes at the LHC

Summary

The scale of quantum gravity could be as low as a few TeV in the existence of extra spatial dimensions or if the Planck scale runs fast due to a large number of particles in a hidden sector. One of the most striking features of low-scale quantum gravity models would be the creation of quantum black holes, i.e. non-thermal black holes with masses around a few TeV, in high energy collisions. This thesis deals with the production and decay mechanisms of quantum black holes at current colliders, such as the Large Hadron Collider (LHC). Firstly, a review of models with low-scale gravity is given. We will present an overview of production and decay mechanism of classical and semi-classical black holes, including the Hoop conjecture criterion, closed trapped surfaces and thermal decay via Hawking radiation. We will then introduce a phenomenological approach of black holes, very differently from the (semi-)classical counterparts, which covers a substantially model independent and specifically established field theory, describing the production of quantum black holes. This is done by matching the amplitude of the quantum black hole processes to the extrapolated semi-classical cross section. All possible decay channels and their probabilities are found for quantum black holes with a continuous and discrete mass spectrum, respectively, by considering different symmetry conservation restrictions for a quantum gravitational theory. In conjunction with these branching ratios, we developed a Monte Carlo integration algorithm to determine the cross sections of specific final states. We extended the algorithm to investigate the enhancement of supersymmetric particle production via quantum black hole processes. Studying such objects proves very important, since it provides new possible insights and restrictions on the quantum black hole model and likewise on the low-scale quantum gravity scenarios.

Acknowledgements

First and foremost, I would like to thank my supervisor, Xavier Calmet, not only for his academical support and inspiration, but also for his patience and understanding in stressful times. I developed many useful skills throughout my years at Sussex and I remain forever thankful for them.

I would also like to thank the other staff in the department, Andrea Banfi, Mark Hindmarsh, Stephan Huber, Sebastian Jaeger, Daniel Litim, and Veronica Sanz, who all always had an open ear and friendly advice.

I am grateful to have had the opportunity to collaborate with several great physicists, such as the BlackMax collaboration, in particular Eram Rizvi and Warren Carlson. I also want to thank Claire Shepherd-Themistocleous and Emmanuel Olaiya for all the useful discussions we had.

Looking back, I think I would never have studied physics without the encouragement of my former physics teacher, Herbert Wulff, and I want to thank him for that.

A big thanks to all my fellow students Mike, Andy, Robert, Denis, Kevin, Edouard, Kostas, Aga, Barry, Glauber, Raul, Susanne, Miguel, Paul, as well as to the postdocs Jorge and Jose, I will miss the conversations, group therapy sessions, and good times we shared. A special thanks to one of the nicest office mates you could ask for, Ting-Cheng, I learned a lot about culture, art, and life from you. There is a lot I can thank my house mate, colleague, and dear friend Jan for, but most of all, I want to thank him for putting up with me.

There are also many people outside the department, who made my time in Brighton special. I want to thank Sally and Inken for all the fun we had on and off the table tennis table. Nicky, I am so grateful to have you as a friend, you constantly supported me and you will remain my favorite coffee buddy until the end of time. Grace, you are an amazing friend and inspiration, many moments with you will remain the most memorable of my life.

I consider myself to be a lucky person because even back home I have remarkable people who have supported me throughout my PhD and before. I want to thank my remarkable friends Vina, Oddel, Sven, Anna, and Jonas. My personal drill instructor and wonderful friend, Esco, thanks for always believing in me and for not allowing me to ever give up.

I also want to thank my parents, Birgit and Dietrich Gausmann, who literally never ceased to support me with their love and trust in me, and thanks to the best big brother in the world, Daniel Gausmann. Both my grandmothers, Irmgard Gausmann and Ursula Holtze, will always be special role models for me and I will aspire to live my life with as much strength and kindness as they did.

I cannot express enough gratitude to my partner, Kris, for being simply exceptional in supporting me, motivating me, and making me unbelievably happy.

This work was supported by a SEPnet studentship and I am much obliged for the chance I have been given.

What is now proved was once only imagined.

- William Blake

Contents

List of Tables

List of Figures

Chapter 1

Introduction

Despite the efforts of many physicists extensively studying two of the important pillars of theoretical physics, namely Einstein's theory of general relativity and the quantum field description of particles known as the Standard Model (SM), finding a quantum description of gravity to unify these theories still proves to be one of the biggest challenges of contemporary physics. One of the major recent theoretical developments was the perception that the Planck mass, the energy scale at which gravitational effects become relevant, is not fundamentally fixed to a certain value but could be anywhere between a few TeVs and the dimensional analysis estimate of $\sim 10^{19}$ GeV. If one assumes that a severe fine tuning cannot be the solution to the unnatural span of particle masses, in particular how small they are compared to the Planck mass, one would suppose that there are new physics effects around a few TeV. The vigorous attention to models introducing a low quantum gravitational theory[1–4] is comprehensible, since they not only address explanations to the conceptual issue of the hierarchy problem but they might provide the possibility of observing quantum gravitational effects at current measurements, such as the Large Hadron Collider (LHC) [5] at the European Organization for Nuclear Science (CERN); an impossible task for conventional models of short distance space-time. Collider physics is not only a powerful tool to provide tests of existing theories but might produce new particles and hence probe new physics. Without a doubt, one of the most interesting consequences of low scale quantum gravitational effects would be the creation of microscopic black holes in a high energy collision. Black holes are fascinating objects because they involve physics under extreme conditions and might provide us with insights completely unknown to date. Low scale quantum gravity led to impressive progress in the research of small black holes created in collider experiments, where one expects matter that experiences a gravitational collapse to form a black hole.

This thesis deals with quantum black holes (QBHs), non-thermal microscopic black holes, very different from their astrophysical counterparts, with masses expected to be close to the Planck scale. Other than for semi-classical black holes, which have been studied thoroughly [6–13] and would not be created even in the most optimistic case of a few TeV Planck scale, the center of mass energy at current experiments might be sufficient to produce these quantum analogs of black holes numerously. Although they do not decay via Hawking radiation, they could have very distinct signatures with hardly any or no SM background. The creation and decay of QBHs would enable us to learn about quantum gravity, especially which symmetries would be conserved by it, and gain more insights about the limits involved in low scale gravity models; QBHs signals would be the first indication of low scale gravity. The following chapters of this thesis are structured as follows:

- Chapter 2 reviews important background material, i.e. the lowering of the fundamental Planck scale in different models.

- Chapter 3 covers black hole formation and decay in high energy collisions. Classical and semi-classical black hole mechanisms are revised and the physics of QBHs introduced.

- In Chapter 4 we establish a field theoretical description of QBH production and interaction with SM particles, by matching the amplitude of the quantum black hole processes to the extrapolated semi-classical cross section. This is based on work published in [14] by the author, X. Calmet, and D. Fragkakis. All calculations presented in this work, i.e. the cross section matching and the proposed bounds of the fundamental Planck scale, have been derived by the author.

- Chapter 5 deals with the production and decay of QBHs with a continuous mass spectrum. The theoretical part of this chapter is based on work published by X. Calmet, D. Fragkakis, and the author in [15] as well as work published by the author and X. Calmet in [16]. The branching ratios presented in this chapter were calculated by the author as well as the implementation of these into a Monte Carlo algorithm, which was rewritten, improved, and adapted from previous code developed by the authors of [17]. The development of this code is part of the BlackMax project [13] and will be covered in the new version of BlackMax. We showed that the developed cross sections are non-negligible. Some of the results are presented in this chapter for the first time and are not published elsewhere.

- In Chapter 6 an extension of the previously discussed objects to a discrete mass spectrum is presented. The content of this chapter is in large parts based on work published [16] by the author and X. Calmet as well as partially on work published in [15]. The Monte Carlo algorithm was adapted by the author and the slightly differing results to the published ones are due to a change of the use of a specific parton distribution functions to allow comparisons with the previous chapter.

- In Chapter 7, the theory of QBH processes and the Monte Carlo algorithm are extended to include supersymmetric particle production. The continuous as well as the discrete mass spectrum are considered and cross sections for all decay products, based on for this purpose established branching ratios, are given. The presented calculations and assumptions are original work of the author in collaboration with X. Calmet and D. Fragkakis, and are yet to be published.

Chapter 2

Low-scale quantum gravity

One of the biggest challenges contemporary physics faces is the explanation of the large hierarchy between the weak scale and the fundamental Planck scale, at which quantum gravity effects supposedly become strong. In other words, it is still unknown why the gravitational force is so much weaker than all other Standard Model interactions. The unification of scales has been illustrated in Figure 2.1.

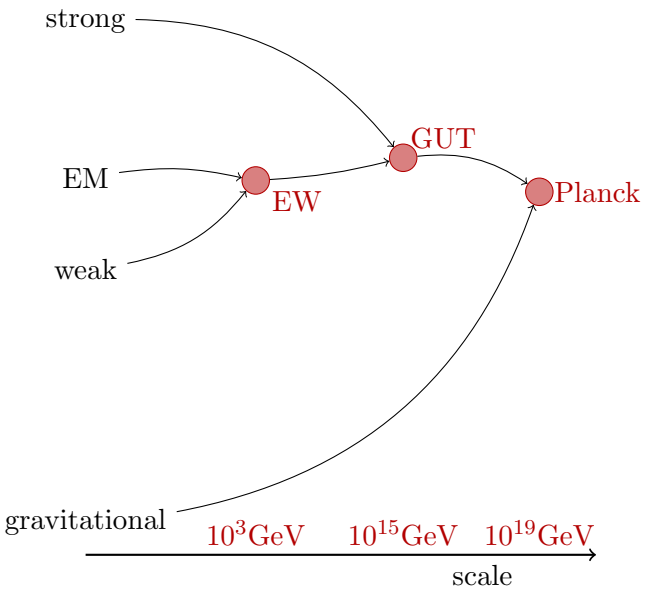

Figure 2.1: *Abstract illustration of the unification of physical scales. The four fundamental forces (strong, electromagnetic (EM), weak and gravitational) are sketched according to their strength. The EM and weak forces unify to the electroweak (EW) force, which then again combines with the strong force to a grand unified theory (GUT). The Planck scale describes the energy regime at which the GUT forces and gravity merge.*

The gravitational laws have only been tested up to ~ 0.056mm [18] which corresponds

to a much smaller energy scale ($\sim 10^{-2}$eV) than the one currently explored at particle accelerators such as the LHC (Large Hadron Collider). For a review on experimental verifications of gravitational laws see also [19][1]. In general, a lowering of the energy scale, at which quantum gravitational effects become strong, might yield very interesting signatures, e.g. the creation of microscopic black holes as described in chapter 3.

There have been several models suggesting a lowering of the Planck mass to a TeV level. This chapter will first revise two theoretically successful models which both introduce extra spatial dimensions: a model proposing a large volume of extra dimensions [1, 2, 20] and one in which the decoupling of the Planck mass originates from a warped extra dimension [3, 21]. It concludes with a model that suggests a low scale quantum gravity through a running of the gravitational coupling in four dimensions [4].

2.1 Extra spatial dimensions

In 1921, only a few years after Einstein proposed his theory of gravity, Kaluza and Klein came up with a model introducing an additional compact spatial dimension [22, 23]. This theory, known as the Kaluza-Klein (KK) model, attempts to unify electromagnetism with gravity. The consideration of extra spatial dimensions also found its motivation in string theoretical models which are formulated with at least ten dimensions. Traditionally, one considered the extra dimensions to be of the order of the Planck length

$$l_P = \frac{\hbar}{M_P c} \sim 1.62 \times 10^{-35}\,\mathrm{m} \quad , \tag{2.1}$$

with $\hbar$ being the reduced Planck constant, c the speed of light and M_P is the Planck mass which is given by dimensional analysis as

$$M_P = \left[\frac{\hbar c}{G_N}\right]^{1/2} \sim 2.18 \times 10^{-8}\,\mathrm{kg} = 1.22 \times 10^{19}\,\mathrm{GeV} \quad , \tag{2.2}$$

where G_N is Newton's gravitational constant. For figurative purposes, these calculations deviate from natural units. With the size of the extra dimension substantially smaller than any observable length scale, it is straightforward to see that an experimental verification of any physical phenomenon at scales around the Planck scale is, at least in the foreseeable future, not attainable.

Studies in the past 20 years have shown that the size of the extra dimensions might be reasonably larger than the Planck length and therefore not necessarily attached to it. The size of the extra dimension does not affect the original conception of our world being

[1] In review "Experimental tests of gravitational theory".

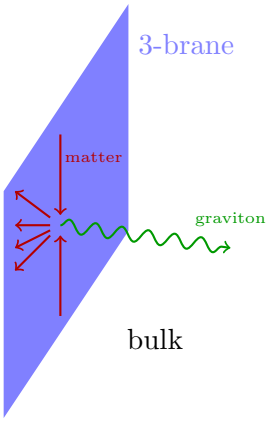

Figure 2.2: *Illustration of the propagation of Standard Model matter fields (red arrows) restricted to the 3-brane and gravitational fields which can escape to the higher dimensional bulk.*

localized on a four-dimensional hypersurface, typically known as the 3-brane, embedded in the bulk which is a higher-dimensional space. As pictured in Figure 2.2, observable matter interacting through Standard Model fields is restricted to the 3-brane whereas gravitational fields can propagate also in the bulk. Since only gravitons or to date unobserved fields propagate into the bulk, the introduction of extra dimensions does not contradict current observations.

The lowering of the Planck mass for each of the two most well-known models, respectively, has been well described in several reviews, i.e. [24–27] which will be closely followed in the next two sections.

2.1.1 ADD model

In 1998 Nima Arkani-Hamed, Savas Dimopoulos, and Gia Dvali proposed a theory [1, 2, 20] in which the four-dimensional 3-brane is embedded in a $(4+n)$-dimensional flat space. This was motivated by string theoretical models developed by Ignatios Antoniadis [28] which predicted the existence of large extra dimensions.

The 3-brane is spanned by (3+1) non-compact dimensions and n denotes the compact spatial dimensions. Figure 2.3 visualizes the compactification of one extra dimension.

Keeping in mind that gravity is a geometrical property of space, it is unambiguous to extend General Relativity to an arbitrary number of spatial dimensions. It has to be noted, however, that in a higher-dimensional space-time, the fundamental gravitational coupling G_* of the bulk does not necessarily correspond to Newton's gravitational constant

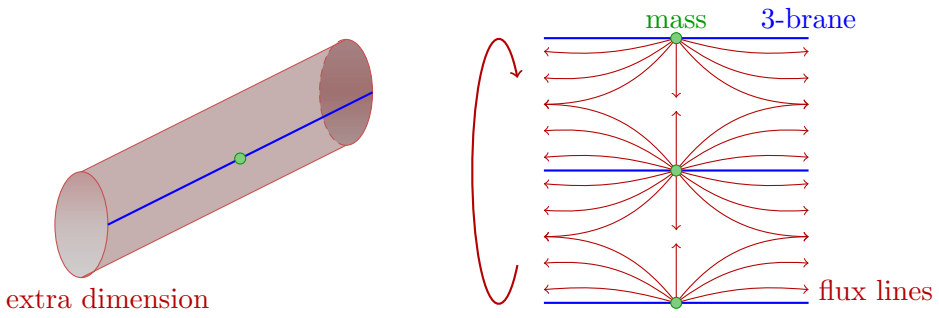

Figure 2.3: *The compactification of one extra dimension: All ordinary matter fields, here visualized by the test masses (green dots), are restricted to the 3-brane (blue thick lines). The extra dimension is compactified on a circle with radius R. If the size of the extra dimension $L = 2\pi R$ is smaller than the distance in the 3-brane, the flux lines from the test masses will run parallel to the brane.*

G_N. For the $(4+n)$-dimensional space, one finds thus the following action:

$$S_* = -\frac{1}{16\pi G_*} \int \mathrm{d}^{4+n}x \sqrt{|g_*|} R_* \quad , \tag{2.3}$$

where g_* is the determinant of the higher-dimensional metric and R_* the Ricci scalar. One assumes that the higher-dimensional metric can be factorized into a four-dimensional and extra-dimensional part:

$$ds^2 = g_{\mu\nu}(x) dx^\mu dx^\nu + \delta_{ab} dy^a dy^b \quad , \tag{2.4}$$

with $g_{\mu\nu}$ being the usual four-dimensional Minkowski metric and x^μ with $\mu = 0, 1, 2, 3$ the coordinates of the 3-brane. The second term represents the line element of the higher-dimensional space with its coordinates y^a with $a = 5, 6, \cdots, n$. The extra dimensions are considered to be flat and thus do not give any additional curvature. We thus find:

$$\sqrt{|g_*|} = \sqrt{|g_{(4)}| \cdot |\delta_{ab}|} = \sqrt{|g_{(4)}|} \quad \text{and} \quad R_* = R_{(4)} \quad , \tag{2.5}$$

where $g_{(4)}$ is the determinant of the four-dimensional metric and $R_{(4)}$ the four-dimensional Ricci scalar. Throughout this thesis, a lower index with numbers in parentheses indicates the dimensionality of the parameter. With these conditions, it is straightforward to integrate out the extra dimensions, finding an expression for the action depending on the volume V_n of the extra dimensions:

$$S_* = -\frac{V_n}{16\pi G_*} \int \mathrm{d}^4 x \sqrt{|g_{(4)}|} R_{(4)} \quad . \tag{2.6}$$

This equation has the same structure as the four-dimensional Einstein-Hilbert action and we can conclude

$$G_* = G_N \cdot V_n \quad . \tag{2.7}$$

It is obvious from this expression that Newton's gravitational constant is not fundamental but scaled by the volume of the extra-dimensional space.

Assume two test masses m_1 and m_2, similar to the one described in Figure 2.3, to be localized on the 3-brane. On the brane itself, the gravitational force $F(r)$ between these masses is described by the standard Newton's law in four dimensions

$$F(r) \sim \frac{m_1 m_2}{M_P^{n+2} \cdot r^2} \quad . \tag{2.8}$$

For illustrative purposes of the physical effects appearing with the existence of extra dimensions, consider one extra dimension compactified on a circle. The 3-brane is then embedded on a torus shaped space-time. For distances r between the two test masses much bigger than the compactification radius R the effect of the extra dimension on the force is negligible and one observes the usual gravitational behavior described in (2.8) divided by the volume of the extra dimensions

$$F(r) \sim \frac{m_1 m_2}{M_P^{n+2} \cdot V_n \cdot r^2} \quad , \quad \text{for} \quad r \gg R \quad . \tag{2.9}$$

In the $(4+n)$-dimensional case, Newton's law for distances much smaller than R is described by the stronger force

$$F(r) \sim \frac{m_1 m_2}{M_*^{n+2} \cdot r^{n+2}} \quad , \quad \text{for} \quad r \ll R \quad . \tag{2.10}$$

Assuming a smooth transition between these two regimes yields the following relation between the fundamental higher-dimensional scale and the Planck scale

$$M_P^2 = M_*^{2+n} \cdot V_n \quad , \tag{2.11}$$

which shows, equivalent to (2.7), that with the existence of extra dimensions, the four-dimensional Planck scale is only an effective scale and the higher-dimensional fundamental scale, at which quantum gravity effects become strong, could be much lower than expected. For a large volume of the extra dimensions, it could be as low as the electroweak scale $M_{EW} \sim 1\,\text{TeV}$, the hierarchy between these scales would only be illusive. It should be noted, however, that although this seemingly solves the hierarchy problem, the model leads to a new hierarchy. The new challenge is to explain the huge difference between the size of the extra dimensions, about one millimeter, and the Planck length, given in (2.1). Another approach, which does not involve this hierarchy between the weak and compactification scale, is the RS model which will be described in the following section.

2.1.2 RS model

Only a year after the proposal of the ADD model, Lisa Randall and Raman Sundrum published a theory which suggests the existence of one warped extra dimension [3, 21]. The idea of curved extra dimensions was first mentioned by Rubakov and Shaposhnikov in 1983 [29], who did not present a substantial model but pointed out the importance of the cosmological constant Λ for these models. Randall and Sundrum suggested a concrete setup, e.g. also described in [27], in which the extra dimension is orbifolded and has the radius R, yielding in a $S^1/\mathbb{Z}_2$ space, i.e. a circle with identified upper and lower halves, as illustrated in Figure 2.4. This leads to the fix points $y = 0$ and $y = \pi R$, at which two 3-branes are located, thus bordering the five-dimensional bulk as shown in Figure 2.5.

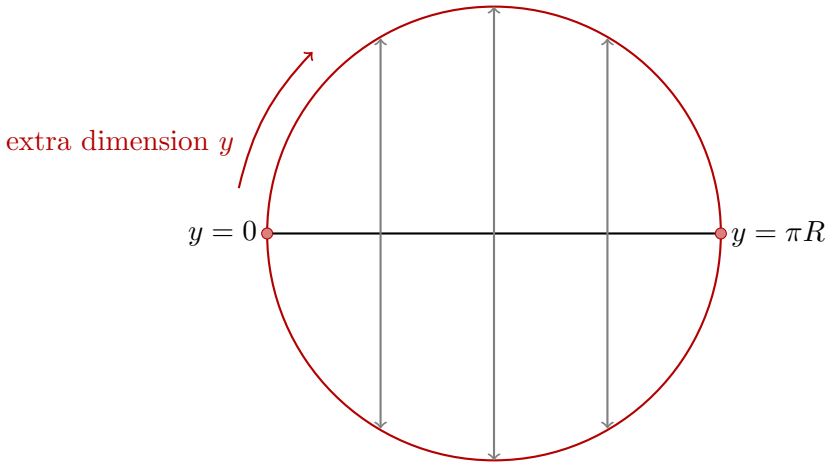

Figure 2.4: *Compactification to $S^1/\mathbb{Z}_2$ orbifold. The upper and lower halves of the one-dimensional sphere are identified and $L = \pi R$.*

The cosmological constant is taken to be negative to ensure a flat metric on the branes. The metric of the five-dimensional setup has the following form

$$ds^2 = \mathrm{e}^{-2A(y)} g_{\mu\nu}(x) dx^\mu dx^\nu + dy^2 \quad , \tag{2.12}$$

where $\mathrm{e}^{-2A(y)}$ is the warp factor and the function $A(y)$, which depends on the coordinates of the extra dimension, will be determined later on. One has to be able to replicate the four-dimensional Minkowski metric at every point along the fifth dimension, evidently including the points $y = 0$ and $y = \pi R$ at which the 3-branes are located. Thus the five-dimensional metric only depends on the coordinates of the extra dimension y.
The classical action is formed out of three parts: the well known gravitational action, and

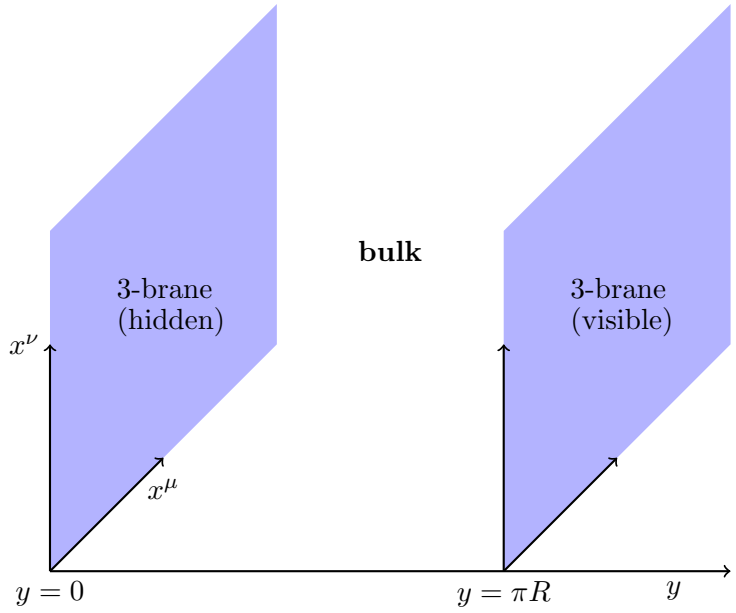

Figure 2.5: *Setup of two four-dimensional 3-branes enclosing the five dimensional bulk.*

one part for our observable and for a hidden 3-brane each:

$$S = S_{grav} + S_{vis} + S_{hid} \tag{2.13}$$

with the action for the bulk

$$S_{grav} = \int \mathrm{d}^4x \int_{-L}^{L} \mathrm{d}y \, \sqrt{-g_*} \left(M_*^3 R_* - \Lambda \right) \quad , \tag{2.14}$$

where R_* is the five-dimensional Ricci tensor, M_* the fundamental scale, and $L = \pi R$. The components for the visible and hidden 3-brane are, respectively [21]:

$$S_{vis/hid} = \int \mathrm{d}^4x \sqrt{-g_{vis/hid}} \left(\mathcal{L} - V \right)_{vis/hid} \quad , \tag{2.15}$$

with $\mathcal{L}_{vis/hid}$ being the Lagrangian of the corresponding 3-brane. $V_{vis/hid}$ is a constant cosmological term, separated out of the Lagrangian as done analogously with the cosmological constant Λ in the bulk action. The function $A(y)$ in the exponent of the warp factor described in (2.12) can be determined with help of the five-dimensional Einstein equations

$$G_{MN} = R_{MN} - \frac{1}{2} g_{MN} R = \kappa^2 T_{MN} \tag{2.16}$$

with G_{MN} being the Einstein tensors, R_{MN} the Ricci tensor and R here meaning the Ricci scalar, which should not be confused with the radius. The indices $M = \mu, 5$ and $N = \nu, 5$ run over the usual Minkowski coordinates combined with an index for the fifth dimension. $\kappa = \dfrac{1}{2M_*^3}$ is Newton's constant in five dimensions. The five-dimensional metric is described by

$$g_{MN} = \mathrm{e}^{-2A(y)} g_{\mu\nu} dx^\mu dx^\nu + \delta_M^5 \delta_N^5 \tag{2.17}$$

and the energy-momentum tensor T_{MN} takes the form

$$T_{MN} = \frac{-2}{\sqrt{-g}} \frac{\delta S_{matter}}{\delta g^{MN}} \quad , \tag{2.18}$$

where S_{matter} is the matter part of the action and all matter particles are confined on the 3-branes. Solving (2.16) one gets for the Einstein tensors

$$G_{\mu\nu} = R_{\mu\nu} - \frac{1}{2} g_{\mu\nu} R = \left(6A'^2 - 3A''\right) g_{\mu\nu} \tag{2.19}$$

$$G_{55} = R_{55} - \frac{1}{2} g_{55} R = 6A'^2 \quad , \tag{2.20}$$

whereas the Ricci scalar is defined as

$$R = g^{MN} R_{MN} = 8A'' - 20A'^2 \tag{2.21}$$

and R_{MN} the Ricci tensor which can be expressed by its components

$$R_{\mu\nu} = \left(A'' - 4A'^2\right) g_{\mu\nu} \tag{2.22}$$

$$R_{55} = 4\left(A'' - A'^2\right) \quad . \tag{2.23}$$

Using (2.20) and the matter part S_{matter} of (2.14), one thus gets for the purely extra-dimensional component of the Einstein tensor

$$G_{55} = 6A'^2 = \frac{-\Lambda}{2M_*^3} \tag{2.24}$$

which gives a constant value for A'^2. Integrating over the coordinate of the extra dimension and taking into account that space is an $S^1/\mathbb{Z}_2$ orbifold which is invariant under the transformation $y \to -y$, the metric (2.12) can be rewritten as

$$ds^2 = \mathrm{e}^{-\sqrt{\frac{-\Lambda}{3M_*^3}}|y|} g_{\mu\nu}(x) dx^\mu dx^\nu + dy^2 \quad . \tag{2.25}$$

From which it can be seen that the exponent of the warp factor can only be real if we define the cosmological constant to be negative. For clarity, a constant is defined as

$$c \equiv \frac{-\Lambda}{3M_*^3} \quad . \tag{2.26}$$

Keeping in mind that one can find an effective four-dimensional action at the visible 3-brane, it can be substituted into the five-dimensional action (2.14). From this it is straightforward to extract the relation for the fundamental Planck scale

$$M_P^2 = \frac{2M_*^3}{c}\left(1 - \mathrm{e}^{-c\pi R}\right) \quad , \tag{2.27}$$

with R being the radius of the extra dimension. Multiplying the metric with the warp factor yields in a lowering of the fundamental mass parameters, as shown in Figure 2.6.

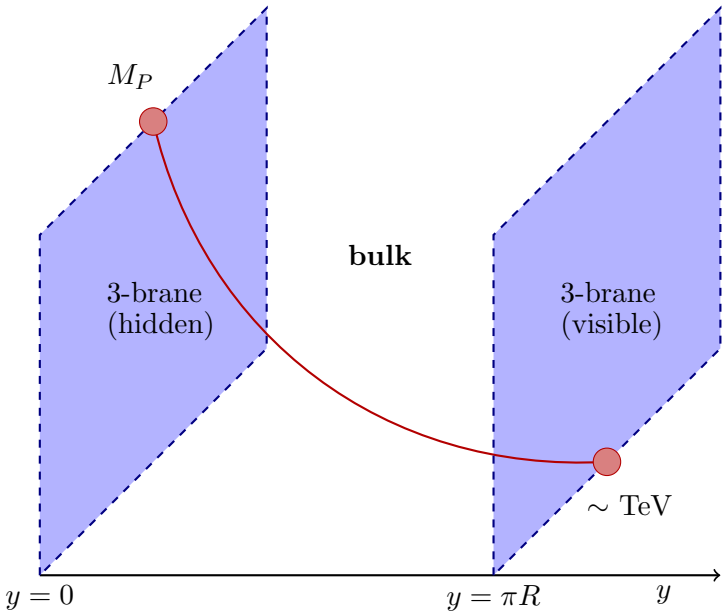

Figure 2.6: *Illustration of the lowering of the Planck scale to a TeV level by multiplication with warp factor.*

2.2 Four-dimensional gravity model at a TeV

In 2008, a model which lowers the Planck scale to a TeV level in four dimensions by introducing a large number of new particles was developed. This chapter will give an overview of this model, using mainly the original paper [4] and [30–32]. As in (2.2), one considers the relation between Newton's gravitational constant G_N and the Planck scale, at which quantum gravitational effects become relevant. In case of one scalar field ϕ which couples only to gravity, one expects an additional term in the action describing gravitational and matter fields:

$$S = \int \mathrm{d}^4x \sqrt{-g_{(4)}} \left(-\frac{R_{(4)}}{16\pi G_N} + \frac{1}{2} g^{\mu\nu}_{(4)} \partial_\mu \phi \partial_\nu \phi + \cdots \right) \quad . \tag{2.28}$$

Examine two non-relativistic sources which exchange a graviton and thus create a gravitational potential between them. Similar to the running of the gauge couplings of the Standard Model, the authors of [4] assume Newton's gravitational constant to be energy scale dependent. The couplings described in (2.28) generate quantum corrections to the graviton propagator. It is shown explicitly in [32] that contributions from diagrams with more than one graviton propagator are suppressed compared to those illustrated in Figure 2.7. Since gravitons interact with each other, they will also run in the loop. Assuming a large new matter content, i.e. in the limit of large N, where N is the number of fields running in the loop, the graviton contribution is negligible [30]. The metric is de-

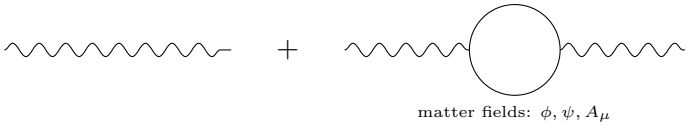

Figure 2.7: *Tree-level and loop corrections of effective graviton propagator in quantum gravity. Quantum corrections from particles with non-zero masses running in the loop. The wavy lines are gravitons, whereas the continuous lines represent matter fields.*

fined as $g_{\mu\nu,(4)} = \eta_{\mu\nu} + h_{\mu\nu}$ with $\eta_{\mu\nu}$ being the four-dimensional Minkowski metric. Loop corrections from the graviton propagator $D_h(q)$ allow for small fluctuations h:

$$D_h(q) \sim \frac{iG_N}{q^2} + \frac{iG_N}{q^2}\Sigma\frac{iG_N}{q^2} \tag{2.29}$$

with q being the graviton momentum, or to be more exact, the two diagrams shown in Figure 2.7, whereas

$$\Sigma \sim -iq^2 \int^{\Xi} \mathrm{d}^4 p D^2(p) p^2 + \cdots \quad . \tag{2.30}$$

$D(p)$ describes the propagation of the particle in the loop with its momentum p and Ξ is the ultraviolet loop momentum cutoff. Redefining G_N yields the expression for Newton's renormalized gravitational constant including the one-loop contribution and thus a scale dependence

$$\frac{1}{G_{N,ren}} = \frac{1}{G_N} + c\,\Xi^2 \quad . \tag{2.31}$$

G_N defines the bare gravitational constant which can be related to a scale, analogously to (2.2) and equally defined in the models with extra dimensions,

$$G_N = \frac{1}{M_P^2} \quad . \tag{2.32}$$

With the scale dependence of the Planck mass, we can define the scale at which quantum gravity effects become large as $M_P(\mu_*) \sim \mu_*$. To allow an observable scale of the order of a TeV, the constant c has to become comparably large ($c \sim 10^{32}$) which will become relevant later in this section. One can establish a Wilsonian running of Newton's gravitational constant depending on the energy scale μ of the following form

$$\frac{1}{G_{N,ren}(\mu)} = \frac{1}{G_{N,ren}} - \frac{N\mu^2}{12\pi} \quad , \tag{2.33}$$

where $N = N_{\text{scalar}} + N_{\text{Weyl}} - 4N_{\text{gauge}}$ indicates the particles - real scalar fields, Weyl fermions and gauge bosons, respectively - which have been integrated out. For the Standard Model, assuming left and right-handed neutrinos to be Dirac particles, we find $N_{SM} = 4 + 48 - 48 = 4$. Expression (2.33) is derived in a heuristic way, a proper

derivation can be found e.g. in [33], see also [34–36], using a heat kernel regularization of one-loop diagrams.

We will now exemplary sketch the derivation of the scalar field result. A scalar field ϕ with minimal coupling to gravity is considered for which the one-loop effective action W is given by [33]

$$\mathrm{e}^{-W} = \int \mathcal{D}\phi\, \mathrm{e}^{-\frac{1}{8\pi}\int \phi(-\Delta+m^2)\phi} = \left(\det(-\Delta+m^2)\right)^{-\frac{1}{2}} \quad . \tag{2.34}$$

The heat kernel can thus be expressed by

$$H(\tau) \equiv \mathrm{Tr}\ \mathrm{e}^{-\tau(-\Delta+m^2)} = \sum_i \mathrm{e}^{-\tau\lambda_i} \tag{2.35}$$

and λ_i are the eigenvalues of $(-\Delta+m^2)$. Comparing these two equations yields

$$W = \frac{1}{2}\ln\left(\det(-\Delta+m^2)\right) = \frac{1}{2}\sum_i \ln(\lambda_i) = -\frac{1}{2}\int_{\epsilon^2}^{\infty} \mathrm{d}\tau \frac{H(\tau)}{\tau} \quad . \tag{2.36}$$

The ultraviolet cutoff ϵ^{-1} had to be introduced to countervail the divergent character of the integral for small values of τ which is mainly due to the behavior of the heat kernel for short times, which can be regularized by the following method. The heat kernel can be written as

$$H(\tau) = \int \mathrm{d}x\, G(x,x',\tau) \tag{2.37}$$

with $G(x,x',\tau)$ representing the Green's function which satisfies the differential equation

$$\left(\frac{\partial}{\partial\tau} - \Delta_x\right) G(x,x',\tau) = 0 \quad , \tag{2.38}$$

$$G(x,x',0) = \delta(x-x') \quad . \tag{2.39}$$

The solution in four-dimensional flat space is

$$G_0(x,x',\tau) = \left(\frac{1}{4\pi\tau}\right)^2 \mathrm{e}^{-\frac{1}{4\tau}(x-x')^2} \quad , \tag{2.40}$$

which has to be generalized by expressing the covariant Laplacian in local coordinates as well as expanding it for small curvatures. This has been done in [37] and yields

$$H(\tau) = -\frac{1}{(4\pi\tau)^2}\left(\int \mathrm{d}^4x\sqrt{-g_{(4)}} + \frac{\tau}{6}\int \mathrm{d}^4x\sqrt{-g_{(4)}}R + \mathcal{O}\left(\tau^{\frac{3}{2}}\right)\right) \quad . \tag{2.41}$$

Inserting this expression into (2.36) gives

$$W = \frac{1}{4\cdot 16\pi^2\epsilon^4}\int \mathrm{d}^4x\sqrt{-g_{(4)}} + \frac{1}{12\cdot 16\pi^2\epsilon^2}\int \mathrm{d}^4x\sqrt{-g_{(4)}}R \quad , \tag{2.42}$$

where only the second term contributes to the gravitational coupling. Thus, comparing this expression to (2.28), we find

$$\frac{1}{G_{N,ren}} = \frac{1}{G_N} + \frac{1}{12\pi\epsilon^2} \quad , \tag{2.43}$$

which noticeably results in a much smaller value for $G_{N,ren}$ compared to the bare value if the scalar field is integrated out, i.e. $\epsilon \to 0$.

Modifying the effective action (2.36) by introducing an infrared cutoff μ as follows

$$W = -\frac{1}{2}\int_{\epsilon^2}^{\mu^{-2}} \mathrm{d}\tau \frac{H(\tau)}{\tau} \tag{2.44}$$

results in a Wilsonian running of Newton's gravitational constant

$$\frac{1}{G_{N,ren}(\mu)} = \frac{1}{G_{N,ren}(0)} - \frac{\mu^2 N_{scalar}}{12\pi} \tag{2.45}$$

with N_{scalar} representing the number of scalars and where for long-distance measurements $G_{N,ren}(0) = G_{N,ren}$, as described in (2.43). It was shown with an analogous calculation in [33] that Weyl fermions give the same contribution in sign and magnitude, whereas gauge bosons contribute oppositely. Using (2.33) of the energy dependent gravitational constant and (2.32), one would get a fundamental Planck scale much lower than traditionally expected

$$M_P^2(\mu) = M_P^2(0) - \frac{\mu^2 N_{scalar}}{12\pi} \quad . \tag{2.46}$$

A TeV Planck scale can only be achieved by introducing $N \sim 10^{32}$ particles with masses smaller than a TeV which has been suggested in [38, 39]. The mass is restricted to a TeV, to allow a running in the loop. These particles only couple to gravity and to none of the other Standard Model interactions, thus carrying no further charges. They are so to speak hidden from the Standard Model. The introduction of these particles will result in weaker gravitational interactions for low energies. Quantum gravity effects would therefore be observable at a few TeV. The number of new degrees of freedom is comparable to the number in models with large extra dimensions. Cosmic ray experiments assume a lower bound on the fundamental Planck mass in four dimensions of the order of 0.5 TeV which has been established in [40] on the basis of black hole production through cosmic ray collisions. The next chapter will give an insight of black hole production, concentrating on microscopic black holes.

Chapter 3

Black holes produced in particle collisions

This chapter deals with the nature and mechanism of black holes created in high-energy collisions. Production and decay of classical and semi-classical black holes are discussed as well as the proposed quantum black holes (QBHs) introduced. This chapter follows the review [25] closely in parts, amended by theory essential for the understanding of this thesis.

The production of black holes in particle collisions provides a way to probe quantum gravity. As described in the previous chapter, the scale at which quantum gravitational effects become relevant is not known from fundamental principles and remains a yet not fully explored parameter of nature. The production and decay of classical black holes (Section 3.2), with center of mass energies going towards infinity, have been well studied and understood. With the understanding of such processes, a semi-classical approach was extrapolated (Section 3.3), in which the black holes have masses of at least 5 to 20 times the Planck mass. To detect objects with such masses, we would need much more energy than accessible at current colliders. By extrapolating to the quantum regime (Section 3.4), the produced black holes have masses of a few TeV, and would in case of a low scale quantum gravity allow us to test quantum gravity at accessible energy levels.

3.1 Quantum gravity and high-energy scattering

Lowering the fundamental Planck scale would enable one to probe physics at a regime with strong gravitational interaction. The creation of black holes in high-energy scattering processes at a lowered scale was first mentioned in [7] where the center of mass energy

$\sqrt{s}$ was assumed to be much larger than the lowered Planck scale M_*. The authors distinguished two different cases depending on the impact parameter b. For an impact parameter bigger than the Schwarzschild radius, which is dependent on the center of mass energy of the colliding particles, one expects both elastic and inelastic processes to occur. In the strong gravity regime, these processes are assumed to be dominated by graviton exchange. For an impact parameter smaller than the Schwarzschild radius and following the Hoop conjecture criterion by Kip Thorne [41], a black hole will be created in such collisions. For more than four dimensions, an extension of the hoop conjecture was developed in [42]. Black holes created under such circumstances are, corresponding to the underlying theory, higher-dimensional objects. Such objects are conceptually not restricted to the 3-brane. It was shown in [43] that black holes mainly radiate on the 3-brane, for further discussion on radiation off and on the 3-brane see also [44]. An elaboration of this appears at the end of section 3.2.2. In the simplest scenario, the produced black hole would be spherically symmetric and neutral and can thus be described by the Schwarzschild metric [45]:

$$\mathrm{d}s^2 = -\left(1-\left(\frac{r_s}{r}\right)^{n+1}\right)\mathrm{d}t^2 + \left(1-\left(\frac{r_s}{r}\right)^{n+1}\right)^{-1}\mathrm{d}r^2 + r^2\mathrm{d}\Omega^2_{(2+n)} \quad , \tag{3.1}$$

where the line element $\mathrm{d}\Omega^2_{(2+n)}$ describes a $(2+n)$-dimensional unit sphere defined as

$$\begin{aligned}\mathrm{d}\Omega^2_{(2+n)} &= \mathrm{d}\theta^2_{(n+1)} \\ &\quad + \sin^2\theta_{(n+1)}\left(\mathrm{d}\theta^2_{(n)} + \sin^2\theta_{(n)}\left(\ldots + \sin^2\theta_{(2)}\left(\mathrm{d}\theta^2_1 + \sin^2\theta_{(1)}\mathrm{d}\varphi^2\right)\right)\right) \quad .\end{aligned} \tag{3.2}$$

For a $(4+n)$-dimensional space with large extra dimensions ($r_s \ll L$), with L being the size of the extra dimensions, the Schwarzschild radius r_s of a black hole can be found by analytically the Einstein equations and is given in [46]. Using the PDG convention [47][1], it takes the form

$$r_s = \frac{1}{M_*\sqrt{\pi}}\left(\frac{M_{BH}}{M_*}\right)^{\frac{1}{n+1}}\left(\frac{8\Gamma\left(\frac{n+3}{2}\right)}{(n+2)}\right)^{\frac{1}{n+1}} \tag{3.3}$$

and depends on the mass of the produced black hole M_{BH}, which is assumed to be much larger than the fundamental scale, allowing to treat the produced black hole as a classical object. The production of classical black holes is elaborated in the following section. In the four-dimensional case ($n = 0$), one finds the well known linear behavior whereas for $n > 0$ a power-law dependence is observed. Due to the dimensionality, the four-dimensional Planck mass M_P is replaced by the fundamental Planck mass M_*. Meade and Randall

[1] For more details on the different conventions for the Planck mass, see appendix A.

pointed out in [48] that a black hole is produced in a collision if the Compton wavelength of the particle

$$\lambda = \frac{2\pi}{\sqrt{s}} \tag{3.4}$$

with center of mass energy of $\sqrt{s}$ lies within the Schwarzschild radius r_s. If this condition applies, (3.3) yields the ratio necessary for the creation of a black hole

$$x_{min} = \frac{\sqrt{s}}{M_*} \quad , \tag{3.5}$$

where the size slightly varies with the number of extra dimensions. If one neglects the factor 2π, the ratio becomes $\sqrt{s} \geq M_*$.

3.2 Production of classical black holes in particle collisions

In the background of strong gravity, the particles of a high-energy collision have been assumed to be gravitational shock waves in many theories, e.g [49–53]. Aichelburg and Sexl presented a well known method in 1970 [49], boosting the Schwarzschild line element using a Lorentz transformation. The Schwarzschild metric is defined by means of the time coordinate t and the spherical coordinates (r, θ, ϕ) as, see e.g. [54] or [55],

$$\mathrm{d}s^2 = -\left(1 - \frac{2m}{r}\right)\mathrm{d}t^2 + \left(1 - \frac{2m}{r}\right)^{-1}\mathrm{d}r^2 + r^2\mathrm{d}\Omega^2 \quad , \tag{3.6}$$

where $r^2\mathrm{d}\Omega = r^2\left(\mathrm{d}\theta^2 + \sin\theta^2\mathrm{d}\phi^2\right)$ describes the geometry of a two-sphere and m is the rest mass. For isotropic coordinates $(t, \bar{r}, \theta, \phi)$, which similarly to Schwarzschild coordinates describe static spherically symmetric systems and only differ from them in the radial coordinate, the line element is given by [55]

$$\mathrm{d}s^2 = -\mathrm{e}^{2\phi}\mathrm{d}t^2 + \mathrm{e}^{2\mu}[\mathrm{d}\bar{r}^2 + \bar{r}^2\mathrm{d}\Omega^2] \tag{3.7}$$

with the functions ϕ and μ dependent of $\bar{r}$. The time coordinate is the same for spherical and isotropic coordinates, whereas the radial coordinates are related via

$$r = \bar{r}\left(1 - \frac{m}{2\bar{r}}\right)^2 \quad . \tag{3.8}$$

With a suitable choice of coordinates

$$(x, y, z) = (\bar{r}\sin\theta\cos\phi\,,\ \bar{r}\sin\theta\sin\phi\,,\ \bar{r}\cos\phi) \tag{3.9}$$

the Schwarzschild metric can be expressed in isotropic coordinates

$$\mathrm{d}s^2 = -\left(\frac{1 - \frac{m}{2\bar{r}}}{1 + \frac{m}{2\bar{r}}}\right)^2\mathrm{d}t^2 + \left(1 + \frac{m}{2\bar{r}}\right)^4\left(\mathrm{d}x^2 + \mathrm{d}y^2 + \mathrm{d}z^2\right) \tag{3.10}$$

for which $\bar{r} = \sqrt{x^2 + y^2 + z^2}$.

Consider a black hole moving along the z-axis. It moves with a speed of $\beta = \sqrt{1 - \frac{1}{\gamma^2}}$ and therefore has a total energy fixed to $\mu = m\gamma$. γ is the Lorentz factor and assumed to be $\gamma \to \infty$, thus describing a large boost in z-direction. It was found in [49][2] that for $\beta = 1$, the metric takes the form

$$\mathrm{d}s^2 = -\mathrm{d}t^2 + \mathrm{d}x^2 + \mathrm{d}y^2 + \mathrm{d}z^2 - 4\mu\,\delta(t-z)\ln(x^2+y^2)\,(\mathrm{d}t - \mathrm{d}z)^2 \quad . \tag{3.11}$$

Expressing this metric with the retarded and advanced time parameters, which can be written in terms of the Minkowski coordinates t and z

$$(u, v) = (t - z, t + z) \tag{3.12}$$

yields

$$\mathrm{d}s^2 = -\mathrm{d}u\mathrm{d}v + \mathrm{d}x^2 + \mathrm{d}y^2 - 4\mu\,\ln(\rho)\delta(u)\mathrm{d}u^2 \quad . \tag{3.13}$$

With x and y as the remaining transverse coordinates, the transverse radius takes the form $\rho = \sqrt{x^2 + y^2}$. For every case except $t = z$, or alternatively $u = 0$, the line element describes a flat metric. For the hypersurface $u \neq 0$, however, a discontinuity occurs due to the delta function and the metric is curved. Assume two identical shock waves of this

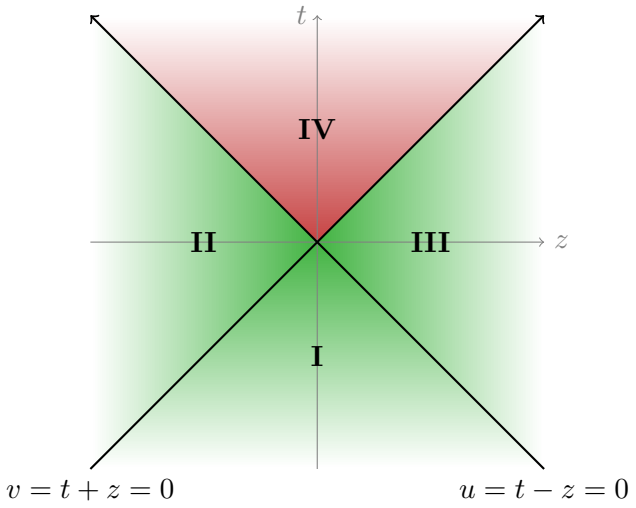

Figure 3.1: *Two Aichelburg-Sexl gravitational shock waves propagating in opposite direction along the z-axis and colliding at $u = v = 0$. The metric in the regions I, II and III remains flat, whereas the space-time of region IV is curved.*

nature, as visualized in Fig. 3.1, one propagating along the $+z$-axis and on the null plane

[2]Note that in this paper another sign notation for the Schwarzschild metric was used and the Lorentz transformation has been carried out in x-direction. It is straightforward to apply the changes suitable for this case.

$u = 0$ and another moving in opposite direction with its center at $v = 0$. A collision occurs at $u = v = 0$ and the space-time can be separated in four different regions. Whereas the regions I–III, at an appropriate distance to the null planes and particularly the collision point $u = v = 0$, are flat, one finds that the region formed after the collision (IV) is curved.

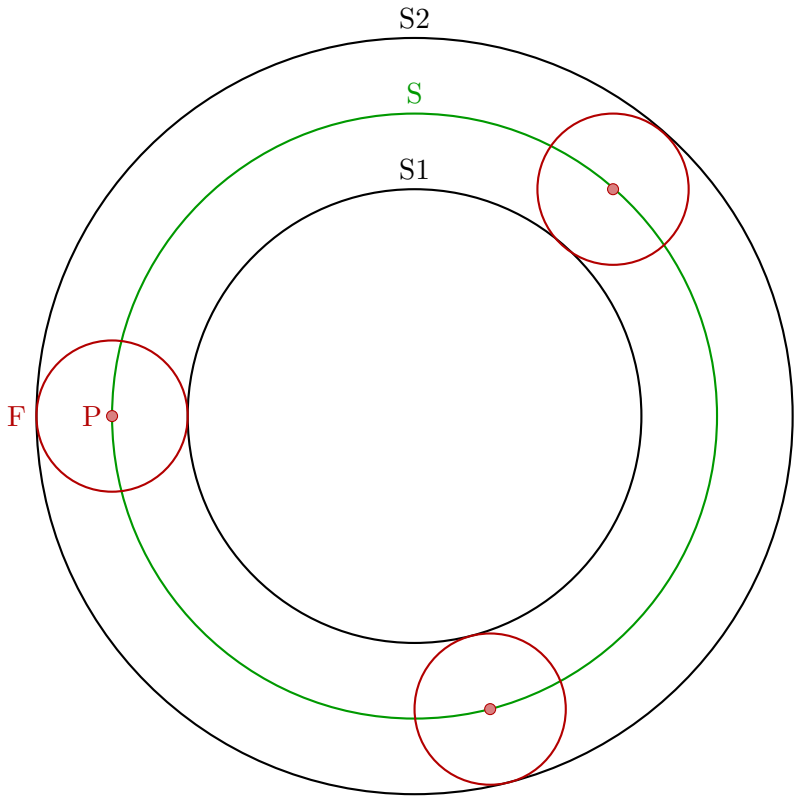

Figure 3.2: *Illustration of a closed trapped surface. P is an arbitrary point (red dot) on the surface S (green circle). If a flash of light F is emitted from P, an incoming and outgoing wavefront of the emitted light are created, S1 and S2 (black circles). If the areas of S1 and S2 are smaller than the area of S, a closed trapped surface is formed.*

To create a black hole in a process including two gravitational shock waves, a closed trapped surface has to be created at the collision. A closed trapped surface is a compact spacelike 2-dimensional surface on which the outgoing null rays perpendicular to the surface are not expanding, see Fig. 3.2 for an illustration of such. In case of the emission of a flash of light from an arbitrary point P on the surface, an incoming wavefront, S1, and an outgoing one, S2, envelope S. If the areas of both S1 and S2 are smaller than the area of S, then S forms a closed trapped surface.

3.2.1 Zero impact parameter

Penrose [56], as well as D'Eath and Payne [51–53], found an analytical solution for the production of a marginally trapped surface, i.e. a surface that separates the trapped surfaces from non-trapped surfaces and to which all outgoing light rays are parallel, in case of a vanishing impact parameter $b = 0$ and for center of mass energies $\sqrt{s}$ going towards infinity. This kind of process resembles a head-on collision, forming a surface of two flat disks with radius ρ_0 at the coordinates [57]

$$(t, z) = (-4\mu \ln(\rho_0), \pm 4\mu \ln(\rho_0)) \quad , \tag{3.14}$$

where each collision partner has the energy $\mu = \frac{\sqrt{s}}{2}$. Taking into account that the boundary lies within the collision surface gives

$$\rho_0 = 4\mu = r_s \quad . \tag{3.15}$$

In a four-dimensional spacetime, a closed-trapped surface can be formed within an area [25]

$$A_{CTS} \equiv 4\pi r_s^2 \geq 32\pi\mu^2 \quad . \tag{3.16}$$

This yields a lower bound on the black hole mass of

$$M_{BH} \equiv \frac{r_s}{2} \geq \sqrt{2}\mu \quad . \tag{3.17}$$

Eardley and Giddings extended this to a higher dimensional scenario, such as described in chapter 2. The closed trapped surface becomes an $(n+2)$-dimensional object with n being the number of extra spatial dimensions. The analytical method, however, can be used in a similar manner. In case of $(n+4)$ dimensions, the Schwarzschild line element (3.6) becomes

$$\begin{aligned} \mathrm{d}s^2 = &- \left(1 - \frac{16\pi M}{(n+2)\Omega_{n+2}} \frac{1}{r^{n+1}}\right) \mathrm{d}t^2 \\ &+ \left(1 - \frac{16\pi M}{(n+2)\Omega_{n+2}} \frac{1}{r^{n+1}}\right)^{-1} \mathrm{d}r^2 + r^2 \mathrm{d}\Omega_{n+2}^2 \quad , \end{aligned} \tag{3.18}$$

where $\mathrm{d}\Omega_{n+2}^2$ is the line element and Ω_{n+2} the volume of an $(n+2)$ sphere. We us an Aichelburg-Sexl boost in z-direction, as done for (3.13), and find

$$\mathrm{d}s^2 = -\mathrm{d}u\mathrm{d}v + \mathrm{d}x^{i2} + \Phi(x^i)\delta(u)\mathrm{d}u^2 \quad , \tag{3.19}$$

where x^i with $i = 1, \ldots, n+2$ denotes the additional transverse coordinates and Φ only depends on the transverse radius $\rho = \sqrt{x^i x_i}$ and is defined in as

$$\Phi = \begin{cases} -4\mu \ln(\rho), & \text{if } n = 0 \quad , \\ \frac{8\pi\mu}{\Omega_{n+1} n \rho^n}, & \text{if } n \geq 1 \quad . \end{cases} \tag{3.20}$$

As in the four-dimensional case, the total energy μ is fixed and an identical shock wave moving in the opposite direction on the z-axis will interact with the shock wave described by (3.19) only at the collision surface $u = v = 0$. Thus (3.15) can be generalized to

$$\rho_0 = \left(\frac{8\pi\mu}{\Omega_{n+1}} \right)^{1/(n+1)} \quad , \tag{3.21}$$

leading to the lower limits on the black hole mass depending on the number of extra dimensions [57]:

	$n=0$	$n=1$	$n=2$	$n=3$	$n=4$	$n=5$	$n=6$	$n=7$
$\frac{M_{BH}}{2\mu}$	0.71	0.67	0.64	0.62	0.61	0.60	0.59	0.58

Table 3.1: *Lower bound on classical black hole mass produced via the collision of two shock waves with zero impact parameter in relation to the number of extra dimensions.*

With an increase of the number of extra dimensions, the mass of the created black holes decreases. Additionally, Eardley and Giddings found that a non-zero impact parameter b effects the mass and extrapolated the previous method which will be described in the following section.

3.2.2 Non-zero impact parameter

As analytically established by Eardley and Giddings in [57], Yoshino and Nambu numerically verified in [58, 59] that even for a non-vanishing impact parameter, meaning a collision which is not head-on, a black hole can be created in a particle collision, for a schematic illustration see Fig. 3.3. Whereas for non-vanishing impact parameters larger

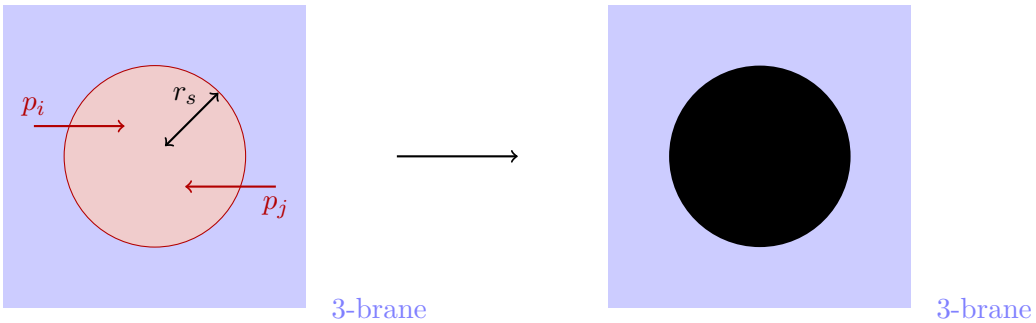

Figure 3.3: *Schematic illustration of a black hole production in a collision of two particles, p_i and p_j, with impact parameter b on the four-dimensional brane.*

than the Schwarzschild radius[3] both, elastic and inelastic processes occur, which are governed by graviton exchange, one finds for impact parameters $b < r_s$ that Thorne's hoop conjecture predicts a creation of a black hole. The hoop conjecture [41] states that black holes with horizons form when and only when an energy 2μ gets compacted into a region with a circumference C that satisfies in four dimensions

$$\frac{C}{4\pi G_N M} \lesssim 1 \quad , \tag{3.22}$$

whereas in a higher dimensional space one finds the following criterion

$$\frac{C}{2\pi r_s(M)} \lesssim 1 \tag{3.23}$$

used in [6–8]. At the instance of the collision, we find the circumference surrounding the colliding particles to be $C \sim 2b$. Comparing this to the minimal center of mass energy needed for the creation of a black hole defined as twice the total energy

$$\mu = \frac{\sqrt{s}}{2} \tag{3.24}$$

and using the inequality (3.23) yields

$$\frac{2b}{2\pi r_s(\sqrt{s})} \lesssim 1 \quad . \tag{3.25}$$

This leads to a maximal impact parameter about the size of the Schwarzschild radius which has to be weighted by a numerical factor $F(n)$, depending on the number of extra dimensions n,

$$b_{\max} = \sqrt{F(n)} r_s(\sqrt{s}) \quad . \tag{3.26}$$

Eardley and Giddings found a solution for an apparent horizon by reducing the question to a boundary-value problem and solved it analytically for the four-dimensional case [57] and found that with an impact parameter smaller than $b \leq b_{\max} \sim 0.8 r_s$, a closed trapped surface is still formed. The black hole mass M_{BH} trapped inside the horizon produced by this surface cannot simply be assumed to be identical to the center of mass energy $\sqrt{s}$, one has to consider inelasticity effects to account for radiated gravitational waves [11]:

$$M_{BH}(z) = y(z)\sqrt{s} \quad . \tag{3.27}$$

The inelasticity function $y(z)$ depends on the rescaled impact parameter $z \equiv b/b_{\max}$ with the maximal impact parameter $b_{\max}$ defined in (3.26). Subsequent to the original work

[3] To be considered for the four dimensional case, higher dimensional models allow for a maximal impact parameter bigger than that as summarized in Table 3.2.

of Eardley and Giddings [57] (and following work by Kohlprath and Veneziano [60]), the authors of [59] numerically determined lower bounds on the inelasticity function $y(z)$ as well as on the form factor $F(n)$ and found that the fraction of the Schwarzschild radius $F(n)$ increases with a rise in extra dimensions. Yoshino and Rychkov improved these numerical factors [61], an overview of the maximal impact parameters is presented in table 3.2. They extended the regime in which the closed trapped surface was produced to $u = 0\,, v \geq 0$, or equivalently $u \geq 0\,, v = 0$, allowing for creations of such surfaces subsequent to the collision of the gravitational waves, which consequently resulted in a boost for the impact parameter.

	$n=0$	$n=1$	$n=2$	$n=3$	$n=4$	$n=5$	$n=6$	$n=7$
$\sqrt{F(n)}$	0.84	1.15	1.33	1.44	1.52	1.57	1.61	1.65

Table 3.2: *Maximal impact parameters for the creation of classical black holes in high energy collisions* $b_{max} = \sqrt{F(n)} \times r_s$

.

In case of a non-zero impact parameter, the production cross section of a black hole produced in a collision can be estimated applying these numerical form factors of order one to the classical, geometrical limit

$$\hat{\sigma} \simeq \pi b^2 = F(n)\pi r_s^2 \quad . \tag{3.28}$$

It has been shown in [62] that even in the case of a collision of two high energetic particles, the process is described classically and not dominated by quantum effects, which will be covered in the following section.

Rewriting the Schwarzschild radius in terms of the center of mass energy of the collision and the fundamental scale, following (3.3), the production cross section becomes

$$\hat{\sigma} \simeq F(n)\pi r_s^2 \sim F(n)\frac{1}{M_*^2}\left(\frac{\sqrt{s}}{M_*}\right)^{\frac{2}{(n+1)}} \quad . \tag{3.29}$$

It is straightforward to see that the cross section increases with a growth in center of mass energy, distinguishing this from conventional perturbative scattering processes. With the rise of energy carried by the incoming particles, the formation of the event horizon would lead to a dominance of this process [7], changing the signatures of short distance physics at this regime dramatically [8].

It should be noted that expression 3.29 is only valid for partons, non-composite particles. Considering the high energies, the interaction happens on a parton level in hadronic

collisions, in which each parton carries a momentum fraction of the composite particle. It is therefore necessary to incorporate the parton distribution functions (PDFs) when considering collisions of composite particles, such as protons p which are used at the LHC. The PDFs, f_i and f_j determine the momentum fraction u and v carried by the parton.[4] The lower bound on the momentum fraction v depends on the fraction u associated with the other parton, whereas u_{min} is defined as

$$u_{min} = \frac{(x_{min} M_*)^2}{y(z)^2 s} \quad , \tag{3.30}$$

$y(z)$ represents inelasticity effects, M_* is the fundamental scale, and

$$x_{min} = \frac{M_{BH,min}}{M_*} \tag{3.31}$$

determines the ratio of the minimal black hole mass $M_{BH,min}$, for which the semi-classical approximation is assumed to be valid, and the fundamental scale. In the semi-classical regime, the ratio is expected to be $x_{min} \approx 3$ to assure validity of the semi-classical calculations [11]. Summing over all possible pairs of partons p_i with sufficient energy to produce a black hole, the cross section takes the form [11]

$$\sigma^{(pp)} = \int_0^1 2z\mathrm{d}z \int_{u_{min}}^1 \mathrm{d}u \int_u^1 \sum_{i,j} \frac{\mathrm{d}v}{v} f_i(u, Q^2) f_j(\frac{u}{v}, Q^2) \hat{\sigma}^{(p_i p_j)} \tag{3.32}$$

$$= \int_0^1 2z\mathrm{d}z \int_{u_{min}}^1 \mathrm{d}u \int_u^1 F(n) \pi r_s^2(us, n, M_*) \sum_{i,j} \frac{\mathrm{d}v}{v} f_i(u, Q^2) f_j(\frac{u}{v}, Q^2) \quad , \tag{3.33}$$

where $\sigma^{(p_i p_j)}$ describes the cross section of a black hole created by partons as described in (3.29) and the rescaled impact parameter is

$$z = \frac{b}{b_{max}} \quad . \tag{3.34}$$

The PDFs depend on the momentum fractions u and v of the considered partons. Q defines the momentum scale at which the PDFs are evaluated. The momentum scale is measured by the inverse length scale related to the type of process. For a gravitational theory and under consideration of a well-defined horizon, the momentum scale $Q^2 \sim r_s^{-2}$ is assumed to be a sensible choice, especially in the limit of high energies [11, 63]. For perturbative hard scattering processes, however, a momentum scale $Q^2 \sim s$ associated with the momentum transfer and thus in the s-channel the center of mass energy is assumed, see e.g. [57]. In case of quantum black holes, objects of masses of a few TeV which will be described in section 3.4, the fundamental Planck scale M_* seems just as natural a choice

[4] The momentum fractions u and v should not be confused with the retarded and advanced time parameters. From now on, u and v define the momentum fractions throughout the rest of this thesis.

for the momentum scale as the length scale associated with the Schwarzschild radius. However, we found that the production cross section is largely insensitive to the choice of momentum scale and we found that for our considered models it only differs by up to 20%, depending on the considered model. The PDFs decrease fast with increasing center of mass energy, counteracting the increase with energy as described before. Plots of the PDFs of relevant partons at the momentum scales $Q^2 \sim s = (14\,\mathrm{TeV})^2$, $Q^2 \sim M_*^2 = (1\,\mathrm{TeV})^2$, and $Q^2 \sim r_s^{-2} \approx (0.41\,\mathrm{TeV})^2$ can be found in appendix B.

3.3 Semi-classical black holes

By extending the classical description through the introduction of quantum states which represent black holes but assuming a substantial overlap with classical black hole trajectories, a semi-classical definition of the black hole states was established by Hsu in [62]. Using a path integral formalism developed in [64, 65], it was shown that the leading contribution to the production amplitude in the semi-classical case is indeed classical and quantum corrections are inconsiderably small. This is valid under the restriction that the small black hole mass is somewhat larger than the Planck mass. A black hole produced in a collision of two particles in opposite direction with center of mass energies much higher than the Planck scale underlies a semi-classical description [8]. For center of mass energies of the order of the Planck scale, a complete description of quantum gravity would be needed which we currently do not possess.

The decay of a semi-classical black hole is a thermal blackbody radiation process and described via Hawking radiation [66], thus dependent on its Hawking temperature which in turn is proportional to the inverse Schwarzschild radius (3.3) and has the form [46]

$$T_H = M_* \left(\frac{M_*}{M_{BH}} \frac{n+2}{8\Gamma\left(\frac{n+3}{2}\right)} \right)^{\frac{1}{n+1}} \frac{n+1}{4\sqrt{\pi}} \quad . \tag{3.35}$$

Higher-dimensional black holes have a lower Hawking temperature, a longer life time

$$\tau \sim \frac{1}{M_*} \left(\frac{M_{BH}}{M_*} \right)^{\frac{n+3}{n+1}} \tag{3.36}$$

and a greater radius (3.3) than their four-dimensional counterparts [67]. Note that the created black hole is smaller than the respective Compton wavelength $\lambda = 2\pi/T_H$. The black hole thus behaves approximately like a point radiator with entropy

$$S = \frac{4}{3}\pi M_{BH} r_s \quad . \tag{3.37}$$

For a thermal decay, the entropy needs to be sufficiently high. This yields an estimate for the ratio between the lowest semi-classical black hole mass and that of the Planck mass of 5 to 20, depending on the chosen low scale quantum gravity theory. In the case of ADD, it is typically taken to be of the order of 5, while it could easily be 20 for RS [48]. For models with large extra dimensions, Emparan, Horowitz, and Myers determined in [43], see also [44], that semi-classical black holes evaporate mainly on the observable 3-brane. Opposing the claims in [7, 68] that due to the high temperature of the black hole compared to the masses of light Kaluza-Klein modes, spin-2 fields with masses starting with the inverse size of the extra dimensions L^{-1} (for $n = 2$, see section 2.1), most of the Hawking radiation will be radiated off into the bulk, the authors of [43] demonstrated that a huge fraction of the energy is taken up by standard model fields and could thus be observed by high energy colliders. Keeping in mind the decomposition of the bulk metric into graviton fields and an infinite tower of Kaluza-Klein modes, they pointed out that the emission of the 3-brane fields is a four-dimensional process and should not be pictured as higher-dimensional bulk fields restricted to a confined area. Additionally, it was indicated that the large number of Kaluza-Klein modes is suppressed by a geometric factor due to the overlap with small black holes and their contribution thus corresponds only to one brane field.

Because of the thermal nature of the evaporation, the black hole is expected to decay into a many-particle final state, not discriminating between the species of the standard model particles but still obeying the local conservation laws [6]. This would lead to a very distinctive signature if observed in particle collisions with sufficient energy. According to [48], it is very unlikely that these signatures will be observed at current colliders because of their insufficient energy to produce semi-classical black holes, which have masses of at least 5-20 TeV, well above threshold. The authors also predict a significant rise in the rate of two-particle final states in the quantum gravitational regime due to a suppression of the multi-particle states as a result of inelasticity effects and black hole entropy, which might lead to a much higher ratio described in (3.5) than formerly expected [8, 12]. This, however, does not exclude (maybe even yet unpredicted) signs of quantum gravitational effects at a TeV level.

In recent years, much progress has been made towards the understanding of the decay of a semi-classical black hole in a particle detector, see e.g. [69], and it is assumed that it proceeds through a number of stages [57, 69]:

1. The first stage is called the *balding phase*. During this stage, the asymmetric black hole sheds its gauge field "hair" and loses its asymmetries via gravitational and gauge

radiation into the bulk. This happens mostly via Schwinger emission.

2. In the second stage, the *spin-down phase*, the spinning, but neutral black hole will lose mass and angular momentum by emitting Hawking and Unruh-Starobinskii radiation.

3. It will then enter the *Schwarzschild phase*, in which the spherical symmetric black hole remains to evaporate via Hawking radiation and gradually decreases in mass in a symmetrical procedure.

4. It will continue to do so until it approaches a mass around the fundamental scale $M_{BH} \sim M_*$, at which it goes over into the *Planck phase*. To explain the no longer semi-classical black hole's behavior at this final stage, a quantum gravitational theory is needed.

A phenomenological approach of black holes which do not undergo the process involving all four stages and with masses of a few TeV will be introduced in the following section.

3.4 Quantum black holes

Other than semi-classical black holes, quantum black holes (QBHs) [17] have masses lower than $5 \times M_*$, i.e. up to a mass where the semi-classical regime is thought to be valid. They are assumed to be non-thermal objects, thus do not pressingly underly the usual black hole thermodynamics and their decay is not described via Hawking radiation. They will not evaporate into many-particle states but only into a few particles, which will most likely be two-particle states [48], distinguishing them from very massive black holes including their astrophysical counterparts as well the much more massive semi-classical black holes created in particle collisions. The horizon of a QBH corresponds to the Schwarzschild radius. With masses of around a few TeV, their production happens for low scale gravity models near threshold and both formation and decay take place over a very short spacetime region. Accordingly, Schwarzschild radius and mass of the QBH approach the quantum gravity scale. The first experimental papers setting limits on the masses of these holes have started to appear, see e.g. [70–73]. Their very short lifetime allows for such objects, produced in collisions of quarks and gluons, to carry an SU(3) color charge, since the QCD length scale is much larger than the size of these objects which is about TeV^{-1} resulting in hadronization being a consequent process. It can hence be uniquely determined by its mass, spin, and gauge charges, making them very interesting objects for particle physicists.

A QBH is thus more resonance-like, this will be elaborated in more detail in the following chapters. We assume that the QBH is created and decays almost instantly, it is thus sensible to imagine it as a short lived gravitational state. This is a fairly strong assumption which is applied throughout this thesis. Other phenomenological approaches consider for instance remnants in the decaying process, see e.g [74–76]. A model to describe these states and their interactions using a quantum field theory is given in chapter 4. A QBH process is expected to conserve local gauge symmetries but no comparable assumptions have been made about global charges. With no complete understanding of quantum gravity, it is not intelligible which global symmetries are conserved. In addition, the important question is raised whether the mass spectrum of the produced QBHs is continuous as for macroscopic black holes or quantized as proposed in [77]. This thesis will examine both cases, covered in chapter 5 and 6, respectively. It is assumed in both cases, however, that their production cross section can be extrapolated from the semi-classical one (3.33). For a continuous mass spectrum, it takes the form

$$\sigma^{(pp)}(s, x_{min}, n, M_*) = \int_0^1 2zdz \int_{\frac{(x_{min}M_*)^2}{y(z)^2 s}}^1 du \int_u^1 \frac{dv}{v} \times F(n)\pi r_s^2(us, n, M_*) \sum_{i,j} f_i(v, Q) f_j(u/v, Q) \tag{3.38}$$

with the $(n+4)$-dimensional Schwarzschild radius given by

$$r_s(us, n, M_*) = k(n) M_*^{-1} [\sqrt{us}/M_*]^{1/(1+n)} \quad , \tag{3.39}$$

where

$$k(n) = \left[2^n \sqrt{\pi}^{n-3} \frac{\Gamma((3+n)/2)}{2+n} \right]^{1/(1+n)} \quad . \tag{3.40}$$

For QBHs with a discrete mass spectrum on the other hand, one considers for the total cross section the sum of the individual ones

$$\sigma_{tot}^{(pp)}(s, n, M_*) = \sum_i \sigma_{QBH}^{(pp)}(s, M_{QBH}^i, n, M_*) \quad . \tag{3.41}$$

The individual cross sections are given by

$$\sigma_{QBH}^{pp}(s, M_{QBH}, n, M_*) = \pi r_s^2(M_{QBH}, n, M_*) \int_0^1 2zdz \int_{\frac{(M_{QBH})^2}{y(z)^2 s}}^1 du \int_u^1 \frac{dv}{v} \times F(n) \sum_{i,j} f_i(v, Q) f_j(u/v, Q) \tag{3.42}$$

with the now constant Schwarzschild radius being

$$r_s(M_{QBH}^2, n, M_*) = k(n) M_*^{-1} [\sqrt{M_{QBH}^2}/M_*]^{1/(1+n)} \tag{3.43}$$

and $k(n)$ remains as in the continuous case before. In the RS model, the number of extra dimensions is fixed to $n = 1$ and the Schwarzschild radius takes the form

$$r_s = M_*^{-1} \left(\frac{2M_{BH}}{3\pi M_*} \right)^{1/2}. \tag{3.44}$$

With energy sufficient enough to produce multi-body final states, the production of semi-classical black holes will dominate, cutting off the production of two-particle final states. The cross section plays an important role, not only to determine approximate values for the likelihood of certain final states to occur (chapters 5, 6 and 7) but also to fix the effective theory which is described in the following chapter.

Chapter 4

Quantum field theory for non-thermal black holes

In this chapter, a substantially model independent field theory describing the production of quantum black holes (QBHs) is presented. The specification *effective* merely indicates that the theory is limited to a certain energy region, which in this case is the realm in which quantum gravity effects become important and the production of non-thermal microscopic black holes [17, 48] might happen. The study of these QBHs provides the opportunity to gain more insights into important physical aspects, such as flavor physics.

This part of the thesis is based on calculations published in [14]. The goal of this work is to find bounds on the fundamental Planck scale M_*, using data on the anomalous magnetic moment of the muon, low energy experiments searching for violation of lepton flavor conservation and bounds on a neutron electric dipole moment. As discussed in chapter 2, one has no certainty for the value of the Planck scale as it was discovered that it might very well be lowered by effects like extra spatial dimensions [1–3] or a large hidden sector [4, 78]. There are several experimental constraints on these theoretical frameworks, leading to a complete exclusion of the model to bounds in the 1 TeV to 100 TeV region, depending on the number of extra-dimensions, see e.g. [70–73] or [19][1].

Since these non-thermal QBHs can be thought of as states which are created and decay almost instantly, they will be treated as short-lived gravitational states. Using a quantum field theory to describe these objects is natural, since these black holes only couple to a few particles. For demonstrative purposes, the QBH will be modeled by a spinless scalar field ϕ which can be charged under the gauge quantum numbers of the Standard Model, but this does obviously not exclude that the QBH could be neutral. The interactions of

[1] In review: "Extra dimensions".

this scalar field with the SM particles p_i and p_j will be chosen in such a way that the geometrical cross section $\sigma \sim \pi r_s^2$, is obtained when calculating $\sigma(p_i + p_j \to \phi)$ where the scalar field ϕ represents the spinless QBH. Although the focus of this work is on the four dimensional case and on a spinless QBHs, our results can be easily generalized to the case of extra-dimensional black holes with spin. As stated before, quantum gravity is assumed to conserve gauge symmetries, which implies that gauge quantum numbers must be preserved by quantum gravitational interactions including QBHs. On the other hand, global symmetries can be violated by quantum gravitational interactions, which might yield to phenomena known in string theory such as Lorentz violating vacua [79]. Lorentz violation effects typically lead to very tight bounds on the scale of quantum gravity. Here we shall assume that Lorentz is not violated and focus on violation of flavor symmetry and CP violation induced by QBH processes.

Due to a black hole's unique identification by its mass, spin, and charge, it is reasonable to describe a black hole by a massive quantum field carrying spin and charge. In case of a QBH created in collisions of quarks or gluons, one would expect them to also carry a QCD color charge as well, since gauge numbers cannot be violated. Furthermore, it is not obvious whether their mass spectrum is continuous or discrete, which will be addressed later on in this thesis. Within the scope of the proposed effective theory, the following Lagrangian for a spinless, neutral QBH ϕ is postulated

$$L_4 = \frac{1}{2}\partial_\mu\phi\,\partial^\mu\phi - \frac{1}{2}M_{BH}^2\phi^2 \quad . \tag{4.1}$$

One expects the first QBH mass to be of the order of the Planck mass. If the spectrum is discrete, one can consider a collection of scalar fields. On the other hand, if the mass spectrum was continuous, the mass of the QBH would increase with the energy of the process. In the following, a discrete mass spectrum is assumed with the focus on the lightest QBH. It shall be noted that the results could be trivially extended to describe a continuous mass spectrum. Considering the higher-dimensional effective Lagrangian

$$L_6 = \frac{C}{\bar{M}_*^2}\,\partial_\mu\partial^\mu\phi\bar{\psi}_1\psi_2 + h.c. \tag{4.2}$$

where C is a momentum-dependent function that will later be adjusted to yield the correct cross section, $\bar{M}_* = M_*/\sqrt{8\pi}$ the reduced Planck mass and ψ_i represents an arbitrary SM fermion field. We shall assume here that the QBH ϕ is neutral, from which follows that the gauge charges of ψ_1 must thus be matched by those of ψ_2. The use of a six-dimensional operator originates from the non-negligible effect of higher-dimensional operators in this energy regime [48] and the suppression of four-dimensional operators for such processes,

i.e. in four dimensions the cross section for black hole production goes as M_*^4.

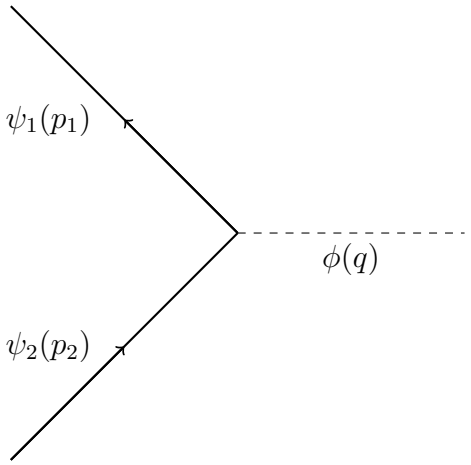

Figure 4.1: *Feynman diagram of the production of a QBH, represented by the scalar field ϕ, created in a collision of two fermions ψ.*

Under consideration of the effective Lagrangian (4.2), one determines the amplitude for the process described in Fig. 4.1

$$\mathcal{A} = q^2 \frac{C}{\bar{M}_*^2} \overline{v}(p_1) u(p_2) \quad , \tag{4.3}$$

where the four-momentum of the ϕ field $q = (p_1 + p_2)$ is the sum of the fermion field momenta, respectively, and u, v denote the fermion spinors. One obtains the following cross section for ϕ production:

$$\sigma\left(2\psi \to \phi\right) = \frac{\pi}{s} |\mathcal{A}|^2 \, \delta(s - M_{BH}^2) \quad , \tag{4.4}$$

where M_{BH} is the mass of the ϕ field, $s = (p_1 + p_2)^2$. Squaring the amplitude yields

$$\begin{aligned} |\mathcal{A}|^2 &= (p_1 + p_2)^4 \frac{C^2}{2\bar{M}_*^4} \operatorname{Tr}\left[\left(\not{p}_1 - m_1\right)\left(\not{p}_2 + m_2\right)\right] \\ &= s^2 \frac{C^2}{\bar{M}_*^4}\left[s - (m_1 + m_2)^2\right] \quad , \end{aligned} \tag{4.5}$$

where m_1 and m_2 are the masses of the fermions ψ_1 and ψ_2. We can now compare this cross section to the geometrical cross section $\sigma = \pi r_s^2$. Note that inelasticity effects have not been considered but could easily be applied. The four-dimensional Schwarzschild radius is given by

$$r_s\left(s, 0, \bar{M}_*\right) = \frac{\sqrt{s}}{4\pi \bar{M}_*^2} \tag{4.6}$$

and one thus finds:

$$C^2 = \frac{9}{4} \frac{4s^{\frac{3}{2}} - 8sM_{BH} + 4\sqrt{s}M_{BH}^2 + \sqrt{s}\Gamma^2}{\Gamma\pi[s - (m_1 + m_2)^2]} \tag{4.7}$$

where Γ is the decay width of ϕ. Note that the following representation was used for the delta function:

$$\delta(s - M_{BH}^2) = \frac{\Gamma M_{BH}}{\pi[(s - M_{BH}^2)^2 + \Gamma^2 M_{BH}^2]} \quad . \tag{4.8}$$

The partial width of ϕ is estimated, as done for the cross section, by extrapolating it from the semi-classical case. For N particles in the final state, one finds [17]

$$\Gamma\left(QBH \to p_1 \dots p_N\right) \sim \left[2\pi \left(\frac{1}{(2\pi)^2}\right)^{(N-1)} \left(\frac{1}{2}\right)^{(N-1)}\right] \pi r_s^2 M_{BH}^3 \quad , \tag{4.9}$$

using the general phase space factors from a decay to N massless particles. Assuming that the mass of the QBH is of the order of the reduced fundamental Planck mass, $\bar{M}_* \sim M_{BH}$, and that the QBH decays into a two particle final state, one finds in the four-dimensional case using (4.6)

$$\Gamma\left(\phi \to \psi_1 + \psi_2\right) \sim \frac{1}{4} r_s^2 M_{BH}^3 = \frac{M_{BH}}{64\pi^2} \quad . \tag{4.10}$$

Since there are about 100 degrees of freedom in the Standard Model, the total width is about hundred times larger. Using this relation gives an estimate for Γ in (4.7). The dimension-six operators introduced in (4.2) have interesting consequences for precise low energy measurements, such as the anomalous magnetic moment of the muon or rare decays forbidden in the Standard Model. They could even lead to new sources of CP violation if a γ_5 is introduced in the effective Lagrangian describing the coupling of the QBH to the fermions

$$L_{6,CP} = \frac{C}{\bar{M}_*^2} \partial_\mu \partial^\mu \phi \bar{\psi}_1 i\gamma_5 \psi_2 + h.c. \quad . \tag{4.11}$$

It is effortless to estimate the one loop induced effective Lagrangian in the low energy regime. Obviously the effective theory is not renormalizable, but one can use power counting arguments to find

$$L_{eff} = \frac{e}{2} \frac{1}{16\pi^2} \sum_{ij} \frac{m_i}{\bar{M}_*^2} \bar{\psi}_i (A_{ij} + B_{ij}\gamma_5) \sigma_{\mu\nu} \psi_j F^{\mu\nu} \quad , \tag{4.12}$$

where m_i is the mass of the heavier of the two fermions, $A_{ij} = A$ and $B_{ij} = B$ are numerical Wilson coefficients which are found to be of order 1. The momentum cutoff of the loop integral is taken to be of the order of the reduced Planck mass. Carefully considering the Dirac structure of the loop diagram (see Fig. 4.2), leads to the chiral suppression factor $m_i/\bar{M}_*$. We find the well known result for the contribution of the loop to the magnetic moment of the muon

$$\Delta a = \frac{1}{16\pi^2} \frac{m_\mu^2}{\bar{M}_*^2} \quad , \tag{4.13}$$

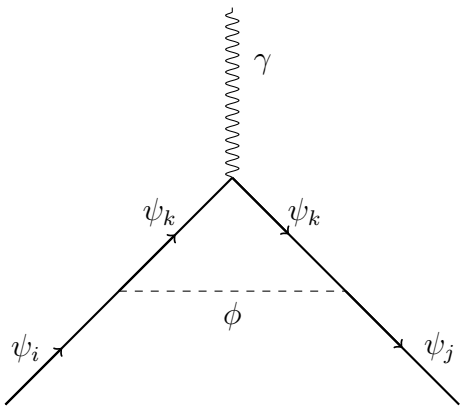

Figure 4.2: *Feynman loop diagram of a QBH treated as a virtual object, describing the production of the QBH from fermions ψ_i and ψ_j and its decay into fermions of the same kind ψ_k which annihilate into a photon γ.*

assuming $|A| = 1$. The γ_5 term of (4.12) does not contribute to the anomalous magnetic moment. Using $\Delta a \sim 10^{-9}$ [80] yields the following bound on the fundamental Planck scale[2]:

$$\bar{M}_* > 266\,\text{GeV} \quad . \tag{4.14}$$

Very few assumptions have been made to obtain this bound: It is assumed that QBHs can be treated as virtual objects which couple to low energy modes and that these non-thermal objects couple to only a few degrees of freedom. Surprisingly, the bound is remarkably low and indicates that QBHs could very well be relevant for LHC physics. Bounds on lepton flavor violating processes also lead to limits on the reduced Planck mass. Unless the lepton number is gauged, QBH processes are expected to lead to transitions which do not preserve lepton number. In case of lepton number violating processes, one finds:

$$\Gamma(\mu \to e\gamma) = e^2 \frac{A^2}{1024\pi^5} \frac{m_\mu^5}{\bar{M}_*^4} \tag{4.15}$$

$$\Gamma(\tau \to e\gamma) = \Gamma(\tau \to \mu\gamma) = e^2 \frac{A^2}{1024\pi^5} \frac{m_\tau^5}{\bar{M}_*^4}. \tag{4.16}$$

The current experimental limit for the muon decay into an electron and photon is $\text{Br}(\mu \to e\gamma) < 1.2 \times 10^{-11}$ and accordingly for the tau $\text{Br}(\tau \to \mu\gamma) < 4.4 \times 10^{-8}$ [80][3], resulting in

[2] With the current value of $\Delta a \approx 2.87 \times 10^{-9}$, taken from [19, review: "The muon anomalous magnetic moment"], one finds a less restricting bound of $\bar{M}_* > 157\,\text{GeV}$.

[3] In summary table: "Leptons".

the following limits on the reduced Planck mass[4]

$$\bar{M}_* > 3 \times 10^4 \,\mathrm{GeV} \tag{4.17}$$

using the bound on the transition $\mu \to e\gamma$ and

$$\bar{M}_* > 3 \times 10^3 \,\mathrm{GeV} \tag{4.18}$$

using the bound on the transition $\tau \to \mu\gamma$.

If CP is violated by QBH processes, the effective Lagrangian also gives a contribution to the electric dipole moment of leptons and quarks of the Standard Model. The Lagrangian gives us the following electric dipole moment of the electron

$$d(e) = \frac{eB}{16\pi^2} \frac{m_e}{\bar{M}_*^2} \quad . \tag{4.19}$$

Using the current experimental constraint $d(e) = (0.07 \pm 0.07) \times 10^{-26} e\,\mathrm{cm}$ [80][5], gives the following bound on the reduced Planck mass[6]:

$$\bar{M}_* > 1 \times 10^4 \,\mathrm{GeV} \tag{4.20}$$

while by using the bound for the muon, i.e. $d(\mu) = (-0.1 \pm 0.9) \times 10^{-19} e\,\mathrm{cm}$, we find

$$\bar{M}_* > 36 \,\mathrm{GeV} \quad . \tag{4.21}$$

Finally, one can also determine a limit by studying the contribution to the electric dipole moment of the neutron. The current bound on the neutron electric dipole moment is $d(n) = 0.29 \times 10^{-25} e\,\mathrm{cm}$ [80][7]. Using

$$d(n) = \frac{4}{3} d(d) - \frac{1}{3} d(u) = \frac{eB}{16\pi^2 \bar{M}_*} \left(\frac{4}{3} \frac{m_d}{\bar{M}_*} - \frac{1}{3} \frac{m_u}{\bar{M}_*} \right) \tag{4.22}$$

gives a bound on the reduced Planck mass of

$$\bar{M}_* \approx 5 \times 10^3 \,\mathrm{GeV} \quad , \tag{4.23}$$

where, following the previous made estimate, it proved reasonable to assume that the Wilson coefficient is $B \sim 1$.

[4] The experimental upper bound for the lepton family violating muon decay into an electron changed to $\mathrm{Br}(\mu \to e\gamma) < 2.4 \times 10^{-12}$, according to [19, summary table: "Leptons"], resulting in an even higher limit for the Planck scale of $\bar{M}_* > 5 \times 10^4 \,\mathrm{GeV}$.

[5] In summary table: "Leptons".

[6] With the most recent upper bound, to be found in [19, summary table: "Leptons"], for the electric dipole moment of the electron of $d(e) < 10.5 \times 10^{-28} e\,\mathrm{cm}$ a slightly lower bound of $\bar{M}_* > 8 \times 10^3 \,\mathrm{GeV}$ is obtained.

[7] In summary table: "Baryons".

Due to the reasonably good agreement between the experimental value and theoretical prediction of the magnetic moment of the muon, a rather low bound on the reduced fundamental Planck scale of 266 GeV (or even lower for the more accurate value of $\Delta a \approx 2.87 \times 10^{-9}$) is found. Studying processes, in which discrete symmetries such as lepton number or CP conservation are violated by quantum gravitational physics, provided much tighter limits on the energy scale, at which quantum gravity effects become sizable, of up to $\sim 10^4$ GeV. Considering that dimension-four operators describing black hole effects are highly suppressed by form factors at low energies, it is assumed that higher-dimension operators will remain at these energies [48], which would make these operators relevant to current colliders in case of a low quantum gravity scale. One could for example examine processes at energies well below the first QBH mass, i.e. $M_{BH}^2 \gg s$, by integrating out the fields ϕ, yielding the dimension-six operators:

$$\mathcal{L} = \frac{C^2}{\bar{M}_*^4} \frac{s^2}{M_{BH}^2} \bar{\psi}\psi\bar{\psi}\psi \quad , \tag{4.24}$$

with C being the same as before, thus being dependent on the momentum. We take a momentum of the order of the typical QCD scale for the momentum of the quarks in the proton. These operators would be applicable to describe non-thermal QBH production in the collisions of quarks. The exchange of a QBH field which violates baryon and lepton numbers generates similar operators. These would obviously also concede proton decay, thus one needs to contemplate the lifetime τ of a proton

$$\tau = \frac{\bar{M}_*^{12}}{m_p^5 C^4 \Lambda_{QCD}^8} \sim \frac{1}{(10^2\ 16\pi)^2} \frac{\bar{M}_*^{10}}{m_p^5 \Lambda_{QCD}^6} \quad , \tag{4.25}$$

where Λ_{QCD} is the typical energy of the quarks in the proton, to find $M_P > 1 \times 10^6$ GeV, using $\tau > 5 \times 10^{33}$ y [80][8]. If low scale quantum gravity is the solution to the weak hierarchy problem, the proton decay problem must be addressed. An obvious solution could be restrict the operators to gauge the baryon or lepton number.

We will now summarize the most important assumptions made in this chapter. To find an effective way of describing the physics of QBHS, the only concrete assumption we make is that the QBH cross section can be extrapolated from the semi-classical case. We thus expect QBHs to be created in the quantum gravitational regime. We assume that QBHs can be treated as short-lived gravitational states which are created and decay almost instantly and couple only to low energy modes. Due to their low mass of the order of a TeV, we expect the QBHs to couple to only a few particles and have a particle-like nature. One can thus describe their physics using a Lagrangian.

[8] In summary table: "Baryons".

It should be stressed again that there is no complete theory describing the effects beyond the fundamental Planck scale. In the succeeding chapters, a theory of the production and decay of QBHs is elaborated, in which many possible scenarios of the nature of quantum gravity are considered, thus enabling one to draw conclusions from restrictions to the fundamental Planck scale as well as the QBH model.

Chapter 5

Quantum black holes with a continuous mass spectrum

This chapter is based on work published in [15] and [16], the results as well as the method will be used in the new version of BlackMax[1] [13], an event generator for microscopic black holes. The code, used to determine the cross sections presented in this chapter, will be included in one of the future versions of BlackMax to complement the currently incorporated models. The main purpose of studying the production and decay mechanisms of QBHs is to gain increased knowledge about gravity at the quantum level, especially at energy regions close to the fundamental Planck scale, as well as to improve the understanding of the model and restrictions concerning these objects. Using the extrapolated cross-section of the semi-classical case, the production mechanism will be described. The classification of QBHs were used to obtain branching ratios, i.e. numbers that determine how likely a created QBH will decay into a certain final state, to establish approximations for specific final state cross sections.

5.1 Production of QBHs with a continuous mass spectrum

Currently, a class of models with low scale quantum gravity predicts that quantum gravitational effects could become important at a few TeVs and is being probed directly by measurements at the Large Hadron Collider (LHC) at CERN, see chapter 2. The production of small black holes at the LHC would be one of the most intriguing signals of low scale quantum gravitational physics, see e.g. [78] for a recent review.

[1] BlackMax Version 3.0 (written in C++), current version to be retrieved from http://blackmax.hepforge.org/.

As introduced in section 3.4, QBHs are quite different from astrophysical black holes in the sense that their masses would be close to the Planck mass. Whereas semi-classical black holes decay via Hawking radiation through several stages (balding, spin-down, Schwarzschild, and Planck phase - see section 3.3 for a detailed description), QBHs decay non-thermally, i.e. their entropy is not high enough to account for a thermal decay. These relatively small black holes presumably decay into only a few particles, each with Compton wavelength of the order of the size of the QBH. It seems unlikely that they would decay to a much larger number of longer wavelength modes. Semi-classical black holes, on the other hand, are thermal objects that are expected to decay via Hawking radiation to many particles, typically of the order of 20, after a spin down phase. This final explosion would lead to a spectacular signature in a detector. It is, however, now well understood [12, 17, 48] that it is very unlikely that semi-classical black holes will be produced at the LHC because the center of mass energy is not high enough.

One could say that in many respects QBH are perhaps more analogous to strongly coupled resonances or bound states than to large black holes. An important question is whether the mass of the quantum black holes is quantized or continuous as expected in the case of macroscopic black holes. Most studies so far are assuming that QBHs have a continuous mass spectrum despite some recent warnings that the quantum black hole masses ought to be quantized [77]. Due to the lack of conviction for either case, this chapter will deal with the continuous case, whereas the following chapter 6 will consider discrete masses for QBHs and discuss the motivation of quantized black holes.

Assuming the extrapolation of the geometrical cross section πr_s^2, the production of QBHs at the LHC is taken to be of the form

$$\sigma^{pp}(s, x_{min}, n, M_*) = \int_0^1 2zdz \int_{\frac{(x_{min}M_*)^2}{y(z)^2 s}}^1 du \int_u^1 \frac{dv}{v} \times F(n)\pi r_s^2(us, n, M_*) \sum_{i,j} f_i(v, Q) f_j(u/v, Q) \tag{5.1}$$

where M_* is the n-dimensional Planck mass, the rescaled impact parameter is defined as $z = b/b_{max}$, $x_{min} = M_{BH,min}/M_*$, n is the number of extra dimensions, $F(n)$ and $y(z)$ are numerical factors introduced by Eardley and Giddings and by Yoshino and Nambu [59, 61] to describe the effects of inelasticity, for more detail see section 3.2.2. f_i and f_j are the parton distribution functions and fall rapidly for high energies. The n-dimensional Schwarzschild radius is given by

$$r_s(us, n, M_*) = k(n) M_*^{-1} [\sqrt{us}/M_*]^{1/(1+n)} \quad , \tag{5.2}$$

where

$$k(n) = \left[2^n \sqrt{\pi}^{n-3} \frac{\Gamma((3+n)/2)}{2+n}\right]^{1/(1+n)} \quad . \tag{5.3}$$

The fact that these QBHs are non-thermal is reflected in the assumption that they decay only to a few particles immediately after their creation. Produced in particle collisions, at the LHC specifically collisions of quarks and gluons, QBHs can be classified with regard to the partons creating the QBH. This classification will be specified in the coming section.

5.2 Classifications of QBHs

It is assumed that QBHs are defined by three quantities: their mass, spin and gauge charges. Importantly, QBHs can have a QCD, or color, charge. This is not in contradiction with confinement since the typical length scale of QCD, i.e., a Fermi, is much larger than the size of a QBH, e.g., TeV^{-1}. The formation and decay of a QBH takes place over a small space-time region, from the QCD perspective it is a short distance process, thus hadronization occurs only subsequently. Their decomposition modes depend on a few assumptions which are as follows

I) Processes involving QBHs conserve QCD and U(1) charges since local gauge symmetries are not violated by gravity. Note that no similar assumption is made about global charges.

II) QBH coupling to long wavelength and highly off-shell perturbative modes is suppressed.

Assumption (II) is necessary so that precision measurements, or, possibly, proton decay do not force the quantum gravity scale to be much larger than the TeV range. It is not implausible that a nonperturbative QBH state couples only weakly to long distance or highly off-shell modes, but strongly to modes of size and energy similar to that of the black hole.

Generically speaking, QBHs form representations of $\mathrm{SU}(3)_c$ and carry a QED charge. The process of two partons p_i, p_j forming a quantum black hole in the c representation of $\mathrm{SU}(3)_c$ and with the QED charge q as it is considered to conserve gauge numbers:

$$p_i + p_j \to \mathrm{QBH}_c^q \quad . \tag{5.4}$$

From the group representations of (anti)quarks as (anti) triplets and gluons as octets in the adjoint representation, we can calculate the multiplicities of the states. The following different transitions are possible at a proton collider:

a) $q + \bar{q}: \ \mathbf{3} \times \overline{\mathbf{3}} = \mathbf{8} + \mathbf{1}$

b) $q + q: \ \mathbf{3} \times \mathbf{3} = \mathbf{6} + \overline{\mathbf{3}}$

c) $\bar{q} + \bar{q}: \ \overline{\mathbf{3}} \times \overline{\mathbf{3}} = \overline{\mathbf{6}} + \mathbf{3}$

d) $q + g: \ \mathbf{3} \times \mathbf{8} = \mathbf{3} + \overline{\mathbf{6}} + \mathbf{15}$

e) $\bar{q} + g: \ \overline{\mathbf{3}} \times \mathbf{8} = \overline{\mathbf{3}} + \mathbf{6} + \overline{\mathbf{15}}$

f) $g + g: \ \mathbf{8} \times \mathbf{8} = \mathbf{1}_S + \mathbf{8}_S + \mathbf{8}_A + \mathbf{10} + \overline{\mathbf{10}}_A + \mathbf{27}_S \quad .$

The subscripts A and S indicate that a state is (anti)symmetric under the interchange of any two quarks. The group representations will be written in bold throughout this thesis. Most of the time the black holes, which are created, carry a $\mathrm{SU}(3)_c$ charge and come in different representations of $\mathrm{SU}(3)_c$ as well as QED charges. There are nine possible electromagnetic charges:

$$0\,, \pm\frac{1}{3}\,, \pm\frac{2}{3}\,, \pm\frac{4}{3} \quad \text{and} \quad \pm 1 \quad ,$$

corresponding to the charges of the colliding quarks and gluons. The classification allows to predict how the black holes will decay. For instance, the production cross-section of a QBH_1^0 is given by

$$\begin{aligned} \sigma^{pp}(s, x_{min}, n, M_*) = \int_0^1 2z dz \int_{\frac{(x_{min} M_*)^2}{y(z)^2 s}}^1 du \int_u^1 \frac{dv}{v} \\ \times F(n) \pi r_s^2(us, n, M_*) \\ \left(\frac{1}{9} \sum_{i,j=q,\bar{q}} f_i(v,Q) f_{\bar{j}}(u/v,Q) + \frac{1}{64} f_g(v,Q) f_g(u/v,Q) \right) \end{aligned} \tag{5.5}$$

where i and j run over all the quarks and anti-quarks subject to the constraint of QED charge neutrality. f_q, f_g are the quark and gluon parton distribution functions, respectively. Additionally, weights according to the spin and gauge number of the partons have been included. For the production of a specific member (i.e., with specified color) of the octet QBH_8^0, one finds the same expression.

It follows a detailed presentation of the branching ratio determination, the listing of the different percentages per explicit QBH, and the application of these on the cross section for a selection of interesting signals.

5.3 Decay of QBHs with a continuous mass spectrum

Little is known about quantum gravity and in particular which symmetry is conserved by quantum gravitational interactions. Thus, one is led to make different assumptions on the type of processes which are allowed by these interactions. Five different models corresponding to different assumptions about which symmetry is conserved or violated by quantum gravity are used to determine the decay branching ratios. Note that the term branching ratio may be misleading as it is not used in its usual sense, i.e. to describe the probability of the decay of a specific particle in a specific mode, but rather to describe the decomposition of a collection of black holes created by the same specific initial states into a specific mode. For all models, Lorentz symmetry is assumed to be conserved and each model takes the full range of Standard Model particles as possible decay products into account. Neutrinos are considered to be Dirac particles which can be both left and right handed. In case of the Higgs boson, we assume that three of the four degrees of freedom merge with the degrees of freedom of the W and Z bosons. The models also allow massless gravitons as possible decay products. Furthermore, the following restrictions on the symmetries for the different models have been considered, respectively:

1. Lepton flavor, quark flavor, B-L and Lorentz invariance conserved,
2. lepton flavor violated, everything else conserved,
3. quark flavor violated, everything else conserved,
4. quark and lepton flavor violated, B-L conserved,
5. and everything violated except Lorentz invariance.

These models cover a multitude of possible global gauge symmetry violations and conservations, with lepton and quark flavor as well as the difference between baryon (B) and lepton (L) number violation not only being potential candidates but also detectable in particle collisions. The classification of QBHs and the assumption that such objects decay into two-particle states allows for a prediction of possible decay products. To determine the number of possible states, one has to consider the color multiplets and spin factors. Due to the high center-of-mass energies, all initial particles are considered to be massless. Using Clebsch-Gordan-coefficients[80][2], one finds that in a collision of two fundamental fermions, which each carry spin 1/2, the created spin-1 state is three times more likely to form than the possible spin-0 state. If a massless vector-boson, carrying spin 1, collides

[2]In review: “Clebsch-Gordan coefficients, spherical harmonics, and d functions”.

with a fundamental fermion, the spin-1/2 state is just half as likely to form compared to the spin-3/2 state. For two gluons, the spin state ratio for the potential spin-0, spin-1 and spin-2 states is 2:3:7. All spin factors are displayed in Table 5.1.

	0	1/2	1
0	0	1/2	1
1/2		0 , 1 1 : 3	1/2 , 3/2 1 : 2
1			0 , 1 , 2 2 : 3 : 7

Table 5.1: *Spin factors for massless particles, determined by Clebsch-Gordan-coefficients [80][4]. Due to considering the gluon to be massless, it cannot carry a magnetization of* $m = 0$*, which yields to the modified numbers. The numbers for the fermion - fermion collision remain the same as stated in the review.*

5.3.1 Branching Ratios of QBHs

In case of a black hole created by two up-quarks and with an incidental $\mathrm{U}(1)_{\mathrm{em}}$ charge of 4/3 (see i.e. Table 5.2), the color factors give $3 \times 3 = 6 + \overline{3}$ for the color states when decaying into two up quarks. This has to be weighted by the spin factors. Since both states, spin-0 as well as spin-1, are possible, one has to multiply the amount of states with the sum of both spin factors:

$$\mathbf{QBH}(\mathbf{u}, \mathbf{u}, \mathbf{4/3}) \to \mathbf{u} + \mathbf{u}: \quad (6+3) \times (1+3) \quad . \tag{5.6}$$

In case of the first two models in which quark flavor is conserved, a quantum black hole can only decay into the quarks with the initial flavor. For all other models all up-type quarks are weighted in the same way. For the models which allow quark and lepton flavor violation, one obtains for instance:

$$\mathbf{QBH}(\mathbf{u}, \mathbf{u}, \mathbf{4/3}) \to \mathbf{l}^{+} + \bar{\mathbf{d}}: \quad (3) \times (1+3)\,. \tag{5.7}$$

By following the same methods and considering the total number of final states, one finds the branching ratios to be the quotient of the number of desired final states divided by the total number of final states. The index “initial” indicates the flavor of the colliding particle, whereas “else” sums over all other type-like particles except the initial one. The

[4] In review: “Clebsch-Gordan coefficients, spherical harmonics, and d functions”.

indices “i” and “j” are used to distinguish between particles of the same flavor and different flavor, i.e. i $\neq$ j. Note that some of the models overlap with those considered in [81]. The branching ratios for all possible QBH classifications are given in table 5.2 to 5.9, in which the integer “0” indicates that the final state is forbidden in that particular model. The first two columns show the particles in the final state. We will explain the notation of the final states using the example of table 5.2, which displays the branching ratios for a QBH produced by two up-type quarks, in the following. The possible final states are two up-type quarks u or an antilepton l^+ and an antidown-type quark $\bar{d}$. In case of models that conserve the quark flavor, it is necessary to distinguish between the initial quark flavor of the quarks producing the QBH and all the other flavors. This is done by using the subscripts “initial” and “else”. Assuming e.g. two and charm-quarks creating a QBH, the final state quarks u_{initial} will have to be charm quarks as well.
The application of the branching ratios to the antiparticle case, respectively, is straightforward and will therefore not be displayed here.

Final state		Branching Ratios [%]				
Particle 1	Particle 2	Model 1	Model 2	Model 3	Model 4	Model 5
u_{initial}	u_{initial}	100	100	16.67	11.11	11.11
u_{else}	u_{else}	0	0	83.33	55.56	55.56
l^+	$\bar{d}$	0	0	0	33.33	33.33

Table 5.2: **QBH(u , u , 4/3)**: *Branching ratios of the decay channels of QBHs created by two up-type quarks (u). “initial” indicates the flavor of the incoming particles, “else” all other up-type quark flavors. l^+ describes an anti-lepton of any generation, $\bar{d}$ an anti-down-type quark.*

Final state		Branching Ratios [%]				
Particle 1	Particle 2	Model 1	Model 2	Model 3	Model 4	Model 5
d_{initial}	d_{initial}	100	100	16.67	8.33	6.67
d_{else}	d_{else}	0	0	83.33	41.67	33.33
l^-	$\bar{d}$	0	0	0	25	20
$\bar{u}$	ν	0	0	0	0	20
$\bar{u}$	$\bar{\nu}$	0	0	0	25	20

Table 5.3: **QBH(d , d , $-2/3$)**: *Branching ratios of the decay channels of QBHs created by two down-type quarks (d). "initial" indicates the flavor of the incoming particles, "else" all other down-type quark flavors. l^- describes a lepton of any generation, $\bar{u}$ an anti-up-type quark, and $\overset{(-)}{\nu}$ an (anti)neutrino.*

Final state		Branching Ratios [%]				
Particle 1	Particle 2	Model 1	Model 2	Model 3	Model 4	Model 5
u_{initial}	$\bar{d}_{\text{initial}}$	100	100	9.42	8.87	8.14
u_{else}	$\bar{d}_{\text{else}}$	0	0	75.39	70.94	65.16
l_{i}^+	ν_{i}	0	0	3.14	2.96	2.71
l_{i}^+	ν_{j}	0	0	0	5.91	5.43
l^+	$\bar{\nu}$	0	0	0	0	8.14
W^+	g	0	0	8.38	7.88	7.24
W^+	γ	0	0	1.05	0.99	0.9
W^+	Z^0	0	0	1.05	0.99	0.9
W^+	H	0	0	0.79	0.74	0.68
W^+	G	0	0	0.79	0.74	0.68

Table 5.4: **QBH(u , $\bar{d}$, 1)**: *Branching ratios of the decay channels of QBHs created by an up- (u) and an anti-down-type quark ($\bar{d}$). "initial" indicates the flavor of the incoming particles, "else" all other (anti)quark flavors. i and j distinguish between particles of different flavors and generations, i.e. $i \neq j$. l^+ describes an anti-lepton of any generation, $\overset{(-)}{\nu}$ an (anti)neutrino.*

Final state		Branching Ratios [%]				
Particle 1	Particle 2	Model 1	Model 2	Model 3	Model 4	Model 5
u_{initial}	d_{initial}	100	100	11.1	6.67	5.56
u_{else}	d_{else}	0	0	88.89	53.33	44.44
l^+	$\bar{u}$	0	0	0	20	16.67
$\bar{d}$	ν	0	0	0	0	16.67
$\bar{d}$	$\bar{\nu}$	0	0	0	20	16.67

Table 5.5: **QBH(**u **,** d **,** $1/3$**)**: *Branching ratios of the decay channels of QBHs created by an up- (u) and down-type quark (d). "initial" indicates the flavor of the incoming particles, "else" all other quark flavors.* l^+ *describes an anti-lepton of any generation,* $\overset{(-)}{\nu}$ *an (anti)neutrino.*

Final state		Branching Ratios [%]				
Particle 1	Particle 2	Model 1	Model 2	Model 3	Model 4	Model 5
u_{initial}	g	72.73	72.73	22.22	22.22	22.22
u_{initial}	γ	9.09	9.09	2.78	2.78	2.78
u_{initial}	Z^0	9.09	9.09	2.78	2.78	2.78
u_{initial}	H	3.03	3.03	0.93	0.93	0.93
u_{initial}	G	6.06	6.06	1.85	1.85	1.85
u_{else}	g	0	0	44.44	44.44	44.44
u_{else}	γ	0	0	5.56	5.56	5.56
u_{else}	Z^0	0	0	5.56	5.56	5.56
u_{else}	H	0	0	1.85	1.85	1.85
u_{else}	G	0	0	3.70	3.70	3.70
d	W^+	0	0	8.33	8.33	8.33

Table 5.6: **QBH(**u **,** g **,** $2/3$**)**: *Branching ratios of the decay channels of QBHs created by an up-type quark (u) and a gluon (g). "initial" indicates the flavor of the incoming particles, "else" all other (anti)quark flavors. d describes a down-type quark.*

Final state		Branching Ratios [%]				
Particle 1	Particle 2	Model 1	Model 2	Model 3	Model 4	Model 5
u_i	$\bar{u}_\mathrm{i}$	29.43	23.33	13.52	12.75	12.07
u_i	$\bar{u}_\mathrm{j}$	0	0	27.03	25.50	24.13
d_i	$\bar{d}_\mathrm{i}$	29.43	23.33	13.52	12.75	12.07
d_i	$\bar{d}_\mathrm{j}$	0	0	27.03	25.50	24.13
l_i^-	l_i^+	3.27	2.59	1.50	1.42	1.34
l_i^-	l_j^+	0	5.18	0	2.83	2.68
ν	ν	0	5.18	0	0	2.68
ν_i	$\bar{\nu}_\mathrm{i}$	3.27	2.59	1.50	1.42	1.34
ν_i	$\bar{\nu}_\mathrm{j}$	0	5.18	0	2.83	2.68
$\bar{\nu}$	$\bar{\nu}$	0	5.18	0	0	2.68
g	g	2.45	1.94	1.13	1.06	1.01
g	γ	2.18	1.73	1.00	0.94	0.89
g	Z^0	8.72	6.91	4.01	3.78	3.58
g	H	6.54	5.18	3.00	2.83	2.68
g	G	6.54	5.18	3.00	2.83	2.68
γ	γ	0.27	0.22	0.13	0.12	0.11
γ	Z^0	1.09	0.86	0.50	0.47	0.45
γ	H	0.82	0.65	0.38	0.35	0.34
γ	G	0.82	0.65	0.38	0.35	0.34
Z^0	Z^0	1.09	0.86	0.50	0.47	0.45
Z^0	H	0.82	0.65	0.38	0.35	0.34
Z^0	G	0.82	0.65	0.38	0.35	0.34
H	H	0.27	0.22	0.13	0.12	0.11
G	G	1.09	0.86	0.50	0.47	0.45
W^-	W^+	1.09	0.86	0.50	0.47	0.45

Table 5.7: **QBH(q_i , $\bar{q}_\mathrm{i}$, 0)**: *Branching ratios of the decay channels of QBHs created by a quark-anti-quark pair of the same flavor. "initial" indicates the flavor of the incoming particles, "else" all other (anti)quark flavors. i and j distinguish between particles of different flavors and generations, i.e. $i \neq j$. (l^+) l^- describes an (anti)lepton of any generation, $\overset{(-)}{\nu}$ an (anti)neutrino, d a down-type quark, and u an up-type quark.*

Final state		Branching Ratios [%]				
Particle 1	Particle 2	Model 1	Model 2	Model 3	Model 4	Model 5
q_{initial}	$\bar{q}_{\text{initial}}$	100.00	100.00	4.51	4.25	4.02
q_{else}	$\bar{q}_{\text{else}}$	0	0	76.60	72.26	68.38
l_{i}^{-}	l_{i}^{+}	0	0	1.50	1.42	1.34
l_{i}^{-}	l_{j}^{+}	0	0	0	2.83	2.68
ν	ν	0	0	0	0	2.68
ν_{i}	$\bar{\nu}_{\text{i}}$	0	0	1.50	1.42	1.34
ν_{i}	$\bar{\nu}_{\text{j}}$	0	0	0	2.83	2.68
$\bar{\nu}$	$\bar{\nu}$	0	0	0	0	2.68
g	g	0	0	1.13	1.06	1.01
g	γ	0	0	1.00	0.94	0.89
g	Z^0	0	0	4.01	3.78	3.58
g	H	0	0	3.00	2.83	2.68
g	G	0	0	3.00	2.83	2.68
γ	γ	0	0	0.13	0.12	0.11
γ	Z^0	0	0	0.50	0.47	0.45
γ	H	0	0	0.38	0.35	0.34
γ	G	0	0	0.38	0.35	0.34
Z^0	Z^0	0	0	0.50	0.47	0.45
Z^0	H	0	0	0.38	0.35	0.34
Z^0	G	0	0	0.38	0.35	0.34
H	H	0	0	0.13	0.12	0.11
G	G	0	0	0.50	0.47	0.45
W^-	W^+	0	0	0.50	0.47	0.45

Table 5.8: **QBH(q_{i} , $\bar{q}_{\text{j}}$, 0)**: *Branching ratios of the decay channels of QBHs created by a quark-anti-quark pair of different flavor. "initial" indicates the flavor of the incoming particles, "else" all other (anti)quark flavors. i and j distinguish between particles of different flavors and generations, i.e. $i \neq j$. (l^+) l^- describes an (anti)lepton of any generation, $\overset{(-)}{\nu}$ an (anti)neutrino, d a down-type quark, and u an up-type quark.*

Final state		Branching Ratios [%]				
Particle 1	Particle 2	Model 1	Model 2	Model 3	Model 4	Model 5
q_i	$\bar{q}_i$	17.65	17.16	13.17	12.97	12.77
q_i	$\bar{q}_j$	0	0	26.34	25.94	25.55
l_i^-	l_i^+	1.04	0.50	0.39	0.38	0.38
l_i^-	l_j^+	0	1.01	0	0.76	0.75
ν	ν	0	0.84	0	0	0.63
ν_i	$\bar{\nu}_i$	1.30	0.50	0.39	0.38	0.38
ν_i	$\bar{\nu}_j$	0	1.01	0	0.76	0.75
$\bar{\nu}$	$\bar{\nu}$	0	1.01	0	0	0.75
g	g	49.83	48.44	37.19	36.62	36.07
g	γ	12.46	12.11	9.30	9.15	9.02
g	Z^0	12.46	12.11	9.30	9.15	9.02
γ	γ	0.78	0.76	0.58	0.57	0.56
γ	Z^0	0.78	0.76	0.58	0.57	0.56
Z^0	Z^0	0.78	0.76	0.58	0.57	0.56
Z^0	H	0	0	0	0	0
Z^0	G	0.61	0.59	0.45	0.45	0.44
H	G	0.17	0.17	0.13	0.13	0.13
H	H	0.61	0.59	0.45	0.45	0.44
G	G	0.78	0.76	0.58	0.57	0.56
W^-	W^+	0.78	0.76	0.58	0.57	0.56

Table 5.9: **QBH(g, g , 0)**: *Branching ratios of the decay channels of QBHs created by two gluons. "initial" indicates the flavor of the incoming particles, "else" all other (anti)quark flavors. i and j distinguish between particles of different flavors and generations, i.e. $i \neq j$. (l^+) l^- describes an (anti)lepton of any generation, $\overset{(-)}{\nu}$ an (anti)neutrino, d a down-type quark, and u an up-type quark.*

5.3.2 Total cross sections of continuous QBH processes

Using a Monte Carlo integration algorithm [82], the total cross section, as described in eq. (5.1), was determined for several center of mass energies as well as different Planck masses. We used the Vegas integration algorithm which is part of the CUBA library for multidimensional integration [83]. CUBA is written in C[5] and includes four independent algorithms: Vegas, Suave, Divonne, and Cuhre. Vegas uses importance sampling for variance reduction, and as every algorithm in CUBA can only solve Riemann integrals of the form:

$$\int_0^1 \mathrm{d}^d x \, f(\vec{x}) \tag{5.8}$$

with $f(\vec{x})$ being a function or subroutine that can be sampled at any point in $\vec{x}_i \in [0,1]^d$. This restriction is not serious because most integrands can be transformed to a unit cube. We use a relative accuracy of $\epsilon_{rel} = 0.001$ for the Monte Carlo method which is negligible compared to the errors due to e.g. PDF choices which we found, however, have no effect on the order of magnitude of the cross section. We used the CTEQ6 PDF set [84] which was initialized via the Les Houches accord PDFs (LHAPDF) interface [85], which gives access to various sets of PDFs. CTEQ is one of the multi-institutional collaborations that test the accuracy of QCD and extracts universal PDFs, see section 3.2.2 for more detail on PDFs. The choice of momentum scale of the PDFs gives an error of up to 20%, depending on the number of extra dimensions, center of mass energy, and the size of the Planck scale. It should be noted, however, that we do not perform an effective fit in field theory in the common sense to describe QBHs but use an effective way to describe the extrapolation of semi-classical BHs. As described in chapter 4, we match the amplitude with the semi-classical cross section and higher-dimensional operators would merely change the function to be matched but not affect the precision of the cross section. Understanding the quantum gravitational regime is still one of the biggest challenges of contemporary physics. To quantify an exact reach of the LHC, a dedicated background study and detector simulations are needed, which goes beyond the scope of this thesis.
Since inelasticity effects are extracted from classical physics and do not necessarily apply in the quantum regime, we assumed no inelasticity effects in the displayed results, i.e. the inelasticity function $y(z) = 1$ as well as the form factors $F(n) = 1$ and do thus not affect the cross section, see section 3.2.2. However, this is an assumption we made regarding the nature of the QBHs and the inelasticity effects by Yoshino and Rychkov [61] can likewise be applied in the numerical determination.

[5] CUBA has a C/C++ interface.

The results for center of mass energies $\sqrt{s} = 7$ to 14 TeV and a fundamental Planck mass M_* ranging from 1 to 5 TeV are displayed in tables 5.10 and 5.11. The shown results are for models with $n = 5, 6, 7$ large extra dimensions (ADD), the Randall-Sundrum (RS) warped extra dimension, and the four-dimensional model described in section 2.2. Although, the neutral QBH_1^0 decays invisibly into the hidden sector in the four-dimensional model, most QBHs created in collisions of quarks and gluons carry a QCD or U(1) charge and their decay into SM particles will not be suppressed, see also [17]. We chose not to display the results for $n = 1, 2, 3,$ and 4 for clarity and because of the tight experimental exclusion bounds on these models.

total σ	Model for low scale quantum gravity				
(in fb)	4 dim[4]	ADD n = 5	ADD n = 6	ADD n = 7	RS
center of mass of $\sqrt{s} = 7\,\text{TeV}$					
$M_* = 1\,\text{TeV}$	3.95×10^{4}	1.60×10^{7}	2.13×10^{7}	2.70×10^{7}	9.34×10^{5}
$M_* = 2\,\text{TeV}$	3.41×10^{2}	1.78×10^{5}	2.39×10^{5}	3.03×10^{5}	9.54×10^{3}
$M_* = 3\,\text{TeV}$	6.40	3.77×10^{3}	5.07×10^{3}	6.46×10^{3}	1.93×10^{2}
$M_* = 4\,\text{TeV}$	9.51×10^{-2}	6.00×10^{1}	8.08×10^{1}	1.03×10^{2}	3.00
$M_* = 5\,\text{TeV}$	5.28×10^{-4}	3.48×10^{-1}	4.70×10^{-1}	5.99×10^{-1}	1.71×10^{-2}
center of mass of $\sqrt{s} = 8\,\text{TeV}$					
$M_* = 1\,\text{TeV}$	6.45×10^{4}	2.49×10^{7}	3.31×10^{7}	4.18×10^{7}	1.47×10^{6}
$M_* = 2\,\text{TeV}$	7.27×10^{2}	3.63×10^{5}	4.87×10^{5}	6.18×10^{5}	1.98×10^{4}
$M_* = 3\,\text{TeV}$	2.09×10^{1}	1.19×10^{4}	1.60×10^{4}	2.03×10^{4}	6.18×10^{2}
$M_* = 4\,\text{TeV}$	6.19×10^{-1}	3.79×10^{2}	5.10×10^{2}	6.50×10^{2}	1.92×10^{1}
$M_* = 5\,\text{TeV}$	1.18×10^{-2}	7.59	1.02×10^{1}	1.30×10^{1}	3.76×10^{-1}
center of mass of $\sqrt{s} = 9\text{TeV}$					
$M_* = 1\,\text{TeV}$	9.76×10^{4}	3.59×10^{7}	4.78×10^{7}	6.04×10^{7}	2.16×10^{6}
$M_* = 2\,\text{TeV}$	1.33×10^{3}	6.37×10^{5}	8.53×10^{5}	1.08×10^{6}	3.52×10^{4}
$M_* = 3\,\text{TeV}$	5.11×10^{1}	2.81×10^{4}	3.77×10^{4}	4.79×10^{4}	1.48×10^{3}
$M_* = 4\,\text{TeV}$	2.34	1.39×10^{3}	1.87×10^{3}	2.38×10^{3}	7.10×10^{1}
$M_* = 5\,\text{TeV}$	8.84×10^{-2}	5.55×10^{1}	7.47×10^{1}	9.52×10^{1}	2.78
center of mass of $\sqrt{s} = 10\text{TeV}$					
$M_* = 1\,\text{TeV}$	1.39×10^{5}	4.93×10^{7}	6.56×10^{7}	8.28×10^{7}	3.00×10^{6}
$M_* = 2\,\text{TeV}$	2.18×10^{3}	1.01×10^{6}	1.35×10^{6}	1.71×10^{6}	5.64×10^{4}
$M_* = 3\,\text{TeV}$	1.03×10^{2}	5.50×10^{4}	7.38×10^{4}	9.37×10^{4}	2.93×10^{3}
$M_* = 4\,\text{TeV}$	6.38	3.70×10^{3}	4.97×10^{3}	6.32×10^{3}	1.91×10^{2}
$M_* = 5\,\text{TeV}$	3.74×10^{-1}	2.29×10^{2}	3.08×10^{2}	3.93×10^{2}	1.16×10^{1}

Table 5.10: *Total cross sections for the production of QBHs with a continuous mass spectrum and for different low-scale gravity models. The center of mass energies range from $\sqrt{s} = 7$ to 10 TeV with considered fundamental Planck masses of $M_* = 1$ to 5 TeV each.*

total σ	Model for low scale quantum gravity				
(in fb)	4 dim[4]	ADD n = 5	ADD n = 6	ADD n = 7	RS
center of mass of $\sqrt{s} = 11\,\text{TeV}$					
$M_* = 1\,\text{TeV}$	1.91×10^{5}	6.51×10^{7}	8.64×10^{7}	1.09×10^{8}	4.01×10^{6}
$M_* = 2\,\text{TeV}$	3.33×10^{3}	1.49×10^{6}	1.99×10^{6}	2.52×10^{6}	8.42×10^{4}
$M_* = 3\,\text{TeV}$	1.84×10^{2}	9.51×10^{4}	1.27×10^{5}	1.62×10^{5}	5.12×10^{3}
$M_* = 4\,\text{TeV}$	1.41×10^{1}	7.97×10^{3}	1.07×10^{4}	1.36×10^{4}	4.15×10^{2}
$M_* = 5\,\text{TeV}$	1.12	6.71×10^{2}	9.03×10^{2}	1.15×10^{3}	3.42×10^{1}
center of mass of $\sqrt{s} = 12\,\text{TeV}$					
$M_* = 1\,\text{TeV}$	2.52×10^{5}	8.32×10^{7}	1.10×10^{8}	1.39×10^{8}	5.17×10^{6}
$M_* = 2\,\text{TeV}$	4.81×10^{3}	2.08×10^{6}	2.77×10^{6}	3.51×10^{6}	1.19×10^{5}
$M_* = 3\,\text{TeV}$	3.00×10^{2}	1.50×10^{5}	2.01×10^{5}	2.55×10^{5}	8.17×10^{3}
$M_* = 4\,\text{TeV}$	2.71×10^{1}	1.49×10^{4}	2.00×10^{4}	2.54×10^{4}	7.83×10^{2}
$M_* = 5\,\text{TeV}$	2.68	1.57×10^{3}	2.11×10^{3}	2.68×10^{3}	8.05×10^{1}
center of mass of $\sqrt{s} = 13\,\text{TeV}$					
$M_* = 1\,\text{TeV}$	3.23×10^{5}	1.04×10^{8}	1.38×10^{8}	1.74×10^{8}	6.50×10^{6}
$M_* = 2\,\text{TeV}$	6.64×10^{3}	2.79×10^{6}	3.72×10^{6}	4.71×10^{6}	1.61×10^{5}
$M_* = 3\,\text{TeV}$	4.55×10^{2}	2.22×10^{5}	2.97×10^{5}	3.77×10^{5}	1.22×10^{4}
$M_* = 4\,\text{TeV}$	4.67×10^{1}	2.51×10^{4}	3.36×10^{4}	4.28×10^{4}	1.33×10^{3}
$M_* = 5\,\text{TeV}$	5.46	3.13×10^{3}	4.21×10^{3}	5.35×10^{3}	1.62×10^{2}
center of mass of $\sqrt{s} = 14\,\text{TeV}$					
$M_* = 1\,\text{TeV}$	4.06×10^{5}	1.27×10^{8}	1.68×10^{8}	2.12×10^{8}	8.00×10^{6}
$M_* = 2\,\text{TeV}$	8.86×10^{3}	3.62×10^{6}	4.82×10^{6}	6.10×10^{6}	2.11×10^{5}
$M_* = 3\,\text{TeV}$	6.56×10^{2}	3.12×10^{5}	4.17×10^{5}	5.29×10^{5}	1.73×10^{4}
$M_* = 4\,\text{TeV}$	7.45×10^{1}	3.91×10^{4}	5.24×10^{4}	6.66×10^{4}	2.09×10^{3}
$M_* = 5\,\text{TeV}$	9.93	5.58×10^{3}	7.49×10^{3}	9.53×10^{3}	2.91×10^{2}

Table 5.11: *Total cross sections for the production of QBHs with a continuous mass spectrum and for different low-scale gravity models. The center of mass energies range from $\sqrt{s} = 11$ to 14 TeV with considered fundamental Planck masses of $M_* = 1$ to 5 TeV each.*

As predicted, the total cross sections increase with the center of mass energy of the incoming particles and with the number of extra dimensions. The higher the fundamental Planck scale, the lower the resulting cross section due to the lower threshold and thus a larger lower bound for the momentum fraction. The drastic decrease is caused by the rapid decrease of the parton distribution functions with rise of momentum, see appendix B.

5.3.3 Specific cross sections for continuous QBHs

The cross section for a specific final state, e.g. QBH $\rightarrow \gamma + \gamma$, is obtained by summing over the production cross sections of the contributing QBHs, which have been multiplied with the desired branching ratio (cf. Table (5.2) to (5.9)):

$$\sigma_{\text{QBH}\rightarrow\text{final state}} = \sum_{\substack{\text{average}\\ \text{initial states}}} \sigma_{\text{initial state}\rightarrow\text{QBH}} \times \text{BR}_{\text{final state,model}} \,. \tag{5.9}$$

In the case of two photon production, the relevant initial states are a quark-anti-quark pair and two gluons, since the produced QBH must be color neutral. There are non-negligible cross sections for all five symmetry models. We sum up the relevant contributions to the cross section and multiply the result with the suitable branching ratios (in this case table 5.7, 5.8, and 5.9). The desired cross section for the chosen final state is given by taking the average over all initial state contributions, see table 5.12 to 5.16 for a listing of calculated cross sections of the two-photon final state. For all final states, we consider the center of mass energies $\sqrt{s} = 7, 8,$ and 14TeV with a Planck mass of $M_* = 1$ to 5 TeV, respectively. The following five low-scale gravity models are adopted: the four-dimensional case, $n = 5, 6, 7$ large extra dimensions, and the warped dimension model.

The results for a QBH decaying into an electron and positron are displayed in table 5.17 to 5.21. As in the case of a two-photon final state, this final state is possible for every considered symmetry model and the QBH cannot carry either color nor QED charge. One thus finds the same initial states as for two-photon decay but with different likelihoods. For the much more exotic signal of a final state containing an electron and antimuon, one finds that the lepton flavor violating process is forbidden in model 1 (conserving all symmetries) and model 3 (allowing only quark flavor violation but not lepton flavor). In the remaining models, the leptons are treated democratically by the quantum gravity, which thus yields to an identical branching ratio to the electron-positron final state.

Table 5.22 and 5.23 depict the cross sections for the creation of an electron and up-quark in model 4 (B-L symmetry conserved, everything but Lorentz invariance can be violated) and model 5 (everything but Lorentz invariance violated), respectively. The QBH from which it decays carries a QED charge of $q = -\frac{1}{3}$, and is, according to Lorentz invariance, restricted to the initial state of an antiup- and antidown-quark. This final state violates both quark and lepton flavor, thus being permitted in the first three models. The same is applicable for the decay into an antimuon and down-quark which is presented in 5.24 and 5.25. In the latter case, the black hole has a charge of $q = \frac{2}{3}$ and can only be produced by two antidown-quarks.

cross section in fb	Model for low scale quantum gravity				
σ (QBH $\to \gamma + \gamma$)	4 dim[4]	ADD n = 5	ADD n = 6	ADD n = 7	RS
CoM energy of $\sqrt{s} = 7$TeV					
$M_* = 1$TeV	3.50×10^{-1}	1.57×10^{2}	2.10×10^{2}	2.66×10^{2}	8.86
$M_* = 3$TeV	1.50×10^{-5}	9.08×10^{-3}	1.22×10^{-2}	1.56×10^{-2}	4.60×10^{-4}
$M_* = 5$TeV	2.99×10^{-10}	1.98×10^{-7}	2.67×10^{-7}	3.41×10^{-7}	9.71×10^{-9}
CoM energy of $\sqrt{s} = 8$TeV					
$M_* = 1$TeV	6.17×10^{-1}	2.64×10^{2}	3.52×10^{2}	4.46×10^{2}	1.51×10^{1}
$M_* = 3$TeV	6.32×10^{-5}	3.73×10^{-2}	5.01×10^{-2}	6.38×10^{-2}	1.91×10^{-3}
$M_* = 5$TeV	9.94×10^{-9}	6.45×10^{-6}	8.70×10^{-6}	1.11×10^{-5}	3.19×10^{-7}
CoM energy of $\sqrt{s} = 14$TeV					
$M_* = 1$TeV	4.71	1.64×10^{3}	2.17×10^{3}	2.75×10^{3}	1.00×10^{2}
$M_* = 3$TeV	4.20×10^{-3}	2.15	2.88	3.66	1.16×10^{-1}
$M_* = 5$TeV	3.25×10^{-5}	1.90×10^{-2}	2.55×10^{-2}	3.24×10^{-2}	9.75×10^{-4}

Table 5.12: *Cross sections for QBHs decaying into two photons with lepton as well as quark flavor, B-L and Lorentz invariance conserved (model 1). Suitable initial states for such a process are a quark and antiquark as well as two gluons.*

cross section in fb	Model for low scale quantum gravity				
σ (QBH $\to \gamma + \gamma$)	4 dim[4]	ADD n = 5	ADD n = 6	ADD n = 7	RS
CoM energy of $\sqrt{s} = 7$TeV					
$M_* = 1$TeV	2.93×10^{-1}	1.32×10^{2}	1.76×10^{2}	2.23×10^{2}	7.42
$M_* = 3$TeV	1.23×10^{-5}	7.47×10^{-3}	1.01×10^{-2}	1.28×10^{-2}	3.79×10^{-4}
$M_* = 5$TeV	2.45×10^{-10}	1.62×10^{-7}	2.19×10^{-7}	2.79×10^{-7}	7.96×10^{-9}
CoM energy of $\sqrt{s} = 8$TeV					
$M_* = 1$TeV	5.17×10^{-1}	2.22×10^{2}	2.96×10^{2}	3.75×10^{2}	1.27×10^{1}
$M_* = 3$TeV	5.20×10^{-5}	3.07×10^{-2}	4.13×10^{-2}	5.25×10^{-2}	1.57×10^{-3}
$M_* = 5$TeV	8.16×10^{-9}	5.30×10^{-6}	7.14×10^{-6}	9.11×10^{-6}	2.62×10^{-7}
CoM energy of $\sqrt{s} = 14$TeV					
$M_* = 1$TeV	4.00	1.40×10^{3}	1.86×10^{3}	2.34×10^{3}	8.53×10^{1}
$M_* = 3$TeV	3.48×10^{-3}	1.78	2.39	3.03	9.62×10^{-2}
$M_* = 5$TeV	2.67×10^{-5}	1.56×10^{-2}	2.10×10^{-2}	2.67×10^{-2}	8.03×10^{-4}

Table 5.13: *Cross sections for QBHs decaying into two photons with lepton flavor violated but quark flavor, B-L and Lorentz invariance conserved (model 2). Suitable initial states for such a process are a quark and antiquark as well as two gluons.*

cross section in fb	Model for low scale quantum gravity				
σ (QBH $\rightarrow \gamma + \gamma$)	4 dim[4]	ADD n = 5	ADD n = 6	ADD n = 7	RS
CoM energy of $\sqrt{s} = 7$TeV					
$M_* = 1$TeV	2.63×10^{-1}	1.18×10^{2}	1.58×10^{2}	2.00×10^{2}	6.67
$M_* = 3$TeV	1.13×10^{-5}	6.84×10^{-3}	9.21×10^{-3}	1.17×10^{-2}	3.47×10^{-4}
$M_* = 5$TeV	2.81×10^{-10}	1.86×10^{-7}	2.51×10^{-7}	3.20×10^{-7}	9.13×10^{-9}
CoM energy of $\sqrt{s} = 8$TeV					
$M_* = 1$TeV	4.66×10^{-1}	2.01×10^{2}	2.68×10^{2}	3.39×10^{2}	1.15×10^{1}
$M_* = 3$TeV	4.70×10^{-5}	2.77×10^{-2}	3.72×10^{-2}	4.74×10^{-2}	1.42×10^{-3}
$M_* = 5$TeV	8.68×10^{-9}	5.63×10^{-6}	7.59×10^{-6}	9.68×10^{-6}	2.78×10^{-7}
CoM energy of $\sqrt{s} = 14$TeV					
$M_* = 1$TeV	3.65	1.28×10^{3}	1.71×10^{3}	2.16×10^{3}	7.83×10^{1}
$M_* = 3$TeV	3.14×10^{-3}	1.61	2.15	2.73	8.66×10^{-2}
$M_* = 5$TeV	2.42×10^{-5}	1.41×10^{-2}	1.90×10^{-2}	2.41×10^{-2}	7.26×10^{-4}

Table 5.14: *Cross sections for QBHs decaying into two photons with quark flavor violated, but lepton flavor, B-L and Lorentz invariance conserved (model 3). Suitable initial states for such a process are a quark and antiquark as well as two gluons.*

cross section in fb	Model for low scale quantum gravity				
σ (QBH $\rightarrow \gamma + \gamma$)	4 dim[4]	ADD n = 5	ADD n = 6	ADD n = 7	RS
CoM energy of $\sqrt{s} = 7$TeV					
$M_* = 1$TeV	2.50×10^{-1}	1.13×10^{2}	1.51×10^{2}	1.91×10^{2}	6.35
$M_* = 3$TeV	1.07×10^{-5}	6.49×10^{-3}	8.73×10^{-3}	1.11×10^{-2}	3.29×10^{-4}
$M_* = 5$TeV	2.66×10^{-10}	1.76×10^{-7}	2.38×10^{-7}	3.03×10^{-7}	8.65×10^{-9}
CoM energy of $\sqrt{s} = 8$TeV					
$M_* = 1$TeV	4.44×10^{-1}	1.91×10^{2}	2.55×10^{2}	3.23×10^{2}	1.09×10^{1}
$M_* = 3$TeV	4.46×10^{-5}	2.63×10^{-2}	3.53×10^{-2}	4.50×10^{-2}	1.35×10^{-3}
$M_* = 5$TeV	8.23×10^{-9}	5.34×10^{-6}	7.19×10^{-6}	9.17×10^{-6}	2.64×10^{-7}
CoM energy of $\sqrt{s} = 14$TeV					
$M_* = 1$TeV	3.49	1.23×10^{3}	1.63×10^{3}	2.06×10^{3}	7.48×10^{1}
$M_* = 3$TeV	2.98×10^{-3}	1.53	2.04	2.60	8.23×10^{-2}
$M_* = 5$TeV	2.30×10^{-5}	1.34×10^{-2}	1.80×10^{-2}	2.29×10^{-2}	6.89×10^{-4}

Table 5.15: *Cross sections for QBHs decaying into two photons with lepton and quark flavor violated, but B-L and Lorentz invariance conserved (model 4). Suitable initial states for such a process are a quark and antiquark as well as two gluons.*

cross section in fb	Model for low scale quantum gravity				
σ (QBH $\rightarrow \gamma + \gamma$)	4 dim[4]	ADD n = 5	ADD n = 6	ADD n = 7	RS
CoM energy of $\sqrt{s} = 7$TeV					
$M_* = 1$TeV	2.39×10^{-1}	1.08×10^{2}	1.44×10^{2}	1.82×10^{2}	6.06
$M_* = 3$TeV	1.02×10^{-5}	6.18×10^{-3}	8.31×10^{-3}	1.06×10^{-2}	3.13×10^{-4}
$M_* = 5$TeV	2.53×10^{-10}	1.68×10^{-7}	2.26×10^{-7}	2.88×10^{-7}	8.22×10^{-9}
CoM energy of $\sqrt{s} = 8$TeV					
$M_* = 1$TeV	4.24×10^{-1}	1.83×10^{2}	2.44×10^{2}	3.09×10^{2}	1.04×10^{1}
$M_* = 3$TeV	4.25×10^{-5}	2.50×10^{-2}	3.36×10^{-2}	4.28×10^{-2}	1.28×10^{-3}
$M_* = 5$TeV	7.83×10^{-9}	5.07×10^{-6}	6.84×10^{-6}	8.72×10^{-6}	2.51×10^{-7}
CoM energy of $\sqrt{s} = 14$TeV					
$M_* = 1$TeV	3.33	1.17×10^{3}	1.56×10^{3}	1.97×10^{3}	7.16×10^{1}
$M_* = 3$TeV	2.84×10^{-3}	1.45	1.95	2.47	7.84×10^{-2}
$M_* = 5$TeV	2.19×10^{-5}	1.27×10^{-2}	1.71×10^{-2}	2.18×10^{-2}	6.56×10^{-4}

Table 5.16: *Cross sections for QBHs decaying into two photons with lepton and quark flavor, as well as B-L violated and only Lorentz invariance conserved (model 5). Suitable initial states for such a process are a quark and antiquark as well as two gluons.*

cross section in fb	Model for low scale quantum gravity				
σ (QBH $\rightarrow e^+ + e^-$)	4 dim[4]	ADD n = 5	ADD n = 6	ADD n = 7	RS
CoM energy of $\sqrt{s} = 7$TeV					
$M_* = 1$TeV	3.14×10^{-1}	1.40×10^{2}	1.86×10^{2}	2.36×10^{2}	7.90
$M_* = 3$TeV	1.43×10^{-5}	8.71×10^{-3}	1.17×10^{-2}	1.49×10^{-2}	4.41×10^{-4}
$M_* = 5$TeV	2.91×10^{-10}	1.93×10^{-7}	2.60×10^{-7}	3.32×10^{-7}	9.46×10^{-9}
CoM energy of $\sqrt{s} = 8$TeV					
$M_* = 1$TeV	5.46×10^{-1}	2.31×10^{2}	3.09×10^{2}	3.91×10^{2}	1.33×10^{1}
$M_* = 3$TeV	6.04×10^{-5}	3.56×10^{-2}	4.78×10^{-2}	6.09×10^{-2}	1.82×10^{-3}
$M_* = 5$TeV	9.63×10^{-9}	6.25×10^{-6}	8.43×10^{-6}	1.08×10^{-5}	3.09×10^{-7}
CoM energy of $\sqrt{s} = 14$TeV					
$M_* = 1$TeV	3.94	1.33×10^{3}	1.77×10^{3}	2.23×10^{3}	8.23×10^{1}
$M_* = 3$TeV	3.91×10^{-3}	2.00	2.67	3.39	1.08×10^{-1}
$M_* = 5$TeV	3.11×10^{-5}	1.81×10^{-2}	2.44×10^{-2}	3.10×10^{-2}	9.33×10^{-4}

Table 5.17: *Cross sections for production of a QBH decaying into an electron and positron with lepton as well as quark flavor, B-L and Lorentz invariance conserved (model 1). Suitable initial states for such a process are a quark and antiquark as well as two gluons.*

cross section in fb	Model for low scale quantum gravity				
$\sigma\,(\mathrm{QBH} \to \mathrm{e}^+ + \mathrm{e}^-)$ or $\sigma\,(\mathrm{QBH} \to \mu^+ + \mathrm{e}^-)$	4 dim[4]	ADD n = 5	ADD n = 6	ADD n = 7	RS
CoM energy of $\sqrt{\mathrm{s}} = 7\mathrm{TeV}$					
$M_* = 1\mathrm{TeV}$	2.59×10^{-1}	1.15×10^{2}	1.54×10^{2}	1.95×10^{2}	6.52
$M_* = 3\mathrm{TeV}$	1.17×10^{-5}	7.12×10^{-3}	9.58×10^{-3}	1.22×10^{-2}	3.61×10^{-4}
$M_* = 5\mathrm{TeV}$	2.38×10^{-10}	1.58×10^{-7}	2.13×10^{-7}	2.71×10^{-7}	7.73×10^{-9}
CoM energy of $\sqrt{\mathrm{s}} = 8\mathrm{TeV}$					
$M_* = 1\mathrm{TeV}$	4.51×10^{-1}	1.91×10^{2}	2.55×10^{2}	3.23×10^{2}	1.10×10^{1}
$M_* = 3\mathrm{TeV}$	4.94×10^{-5}	2.91×10^{-2}	3.91×10^{-2}	4.98×10^{-2}	1.49×10^{-3}
$M_* = 5\mathrm{TeV}$	7.87×10^{-9}	5.11×10^{-6}	6.89×10^{-6}	8.78×10^{-6}	2.53×10^{-7}
CoM energy of $\sqrt{\mathrm{s}} = 14\mathrm{TeV}$					
$M_* = 1\mathrm{TeV}$	3.28	1.11×10^{3}	1.47×10^{3}	1.86×10^{3}	6.86×10^{1}
$M_* = 3\mathrm{TeV}$	3.21×10^{-3}	1.64	2.20	2.79	8.85×10^{-2}
$M_* = 5\mathrm{TeV}$	2.54×10^{-5}	1.48×10^{-2}	1.99×10^{-2}	2.54×10^{-2}	7.63×10^{-4}

Table 5.18: *Cross sections for QBHs decaying into an electron and positron, or alternatively into an electron and anti-muon, with lepton flavor violated, but quark flavor, B-L and Lorentz invariance conserved (model 2). The center of mass energies* $\sqrt{s} = 7, 8,$ *and* 14TeV *are considered with a Planck mass of* $M_* = 1 - 5\mathrm{TeV}$*, respectively. The following five low-scale gravity models are adopted: the four-dimensional case,* $n = 5, 6, 7$ *large extra dimensions, and the warped dimension model. Suitable initial states for such a process are a quark and antiquark as well as two gluons. The decay into an electron and anti-muon is forbidden in model 1 and 3. Due to the symmetry restrictions in models 2, 4 and 5 the cross sections of both cases are identical.*

cross section in fb	Model for low scale quantum gravity				
$\sigma\,(\mathrm{QBH} \to \mathrm{e}^+ + \mathrm{e}^-)$	4 dim[4]	ADD n = 5	ADD n = 6	ADD n = 7	RS
CoM energy of $\sqrt{\mathrm{s}} = 7\mathrm{TeV}$					
$M_* = 1\mathrm{TeV}$	2.40×10^{-1}	1.07×10^{2}	1.43×10^{2}	1.82×10^{2}	6.06
$M_* = 3\mathrm{TeV}$	1.09×10^{-5}	6.61×10^{-3}	8.89×10^{-3}	1.13×10^{-2}	3.35×10^{-4}
$M_* = 5\mathrm{TeV}$	2.76×10^{-10}	1.83×10^{-7}	2.47×10^{-7}	3.15×10^{-7}	8.97×10^{-9}
CoM energy of $\sqrt{\mathrm{s}} = 8\mathrm{TeV}$					
$M_* = 1\mathrm{TeV}$	4.21×10^{-1}	1.80×10^{2}	2.40×10^{2}	3.04×10^{2}	1.03×10^{1}
$M_* = 3\mathrm{TeV}$	4.53×10^{-5}	2.66×10^{-2}	3.58×10^{-2}	4.56×10^{-2}	1.37×10^{-3}
$M_* = 5\mathrm{TeV}$	8.49×10^{-9}	5.50×10^{-6}	7.42×10^{-6}	9.46×10^{-6}	2.72×10^{-7}
CoM energy of $\sqrt{\mathrm{s}} = 14\mathrm{TeV}$					
$M_* = 1\mathrm{TeV}$	3.16	1.09×10^{3}	1.45×10^{3}	1.83×10^{3}	6.70×10^{1}
$M_* = 3\mathrm{TeV}$	2.95×10^{-3}	1.51	2.02	2.57	8.14×10^{-2}
$M_* = 5\mathrm{TeV}$	2.33×10^{-5}	1.36×10^{-2}	1.83×10^{-2}	2.32×10^{-2}	7.00×10^{-4}

Table 5.19: *Cross sections for QBHs decaying into an electron and positron with quark flavor violated, but lepton flavor, B-L and Lorentz invariance conserved (model 3). The center of mass energies* $\sqrt{s} = 7, 8,$ *and* 14TeV *are considered with a Planck mass of* $M_* = 1 - 5\mathrm{TeV}$*, respectively. The following five low-scale gravity models are adopted: the four-dimensional case,* $n = 5, 6, 7$ *large extra dimensions, and the warped dimension model. Suitable initial states for such a process are a quark and antiquark as well as two gluons.*

cross section in fb	Model for low scale quantum gravity				
$\sigma\,(\mathrm{QBH} \to \mathrm{e}^+ + \mathrm{e}^-)$ or $\sigma\,(\mathrm{QBH} \to \mu^+ + \mathrm{e}^-)$	4 dim[4]	ADD n = 5	ADD n = 6	ADD n = 7	RS
CoM energy of $\sqrt{\mathrm{s}} = 7\mathrm{TeV}$					
$M_* = 1\mathrm{TeV}$	2.28×10^{-1}	1.02×10^{2}	1.36×10^{2}	1.72×10^{2}	5.75
$M_* = 3\mathrm{TeV}$	1.03×10^{-5}	6.26×10^{-3}	8.42×10^{-3}	1.07×10^{-2}	3.18×10^{-4}
$M_* = 5\mathrm{TeV}$	2.62×10^{-10}	1.73×10^{-7}	2.34×10^{-7}	2.98×10^{-7}	8.50×10^{-9}
CoM energy of $\sqrt{\mathrm{s}} = 8\mathrm{TeV}$					
$M_* = 1\mathrm{TeV}$	4.00×10^{-1}	1.71×10^{2}	2.28×10^{2}	2.89×10^{2}	9.80
$M_* = 3\mathrm{TeV}$	4.29×10^{-5}	2.52×10^{-2}	3.39×10^{-2}	4.32×10^{-2}	1.29×10^{-3}
$M_* = 5\mathrm{TeV}$	8.04×10^{-9}	5.21×10^{-6}	7.03×10^{-6}	8.96×10^{-6}	2.58×10^{-7}
CoM energy of $\sqrt{\mathrm{s}} = 14\mathrm{TeV}$					
$M_* = 1\mathrm{TeV}$	3.01	1.04×10^{3}	1.38×10^{3}	1.74×10^{3}	6.37×10^{1}
$M_* = 3\mathrm{TeV}$	2.80×10^{-3}	1.43	1.92	2.43	7.71×10^{-2}
$M_* = 5\mathrm{TeV}$	2.21×10^{-5}	1.29×10^{-2}	1.73×10^{-2}	2.20×10^{-2}	6.63×10^{-4}

Table 5.20: *Cross sections for QBHs decaying into an electron and positron , or alternatively into an electron and anti-muon, with lepton as well as quark flavor violated, but B-L and Lorentz invariance conserved (model 4). The center of mass energies* $\sqrt{s} = 7, 8,$ *and* $14\mathrm{TeV}$ *are considered with a Planck mass of* $M_* = 1 - 5\mathrm{TeV}$*, respectively. The following five low-scale gravity models are adopted: the four-dimensional case,* $n = 5, 6, 7$ *large extra dimensions, and the warped dimension model. Suitable initial states for such a process are a quark and antiquark as well as two gluons. The decay into an electron and anti-muon is forbidden in model 1 and 3. Due to the symmetry restrictions in models 2, 4 and 5 the cross sections of both cases are identical.*

cross section in fb	Model for low scale quantum gravity				
$\sigma\,(\mathrm{QBH} \to \mathrm{e}^+ + \mathrm{e}^-)$ or $\sigma\,(\mathrm{QBH} \to \mu^+ + \mathrm{e}^-)$	4 dim[4]	ADD n = 5	ADD n = 6	ADD n = 7	RS
CoM energy of $\sqrt{\mathrm{s}} = 7\mathrm{TeV}$					
$M_* = 1\mathrm{TeV}$	2.17×10^{-1}	9.69×10^{1}	1.29×10^{2}	1.64×10^{2}	5.47
$M_* = 3\mathrm{TeV}$	9.82×10^{-6}	5.95×10^{-3}	8.00×10^{-3}	1.02×10^{-2}	3.02×10^{-4}
$M_* = 5\mathrm{TeV}$	2.49×10^{-10}	1.65×10^{-7}	2.22×10^{-7}	2.83×10^{-7}	8.07×10^{-9}
CoM energy of $\sqrt{\mathrm{s}} = 8\mathrm{TeV}$					
$M_* = 1\mathrm{TeV}$	3.81×10^{-1}	1.63×10^{2}	2.17×10^{2}	2.75×10^{2}	9.33
$M_* = 3\mathrm{TeV}$	4.07×10^{-5}	2.40×10^{-2}	3.22×10^{-2}	4.10×10^{-2}	1.23×10^{-3}
$M_* = 5\mathrm{TeV}$	7.64×10^{-9}	4.95×10^{-6}	6.67×10^{-6}	8.51×10^{-6}	2.45×10^{-7}
CoM energy of $\sqrt{\mathrm{s}} = 14\mathrm{TeV}$					
$M_* = 1\mathrm{TeV}$	2.87	9.88×10^{2}	1.31×10^{3}	1.66×10^{3}	6.07×10^{1}
$M_* = 3\mathrm{TeV}$	2.66×10^{-3}	1.36	1.82	2.31	7.34×10^{-2}
$M_* = 5\mathrm{TeV}$	2.10×10^{-5}	1.22×10^{-2}	1.64×10^{-2}	2.09×10^{-2}	6.30×10^{-4}

Table 5.21: *Cross sections for QBHs decaying into an electron and positron, or alternatively into an electron and anti-muon, with lepton as well as quark flavor, B-L violated, and only Lorentz invariance conserved (model 5). The center of mass energies* $\sqrt{s} = 7, 8,$ *and* $14\mathrm{TeV}$ *are considered with a Planck mass of* $M_* = 1 - 5\mathrm{TeV}$*, respectively. The following five low-scale gravity models are adopted: the four-dimensional case,* $n = 5, 6, 7$ *large extra dimensions, and the warped dimension model. Suitable initial states for such a process are a quark and antiquark as well as two gluons. The decay into an electron and anti-muon is forbidden in model 1 and 3. Due to the symmetry restrictions in models 2, 4 and 5 the cross sections of both cases are identical.*

cross section in fb	Model for low scale quantum gravity				
$\sigma\,(\mathrm{QBH} \to u + \mathrm{e}^-)$	4 dim[4]	ADD n = 5	ADD n = 6	ADD n = 7	RS
center of mass of $\sqrt{\mathrm{s}} = 7\,\mathrm{TeV}$					
$M_* = 1\,\mathrm{TeV}$	$5.04{\times}10^{-2}$	$2.46{\times}10^{1}$	$3.29{\times}10^{1}$	$4.18{\times}10^{1}$	1.35
$M_* = 3\,\mathrm{TeV}$	$4.89{\times}10^{-7}$	$3.01{\times}10^{-4}$	$4.06{\times}10^{-4}$	$5.17{\times}10^{-4}$	$1.52{\times}10^{-5}$
$M_* = 5\,\mathrm{TeV}$	$5.68{\times}10^{-12}$	$3.76{\times}10^{-9}$	$5.07{\times}10^{-9}$	$6.47{\times}10^{-9}$	$1.84{\times}10^{-10}$
center of mass of $\sqrt{\mathrm{s}} = 8\,\mathrm{TeV}$					
$M_* = 1\,\mathrm{TeV}$	$9.91{\times}10^{-2}$	$4.66{\times}10^{1}$	$6.24{\times}10^{1}$	$7.91{\times}10^{1}$	2.59
$M_* = 3\,\mathrm{TeV}$	$2.61{\times}10^{-6}$	$1.58{\times}10^{-3}$	$2.12{\times}10^{-3}$	$2.70{\times}10^{-3}$	$8.01{\times}10^{-5}$
$M_* = 5\,\mathrm{TeV}$	$2.04{\times}10^{-10}$	$1.33{\times}10^{-7}$	$1.79{\times}10^{-7}$	$2.29{\times}10^{-7}$	$6.56{\times}10^{-9}$
center of mass of $\sqrt{\mathrm{s}} = 14\,\mathrm{TeV}$					
$M_* = 1\,\mathrm{TeV}$	1.08	$4.26{\times}10^{2}$	$5.68{\times}10^{2}$	$7.18{\times}10^{2}$	$2.50{\times}10^{1}$
$M_* = 3\,\mathrm{TeV}$	$4.13{\times}10^{-4}$	$2.24{\times}10^{-1}$	$3.00{\times}10^{-1}$	$3.82{\times}10^{-1}$	$1.18{\times}10^{-2}$
$M_* = 5\,\mathrm{TeV}$	$1.48{\times}10^{-6}$	$8.89{\times}10^{-4}$	$1.20{\times}10^{-3}$	$1.52{\times}10^{-3}$	$4.53{\times}10^{-5}$

Table 5.22: *Cross sections for QBHs decaying into an electron and up-quark with lepton as well as quark flavor violated, but B-L and Lorentz invariance conserved (model 4). The suitable initial state for such a process is an antiup-quark and an antidown-quark.*

cross section in fb	Model for low scale quantum gravity				
$\sigma\,(\mathrm{QBH} \to u + \mathrm{e}^-)$	4 dim[4]	ADD n = 5	ADD n = 6	ADD n = 7	RS
center of mass of $\sqrt{\mathrm{s}} = 7\,\mathrm{TeV}$					
$M_* = 1\,\mathrm{TeV}$	$4.20{\times}10^{-2}$	$2.05{\times}10^{1}$	$2.74{\times}10^{1}$	$3.48{\times}10^{1}$	1.12
$M_* = 3\,\mathrm{TeV}$	$4.08{\times}10^{-7}$	$2.51{\times}10^{-4}$	$3.38{\times}10^{-4}$	$4.31{\times}10^{-4}$	$1.27{\times}10^{-5}$
$M_* = 5\,\mathrm{TeV}$	$4.73{\times}10^{-12}$	$3.13{\times}10^{-9}$	$4.23{\times}10^{-9}$	$5.39{\times}10^{-9}$	$1.54{\times}10^{-10}$
center of mass of $\sqrt{\mathrm{s}} = 8\,\mathrm{TeV}$					
$M_* = 1\,\mathrm{TeV}$	$8.26{\times}10^{-2}$	$3.89{\times}10^{1}$	$5.20{\times}10^{1}$	$6.59{\times}10^{1}$	2.16
$M_* = 3\,\mathrm{TeV}$	$2.18{\times}10^{-6}$	$1.31{\times}10^{-3}$	$1.77{\times}10^{-3}$	$2.25{\times}10^{-3}$	$6.68{\times}10^{-5}$
$M_* = 5\,\mathrm{TeV}$	$1.70{\times}10^{-10}$	$1.11{\times}10^{-7}$	$1.49{\times}10^{-7}$	$1.90{\times}10^{-7}$	$5.47{\times}10^{-9}$
center of mass of $\sqrt{\mathrm{s}} = 14\,\mathrm{TeV}$					
$M_* = 1\,\mathrm{TeV}$	$8.96{\times}10^{-1}$	$3.55{\times}10^{2}$	$4.73{\times}10^{2}$	$5.99{\times}10^{2}$	$2.09{\times}10^{1}$
$M_* = 3\,\mathrm{TeV}$	$3.44{\times}10^{-4}$	$1.87{\times}10^{-1}$	$2.50{\times}10^{-1}$	$3.18{\times}10^{-1}$	$9.86{\times}10^{-3}$
$M_* = 5\,\mathrm{TeV}$	$1.24{\times}10^{-6}$	$7.41{\times}10^{-4}$	$9.97{\times}10^{-4}$	$1.27{\times}10^{-3}$	$3.78{\times}10^{-5}$

Table 5.23: *Cross sections for QBHs decaying into an electron and up-quark with lepton as well as quark flavor, and B-L violated and only Lorentz invariance conserved (model 5). The suitable initial state for such a process is an antiup-quark and an antidown-quark.*

cross section in fb	Model for low scale quantum gravity				
$\sigma\,(\mathrm{QBH} \to d + \mu^+)$	4 dim[4]	ADD n = 5	ADD n = 6	ADD n = 7	RS
center of mass of $\sqrt{s} = 7\,\mathrm{TeV}$					
$M_* = 1\,\mathrm{TeV}$	6.58×10^{-2}	3.27×10^{1}	4.38×10^{1}	5.56×10^{1}	1.78
$M_* = 3\,\mathrm{TeV}$	4.18×10^{-7}	2.57×10^{-4}	3.46×10^{-4}	4.41×10^{-4}	1.30×10^{-5}
$M_* = 5\,\mathrm{TeV}$	5.83×10^{-12}	3.86×10^{-9}	5.21×10^{-9}	6.64×10^{-9}	1.89×10^{-10}
center of mass of $\sqrt{s} = 8\,\mathrm{TeV}$					
$M_* = 1\,\mathrm{TeV}$	1.32×10^{-1}	6.31×10^{1}	8.45×10^{1}	1.07×10^{2}	3.48
$M_* = 3\,\mathrm{TeV}$	2.30×10^{-6}	1.39×10^{-3}	1.87×10^{-3}	2.39×10^{-3}	7.07×10^{-5}
$M_* = 5\,\mathrm{TeV}$	1.94×10^{-10}	1.26×10^{-7}	1.70×10^{-7}	2.17×10^{-7}	6.24×10^{-9}
center of mass of $\sqrt{s} = 14\,\mathrm{TeV}$					
$M_* = 1\,\mathrm{TeV}$	1.46	5.80×10^{2}	7.73×10^{2}	9.78×10^{2}	3.41×10^{1}
$M_* = 3\,\mathrm{TeV}$	4.70×10^{-4}	2.59×10^{-1}	3.47×10^{-1}	4.41×10^{-1}	1.36×10^{-2}
$M_* = 5\,\mathrm{TeV}$	1.33×10^{-6}	8.00×10^{-4}	1.08×10^{-3}	1.37×10^{-3}	4.07×10^{-5}

Table 5.24: *Cross sections for QBHs decaying into an anti-muon and down quark with lepton as well as quark flavor violated, but B-L and Lorentz invariance conserved (model 4). The suitable initial state for such a process consists of two antidown-quarks.*

cross section in fb	Model for low scale quantum gravity				
$\sigma\,(\mathrm{QBH} \to d + \mu^+)$	4 dim[4]	ADD n = 5	ADD n = 6	ADD n = 7	RS
center of mass of $\sqrt{s} = 7\,\mathrm{TeV}$					
$M_* = 1\,\mathrm{TeV}$	5.27×10^{-2}	2.62×10^{1}	3.50×10^{1}	4.45×10^{1}	1.43
$M_* = 3\,\mathrm{TeV}$	3.34×10^{-7}	2.06×10^{-4}	2.77×10^{-4}	3.53×10^{-4}	1.04×10^{-5}
$M_* = 5\,\mathrm{TeV}$	4.67×10^{-12}	3.09×10^{-9}	4.16×10^{-9}	5.31×10^{-9}	1.51×10^{-10}
center of mass of $\sqrt{s} = 8\,\mathrm{TeV}$					
$M_* = 1\,\mathrm{TeV}$	1.06×10^{-1}	5.05×10^{1}	6.76×10^{1}	8.57×10^{1}	2.79
$M_* = 3\,\mathrm{TeV}$	1.84×10^{-6}	1.11×10^{-3}	1.50×10^{-3}	1.91×10^{-3}	5.65×10^{-5}
$M_* = 5\,\mathrm{TeV}$	1.56×10^{-10}	1.01×10^{-7}	1.36×10^{-7}	1.74×10^{-7}	4.99×10^{-9}
center of mass of $\sqrt{s} = 14\,\mathrm{TeV}$					
$M_* = 1\,\mathrm{TeV}$	1.17	4.64×10^{2}	6.19×10^{2}	7.83×10^{2}	2.73×10^{1}
$M_* = 3\,\mathrm{TeV}$	3.76×10^{-4}	2.07×10^{-1}	2.78×10^{-1}	3.53×10^{-1}	1.09×10^{-2}
$M_* = 5\,\mathrm{TeV}$	1.07×10^{-6}	6.40×10^{-4}	8.61×10^{-4}	1.10×10^{-3}	3.26×10^{-5}

Table 5.25: *Cross sections for QBHs decaying into an anti-muon and down quark with lepton as well as quark flavor, and B-L violated and only Lorentz invariance conserved (model 5). The suitable initial state for such a process consists of two antidown-quarks.*

Chapter 6

Quantum black holes with a discrete mass spectrum

This chapter will elaborate the effects of a discrete mass spectrum on the model, especially the cross sections, of quantum black holes (QBHs) and is based on work published in [15] and [16].

6.1 Production of QBHs with discrete masses

Till recently, only a continuous mass spectrum had been considered for quantum black holes. This was sensible since most of the physics is extrapolated from the classical black hole case. However, motivated by the existence of a minimal length in models trying to unify quantum mechanics with general relativity [86–89], it was suggested in [15] (see also [77][1]) that non-thermal quantum black hole masses could be quantized in terms of the Planck scale. Due to a partitioned mass distribution, we thus propose the production of plateau-shaped black hole states before reaching the semi-classical regime.
Whereas a continuous quantum black hole is more likely to be seen as gravitational scattering, the phenomenology of the equivalents with discrete masses is rather different. Their behavior is not unlike that of heavy particle states with a very short life time ($\Gamma(QBH \to 2 \text{ particles}) \sim \frac{1}{64\pi^2} M_{QBH}$ using dimensional analysis, as shown in chapter 4), which will decay to a few particles.

[1] In [77] the authors give both a physical and mathematical reason for the proposal of quantized black hole masses. As a physical reason, they argue that a continuous spectrum of finite norm states would also imply an infinite production rate. The mathematical reason they give is based on the fact that any hermitian operator has discrete finite norm eigenfunctions, assuming a Poincare invariant asymptotic background.

Assuming the Planck mass to be $M_* = 1\,\mathrm{TeV}$, we expect about 5 QBH states between the Planck mass before reaching the semi-classical regime. The production cross section of discrete QBHs is given by the sum of the individual cross sections, i.e. distinguished by their mass [15],

$$\sigma_{tot}^{(pp)}(s, n, M_*) = \sum_i \sigma_{QBH}^{(pp)}(s, M_{QBH}^i, n, M_*) \quad . \tag{6.1}$$

Similar to the continuous cross section, see eq. (5.1), the individual cross sections are extrapolated from the semi-classical case and take the form

$$\begin{aligned}\sigma_{QBH}^{pp}(s, M_{QBH}, n, M_*) = \pi r_s^2(M_{QBH}, n, M_*) \int_0^1 2z dz \int_{\frac{(M_{QBH})^2}{y(z)^2 s}}^1 du \int_u^1 \frac{dv}{v} \\ \times F(n) \sum_{i,j} f_i(v, Q) f_j(u/v, Q) \quad ,\end{aligned} \tag{6.2}$$

where M_{QBH} is the mass of the quantum black hole, respectively. One observes a constant Schwarzschild radius, and thus a constant parton level cross section, which relies on the mass of the specific black hole and not on the center of mass energy

$$r_s(M_{QBH}^2, n, M_*) = k(n) M_*^{-1} [M_{QBH}/M_*]^{1/(1+n)} \quad . \tag{6.3}$$

As before, $z \equiv b/b_{max}$ is the rescaled impact parameter and $F\,(n)$ as well as $y(z)$ describe the effects of inelasticity numerically fitted by Yoshino and Nambu [59, 61]. The labels i,j run over the different particles species, f_i,f_j are the parton distribution functions evaluated at the scale of momentum transfer Q and u, v are the momentum fractions of the incoming particles. $k(n)$ remains as in the continuous case

$$k(n) = \left[2^n \sqrt{\pi}^{n-3} \frac{\Gamma((3+n)/2)}{2+n} \right]^{1/(1+n)} \quad . \tag{6.4}$$

Assuming that space-time is quantized at short distances and that there is a minimal length [86–91], the mass distribution is expected to be partitioned in terms of the Planck mass. If the Planck mass is of the order of 1 TeV, one would expect five different black hole states before reaching a continuum in the semi-classical regime. For higher Planck masses, the number of states is hugely dependent on the center of mass energy because of the suppression due to the parton distribution factors. The factors $F(n)$ and the functions $y(z)$ have been calculated in the framework of classical black holes and are not known for non-thermal quantum black holes. We are thus setting the factors $F(n) = 1$ as well as the functions $y(z) = 1$. This is an approximation which is reasonable since these factors have been calculated for classical black holes and may not apply to quantum black holes. However, let us emphasize that the functions $y(z)$ describe the lost energy of the incoming

partons to gravitational radiation. Since this has nothing to do with the decomposition of the black holes or the type of black hole produced, we expect that the functions $y(z)$ for quantum black holes will be similar to the classical case.

One might worry that the cross section for non-thermal black holes could be exponentially suppressed. However, such a suppression has been refuted in [62]: Because of the seminal work of Eardley and Giddings [57], we know that there are classical trajectories with two particle initial conditions which evolve into black holes, the process is clearly not classically forbidden. Furthermore, the time-reversed process is not thermal and involves very special initial (final) conditions.

6.2 Decay of QBHs with quantized masses

Although the physics of the QBHs with discrete masses appears to be very different from the continuous case, the classification of these objects according to their mass, spin, QCD and QED charge remains the same. As it is described in detail in section 5.2, we will only emphasize the keypoints:

- The QBH can carry a $SU(3)_c$ color charge. Considering quarks and gluons as initial particles, the following color states are possible: $\mathbf{1}$, $\overset{(-)}{\mathbf{3}}$, $\overset{(-)}{\mathbf{6}}$, $\mathbf{8}$, $\overset{(-)}{\mathbf{10}}$, $\overset{(-)}{\mathbf{15}}$, $\mathbf{27}$.
- There are nine possible electromagnetic charges: 0, $\pm 1/3$, $\pm 2/3$, $\pm 4/3$, and ± 1.
- The spin factors for the likeliness of a final spin state can be found in table 5.1.

One finds the same branching ratios as given in section 5.3.1, for the five considered models corresponding to the symmetries of the underlying theory, i.e. lepton and quark flavor, B-L, and Lorentz invariance.

6.2.1 Total cross sections of QBHs with discrete masses

As aforementioned, we assume that there are five quantum black hole states between the Planck mass and the continuous semi-classical region. We thus calculate the total cross section for these five states for different models with low scale quantum gravity using a Monte Carlo integration algorithm specifically designed for the discrete mass spectrum [82]. We use the CTEQ6 PDF set and assume for the inelasticity effects $y(z) = 1$ and form factors $F(n) = 1$. Our results can be found in Tables 6.1 to 6.2 which correspond to different center of mass energies ($\sqrt{s} = 7, 8,$ and $14\,\mathrm{TeV}$). We emphasize that these intermediate black holes will have different spins. We are summing over these allowed

spin states in the cross sections given in Tables 6.1 to 6.2. Similar to the continuous case, we present results for models with $n = 5, 6, 7$ large extra dimensions (ADD), the Randall-Sundrum (RS) warped extra dimension, and the four-dimensional model described in section 2.2.

total σ	model for low scale quantum gravity				
(in fb)	4 dim[4]	ADD n = 5	ADD n = 6	ADD n = 7	RS
center of mass energy of $\sqrt{s} = 7\,\text{TeV}$					
$M_* = 1\,\text{TeV}$					
$M_{BH} = 1\,\text{TeV}$	2.10×10^{4}	1.46×10^{7}	1.98×10^{7}	2.52×10^{7}	7.03×10^{5}
$M_{BH} = 2\,\text{TeV}$	4.47×10^{3}	9.81×10^{5}	1.28×10^{6}	1.60×10^{6}	7.48×10^{4}
$M_{BH} = 3\,\text{TeV}$	5.61×10^{2}	6.27×10^{4}	8.03×10^{4}	9.86×10^{4}	6.26×10^{3}
$M_{BH} = 4\,\text{TeV}$	3.31×10^{1}	2.29×10^{3}	2.90×10^{3}	3.52×10^{3}	2.77×10^{2}
$M_{BH} = 5\,\text{TeV}$	5.64×10^{-1}	2.69×10^{1}	3.37×10^{1}	4.06×10^{1}	3.78
$M_* = 3\,\text{TeV}$					
$M_{BH} = 3\,\text{TeV}$	5.24	3.66×10^{3}	4.94×10^{3}	6.31×10^{3}	1.76×10^{2}
$M_{BH} = 6\,\text{TeV}$	4.03×10^{-6}	8.85×10^{-4}	1.16×10^{-3}	1.44×10^{-3}	6.75×10^{-5}
$M_* = 5\,\text{TeV}$					
$M_{BH} = 5\,\text{TeV}$	4.94×10^{-4}	3.45×10^{-1}	4.65×10^{-1}	5.94×10^{-1}	1.66×10^{-2}
center of mass energy of $\sqrt{s} = 8\,\text{TeV}$					
$M_* = 1\,\text{TeV}$					
$M_{BH} = 1\,\text{TeV}$	3.24×10^{4}	2.26×10^{7}	3.05×10^{7}	3.90×10^{7}	1.09×10^{6}
$M_{BH} = 2\,\text{TeV}$	8.96×10^{3}	1.97×10^{6}	2.57×10^{6}	3.20×10^{6}	1.50×10^{5}
$M_{BH} = 3\,\text{TeV}$	1.72×10^{3}	1.92×10^{5}	2.46×10^{5}	3.02×10^{5}	1.92×10^{4}
$M_{BH} = 4\,\text{TeV}$	2.00×10^{2}	1.38×10^{4}	1.75×10^{4}	2.12×10^{4}	1.67×10^{3}
$M_{BH} = 5\,\text{TeV}$	1.14×10^{1}	5.42×10^{2}	6.78×10^{2}	8.18×10^{2}	7.61×10^{1}
$M_* = 3\,\text{TeV}$					
$M_{BH} = 3\,\text{TeV}$	1.64×10^{1}	1.15×10^{4}	1.55×10^{4}	1.98×10^{4}	5.51×10^{2}
$M_{BH} = 6\,\text{TeV}$	1.52×10^{-3}	3.34×10^{-1}	4.36×10^{-1}	5.44×10^{-1}	2.55×10^{-2}
$M_* = 5\,\text{TeV}$					
$M_{BH} = 5\,\text{TeV}$	1.07×10^{-2}	7.47	1.01×10^{1}	1.29×10^{1}	3.59×10^{-1}

Table 6.1: *Total cross sections for the production of QBHs with masses above the chosen reduced Planck mass of $M_* = 1, 3$ and 5 TeV, respectively, and below center of mass energy of the initial particles of 7 and 8 TeV.*

total σ	model for low scale quantum gravity				
(in fb)	4 dim[4]	ADD n = 5	ADD n = 6	ADD n = 7	RS
center of mass energy of $\sqrt{s} = 14\,\text{TeV}$					
$M_* = 1\,\text{TeV}$					
$M_{BH} = 1\,\text{TeV}$	1.61×10^{5}	1.12×10^{8}	1.52×10^{8}	1.94×10^{8}	5.40×10^{6}
$M_{BH} = 2\,\text{TeV}$	8.39×10^{4}	1.84×10^{7}	2.41×10^{7}	3.00×10^{7}	1.41×10^{6}
$M_{BH} = 3\,\text{TeV}$	4.09×10^{4}	4.57×10^{6}	5.85×10^{6}	7.19×10^{6}	4.56×10^{5}
$M_{BH} = 4\,\text{TeV}$	1.79×10^{4}	1.24×10^{6}	1.56×10^{6}	1.90×10^{6}	1.50×10^{5}
$M_{BH} = 5\,\text{TeV}$	6.84×10^{3}	3.26×10^{5}	4.08×10^{5}	4.92×10^{5}	4.58×10^{4}
$M_* = 3\,\text{TeV}$					
$M_{BH} = 3\,\text{TeV}$	4.19×10^{2}	2.92×10^{5}	3.94×10^{5}	5.04×10^{5}	1.40×10^{4}
$M_{BH} = 6\,\text{TeV}$	2.10×10^{1}	4.61×10^{3}	6.02×10^{3}	7.50×10^{3}	3.51×10^{2}
$M_{BH} = 9\,\text{TeV}$	1.80×10^{-1}	2.01×10^{1}	2.58×10^{1}	3.17×10^{1}	2.01
$M_{BH} = 12\,\text{TeV}$	1.61×10^{-5}	1.12×10^{-3}	1.41×10^{-3}	1.71×10^{-3}	1.35×10^{-4}
$M_* = 5\,\text{TeV}$					
$M_{BH} = 5\,\text{TeV}$	7.69	5.36×10^{3}	7.24×10^{3}	9.25×10^{3}	2.58×10^{2}
$M_{BH} = 10\,\text{TeV}$	1.98×10^{-3}	4.34×10^{-1}	5.67×10^{-1}	7.07×10^{-1}	3.31×10^{-2}

Table 6.2: *Total cross sections for the production of QBHs with masses above the chosen reduced Planck mass of $M_* = 1, 3$ and $5\,\text{TeV}$, respectively, and below center of mass energy of the initial particles of 14 TeV.*

Due to the quantized energy levels, one finds that the total cross sections in case of a discrete mass spectrum are smaller than the cross sections determined for the continuous case. We again observe an increase of the cross section with growing center of mass energy and a decrease for higher Planck masses.

6.2.2 Specific cross sections for discrete QBHs

Different to the continuous case, we need to also sum over the mass states to determine the cross section for a specific final state:

$$\sigma_{\text{QBH}\to\text{final state}} = \sum_{\substack{\text{average}\\ \text{initial states}}} \sum_{\text{masses}} \sigma_{\text{initial state}\to\text{QBH}_{\text{mass}}} \times \text{BR}_{\text{final state,model}} \,. \tag{6.5}$$

Each cross section for a specific initial states was calculated via equations (6.1) and (6.2) by using a Monte Carlo integration algorithm. Assuming a specific model, we sum up the cross sections for all contributing masses up to the center of mass energy and then multiply the result with the suitable branching ratios (Table 5.2 to 5.9). The desired cross section for the chosen final state is given by taking the average over all initial state contributions. We calculated the cross sections for the same final states as given in section 5.3.3 to compare the results. As in the continuous case, the results are shown for center of mass energies $\sqrt{s} = 7, 8,$ and 14TeV and for the Planck masses of $M_* = 1, 3,$ and 5TeV which suffices to understand the diversifications. Thus, one finds the cross sections for all suitable discrete QBHs, i.e. with all different masses and possible initial states, decaying into two photons in table 6.3 to 6.7 for the appropriate symmetry model, respectively. Table 6.8 to 6.12 give numbers for the final states of an electron and positron as well as for an electron and antimuon if the symmetry restrictions allow such a process. The lepton and quark flavor violating processes of a QBH decaying into an electron and up-quark (table 6.13, 6.14) as well as into an antimuon and down-quark (table 6.15,6.16) are given for model 4 and 5. The limitations to all shown creation processes, including the possible initial states, can be found in section 5.3.3 or partially in the table captions. To allow for a useful comparison, the same low-scale gravity models as for the continuous case, that is the four-dimensional case proposed in [4], three models with $n = 5, 6,$ and 7 large extra dimensions, as well as the warped dimension model.

cross section in fb	model for low scale quantum gravity				
$\sigma\,(\mathrm{QBH} \to \gamma + \gamma)$	4 dim[4]	ADD n = 5	ADD n = 6	ADD n = 7	RS
CoM energy of $\sqrt{s} = 7$TeV					
$M_* = 1$TeV	2.33×10^{-1}	1.51×10^{2}	2.03×10^{2}	2.60×10^{2}	7.39
$M_* = 3$TeV	1.27×10^{-5}	8.85×10^{-3}	1.19×10^{-2}	1.53×10^{-2}	4.25×10^{-4}
$M_* = 5$TeV	2.81×10^{-10}	1.96×10^{-7}	2.65×10^{-7}	3.38×10^{-7}	9.42×10^{-9}
CoM energy of $\sqrt{s} = 8$TeV					
$M_* = 1$TeV	4.08×10^{-1}	2.56×10^{2}	3.45×10^{2}	4.40×10^{2}	1.27×10^{1}
$M_* = 3$TeV	5.18×10^{-5}	3.61×10^{-2}	4.88×10^{-2}	6.23×10^{-2}	1.74×10^{-3}
$M_* = 5$TeV	9.13×10^{-9}	6.37×10^{-6}	8.60×10^{-6}	1.10×10^{-5}	3.06×10^{-7}
CoM energy of $\sqrt{s} = 14$TeV					
$M_* = 1$TeV	3.35	1.69×10^{3}	2.28×10^{3}	2.90×10^{3}	8.88×10^{1}
$M_* = 3$TeV	2.97×10^{-3}	2.05	2.77	3.53	9.87×10^{-2}
$M_* = 5$TeV	2.63×10^{-5}	1.83×10^{-2}	2.48×10^{-2}	3.16×10^{-2}	8.81×10^{-4}

Table 6.3: *Cross sections for discrete QBHs decaying into two photons with lepton as well as quark flavor, B-L and Lorentz invariance conserved (model 1). Suitable initial states for such a process are a quark and antiquark as well as two gluons.*

cross section in fb	model for low scale quantum gravity				
$\sigma\,(\mathrm{QBH} \to \gamma + \gamma)$	4 dim[4]	ADD n = 5	ADD n = 6	ADD n = 7	RS
CoM energy of $\sqrt{s} = 7$TeV					
$M_* = 1$TeV	1.95×10^{-1}	1.26×10^{2}	1.70×10^{2}	2.18×10^{2}	6.19
$M_* = 3$TeV	1.04×10^{-5}	7.28×10^{-3}	9.83×10^{-3}	1.26×10^{-2}	3.50×10^{-4}
$M_* = 5$TeV	2.30×10^{-10}	1.61×10^{-7}	2.17×10^{-7}	2.77×10^{-7}	7.72×10^{-9}
CoM energy of $\sqrt{s} = 8$TeV					
$M_* = 1$TeV	3.42×10^{-1}	2.15×10^{2}	2.90×10^{2}	3.70×10^{2}	1.06×10^{1}
$M_* = 3$TeV	4.27×10^{-5}	2.98×10^{-2}	4.02×10^{-2}	5.13×10^{-2}	1.43×10^{-3}
$M_* = 5$TeV	7.49×10^{-9}	5.23×10^{-6}	7.06×10^{-6}	9.01×10^{-6}	2.51×10^{-7}
CoM energy of $\sqrt{s} = 14$TeV					
$M_* = 1$TeV	2.84	1.44×10^{3}	1.94×10^{3}	2.47×10^{3}	7.55×10^{1}
$M_* = 3$TeV	2.46×10^{-3}	1.70	2.29	2.93	8.19×10^{-2}
$M_* = 5$TeV	2.17×10^{-5}	1.51×10^{-2}	2.04×10^{-2}	2.61×10^{-2}	7.26×10^{-4}

Table 6.4: *Cross sections for discrete QBHs decaying into two photons with lepton flavor violated but quark flavor, B-L and Lorentz invariance conserved (model 2). Suitable initial states for such a process are a quark and antiquark as well as two gluons.*

cross section in fb	model for low scale quantum gravity				
$\sigma\,(\mathrm{QBH} \to \gamma + \gamma)$	4 dim[4]	ADD n = 5	ADD n = 6	ADD n = 7	RS
CoM energy of $\sqrt{s} = 7$TeV					
$M_* = 1$TeV	1.75×10^{-1}	1.14×10^{2}	1.53×10^{2}	1.96×10^{2}	5.57
$M_* = 3$TeV	9.56×10^{-6}	6.67×10^{-3}	9.00×10^{-3}	1.15×10^{-2}	3.20×10^{-4}
$M_* = 5$TeV	2.64×10^{-10}	1.84×10^{-7}	2.49×10^{-7}	3.18×10^{-7}	8.85×10^{-9}
CoM energy of $\sqrt{s} = 8$TeV					
$M_* = 1$TeV	3.09×10^{-1}	1.94×10^{2}	2.62×10^{2}	3.34×10^{2}	9.61
$M_* = 3$TeV	3.85×10^{-5}	2.68×10^{-2}	3.62×10^{-2}	4.63×10^{-2}	1.29×10^{-3}
$M_* = 5$TeV	7.96×10^{-9}	5.55×10^{-6}	7.50×10^{-6}	9.58×10^{-6}	2.67×10^{-7}
CoM energy of $\sqrt{s} = 14$TeV					
$M_* = 1$TeV	2.59	1.32×10^{3}	1.78×10^{3}	2.27×10^{3}	6.91×10^{1}
$M_* = 3$TeV	2.22×10^{-3}	1.53	2.07	2.64	7.37×10^{-2}
$M_* = 5$TeV	1.96×10^{-5}	1.37×10^{-2}	1.84×10^{-2}	2.36×10^{-2}	6.56×10^{-4}

Table 6.5: *Cross sections for discrete QBHs decaying into two photons with quark flavor violated, but lepton flavor, B-L and Lorentz invariance conserved (model 3). Suitable initial states for such a process are a quark and antiquark as well as two gluons.*

cross section in fb	model for low scale quantum gravity				
$\sigma\,(\mathrm{QBH} \to \gamma + \gamma)$	4 dim[4]	ADD n = 5	ADD n = 6	ADD n = 7	RS
CoM energy of $\sqrt{s} = 7$TeV					
$M_* = 1$TeV	1.67×10^{-1}	1.08×10^{2}	1.46×10^{2}	1.86×10^{2}	5.30
$M_* = 3$TeV	9.07×10^{-6}	6.32×10^{-3}	8.54×10^{-3}	1.09×10^{-2}	3.04×10^{-4}
$M_* = 5$TeV	2.50×10^{-10}	1.75×10^{-7}	2.36×10^{-7}	3.01×10^{-7}	8.39×10^{-9}
CoM energy of $\sqrt{s} = 8$TeV					
$M_* = 1$TeV	2.94×10^{-1}	1.85×10^{2}	2.50×10^{2}	3.19×10^{2}	9.15
$M_* = 3$TeV	3.65×10^{-5}	2.55×10^{-2}	3.44×10^{-2}	4.39×10^{-2}	1.22×10^{-3}
$M_* = 5$TeV	7.55×10^{-9}	5.26×10^{-6}	7.11×10^{-6}	9.08×10^{-6}	2.53×10^{-7}
CoM energy of $\sqrt{s} = 14$TeV					
$M_* = 1$TeV	2.47	1.26×10^{3}	1.70×10^{3}	2.16×10^{3}	6.60×10^{1}
$M_* = 3$TeV	2.11×10^{-3}	1.45	1.96	2.51	7.01×10^{-2}
$M_* = 5$TeV	1.86×10^{-5}	1.30×10^{-2}	1.75×10^{-2}	2.23×10^{-2}	6.22×10^{-4}

Table 6.6: *Cross sections for discrete QBHs decaying into two photons with lepton as well as quark flavor violated, but B-L and Lorentz invariance conserved (model 4). Suitable initial states for such a process are a quark and antiquark as well as two gluons.*

cross section in fb	model for low scale quantum gravity				
$\sigma\,(\mathrm{QBH} \to \gamma + \gamma)$	4 dim[4]	ADD n = 5	ADD n = 6	ADD n = 7	RS
CoM energy of $\sqrt{s} = 7$TeV					
$M_* = 1$TeV	1.59×10^{-1}	1.03×10^{2}	1.39×10^{2}	1.78×10^{2}	5.06
$M_* = 3$TeV	8.62×10^{-6}	6.02×10^{-3}	8.12×10^{-3}	1.04×10^{-2}	2.89×10^{-4}
$M_* = 5$TeV	2.38×10^{-10}	1.66×10^{-7}	2.24×10^{-7}	2.86×10^{-7}	7.97×10^{-9}
CoM energy of $\sqrt{s} = 8$TeV					
$M_* = 1$TeV	2.81×10^{-1}	1.77×10^{2}	2.38×10^{2}	3.04×10^{2}	8.74
$M_* = 3$TeV	3.47×10^{-5}	2.42×10^{-2}	3.27×10^{-2}	4.18×10^{-2}	1.16×10^{-3}
$M_* = 5$TeV	7.18×10^{-9}	5.00×10^{-6}	6.76×10^{-6}	8.63×10^{-6}	2.40×10^{-7}
CoM energy of $\sqrt{s} = 14$TeV					
$M_* = 1$TeV	2.36	1.21×10^{3}	1.63×10^{3}	2.07×10^{3}	6.31×10^{1}
$M_* = 3$TeV	2.01×10^{-3}	1.38	1.87	2.39	6.67×10^{-2}
$M_* = 5$TeV	1.77×10^{-5}	1.23×10^{-2}	1.66×10^{-2}	2.13×10^{-2}	5.92×10^{-4}

Table 6.7: *Cross sections for discrete QBHs decaying into two photons with lepton as well as quark flavor, B-L violated and only Lorentz invariance conserved (model 5). Suitable initial states for such a process are a quark and antiquark as well as two gluons.*

cross section in fb	model for low scale quantum gravity				
$\sigma\,(\mathrm{QBH} \to \mathrm{e}^+ + \mathrm{e}^-)$	4 dim[4]	ADD n = 5	ADD n = 6	ADD n = 7	RS
CoM energy of $\sqrt{s} = 7$TeV					
$M_* = 1$TeV	2.07×10^{-1}	1.34×10^{2}	1.81×10^{2}	2.31×10^{2}	6.58
$M_* = 3$TeV	1.22×10^{-5}	8.48×10^{-3}	1.15×10^{-2}	1.46×10^{-2}	4.08×10^{-4}
$M_* = 5$TeV	2.74×10^{-10}	1.91×10^{-7}	2.58×10^{-7}	3.30×10^{-7}	9.18×10^{-9}
CoM energy of $\sqrt{s} = 8$TeV					
$M_* = 1$TeV	3.60×10^{-1}	2.24×10^{2}	3.03×10^{2}	3.86×10^{2}	1.11×10^{1}
$M_* = 3$TeV	4.95×10^{-5}	3.45×10^{-2}	4.66×10^{-2}	5.95×10^{-2}	1.66×10^{-3}
$M_* = 5$TeV	8.85×10^{-9}	6.17×10^{-6}	8.33×10^{-6}	1.06×10^{-5}	2.96×10^{-7}
CoM energy of $\sqrt{s} = 14$TeV					
$M_* = 1$TeV	2.82	1.39×10^{3}	1.87×10^{3}	2.38×10^{3}	7.34×10^{1}
$M_* = 3$TeV	2.76×10^{-3}	1.90	2.57	3.28	9.16×10^{-2}
$M_* = 5$TeV	2.52×10^{-5}	1.75×10^{-2}	2.37×10^{-2}	3.03×10^{-2}	8.43×10^{-4}

Table 6.8: *Cross sections for production of a QBH decaying into an electron and positron with lepton as well as quark flavor, B-L and Lorentz invariance conserved (model 1). Suitable initial states for such a process are a quark and antiquark as well as two gluons.*

cross section in fb	model for low scale quantum gravity				
$\sigma\,(\mathrm{QBH} \to \mathrm{e}^+ + \mathrm{e}^-)$ or $\sigma\,(\mathrm{QBH} \to \mu^+ + \mathrm{e}^-)$	4 dim[4]	ADD n = 5	ADD n = 6	ADD n = 7	RS
CoM energy of $\sqrt{\mathrm{s}} = 7\mathrm{TeV}$					
$M_* = 1\mathrm{TeV}$	1.71×10^{-1}	1.11×10^{2}	1.49×10^{2}	1.90×10^{2}	5.43
$M_* = 3\mathrm{TeV}$	9.95×10^{-6}	6.94×10^{-3}	9.37×10^{-3}	1.20×10^{-2}	3.33×10^{-4}
$M_* = 5\mathrm{TeV}$	2.24×10^{-10}	1.56×10^{-7}	2.11×10^{-7}	2.69×10^{-7}	7.49×10^{-9}
CoM energy of $\sqrt{\mathrm{s}} = 8\mathrm{TeV}$					
$M_* = 1\mathrm{TeV}$	2.97×10^{-1}	1.86×10^{2}	2.50×10^{2}	3.19×10^{2}	9.19
$M_* = 3\mathrm{TeV}$	4.05×10^{-5}	2.82×10^{-2}	3.81×10^{-2}	4.87×10^{-2}	1.36×10^{-3}
$M_* = 5\mathrm{TeV}$	7.23×10^{-9}	5.04×10^{-6}	6.81×10^{-6}	8.69×10^{-6}	2.42×10^{-7}
CoM energy of $\sqrt{\mathrm{s}} = 14\mathrm{TeV}$					
$M_* = 1\mathrm{TeV}$	2.34	1.16×10^{3}	1.56×10^{3}	1.98×10^{3}	6.11×10^{1}
$M_* = 3\mathrm{TeV}$	2.26×10^{-3}	1.56	2.11	2.69	7.52×10^{-2}
$M_* = 5\mathrm{TeV}$	2.06×10^{-5}	1.44×10^{-2}	1.94×10^{-2}	2.48×10^{-2}	6.90×10^{-4}

Table 6.9: *Cross sections for discrete QBHs decaying into an electron and positron, or alternatively into an electron and anti-muon, with lepton flavor violated, but quark flavor, B-L and Lorentz invariance conserved (model 2). The center of mass energies* $\sqrt{s} = 7, 8,$ *and* 14TeV *are considered with a Planck mass of* $M_* = 1, 3,$ *and* 5TeV*, respectively. The following five low-scale gravity models are adopted: the four-dimensional case,* $n = 5, 6, 7$ *large extra dimensions, and the warped dimension model. Suitable initial states for such a process are a quark and antiquark as well as two gluons. The decay into an electron and anti-muon is forbidden in model 1 and 3. Due to the symmetry restrictions in models 2, 4 and 5 the cross sections of both cases are identical.*

cross section in fb	model for low scale quantum gravity				
$\sigma\,(\mathrm{QBH} \to \mathrm{e}^+ + \mathrm{e}^-)$	4 dim[4]	ADD n = 5	ADD n = 6	ADD n = 7	RS
CoM energy of $\sqrt{\mathrm{s}} = 7\mathrm{TeV}$					
$M_* = 1\mathrm{TeV}$	1.59×10^{-1}	1.03×10^{2}	1.39×10^{2}	1.77×10^{2}	5.05
$M_* = 3\mathrm{TeV}$	9.22×10^{-6}	6.43×10^{-3}	8.69×10^{-3}	1.11×10^{-2}	3.09×10^{-4}
$M_* = 5\mathrm{TeV}$	2.60×10^{-10}	1.81×10^{-7}	2.44×10^{-7}	3.12×10^{-7}	8.70×10^{-9}
CoM energy of $\sqrt{\mathrm{s}} = 8\mathrm{TeV}$					
$M_* = 1\mathrm{TeV}$	2.79×10^{-1}	1.75×10^{2}	2.35×10^{2}	3.00×10^{2}	8.63
$M_* = 3\mathrm{TeV}$	3.70×10^{-5}	2.58×10^{-2}	3.48×10^{-2}	4.45×10^{-2}	1.24×10^{-3}
$M_* = 5\mathrm{TeV}$	7.78×10^{-9}	5.43×10^{-6}	7.33×10^{-6}	9.36×10^{-6}	2.61×10^{-7}
CoM energy of $\sqrt{\mathrm{s}} = 14\mathrm{TeV}$					
$M_* = 1\mathrm{TeV}$	2.25	1.13×10^{3}	1.52×10^{3}	1.93×10^{3}	5.94×10^{1}
$M_* = 3\mathrm{TeV}$	2.08×10^{-3}	1.44	1.94	2.48	6.92×10^{-2}
$M_* = 5\mathrm{TeV}$	1.89×10^{-5}	1.31×10^{-2}	1.78×10^{-2}	2.27×10^{-2}	6.32×10^{-4}

Table 6.10: *Cross sections for discrete QBHs decaying into an electron and positron with quark flavor violated, but lepton flavor, B-L and Lorentz invariance conserved (model 3). Suitable initial states for such a process are a quark and antiquark as well as two gluons.*

cross section in fb	model for low scale quantum gravity				
$\sigma\,(\mathrm{QBH} \to \mathrm{e}^+ + \mathrm{e}^-)$ or $\sigma\,(\mathrm{QBH} \to \mu^+ + \mathrm{e}^-)$	4 dim[4]	ADD n = 5	ADD n = 6	ADD n = 7	RS
CoM energy of $\sqrt{\mathrm{s}} = 7\mathrm{TeV}$					
$M_* = 1\mathrm{TeV}$	1.51×10^{-1}	9.78×10^{1}	1.32×10^{2}	1.68×10^{2}	4.80
$M_* = 3\mathrm{TeV}$	8.74×10^{-6}	6.10×10^{-3}	8.23×10^{-3}	1.05×10^{-2}	2.93×10^{-4}
$M_* = 5\mathrm{TeV}$	2.46×10^{-10}	1.71×10^{-7}	2.31×10^{-7}	2.96×10^{-7}	8.24×10^{-9}
CoM energy of $\sqrt{\mathrm{s}} = 8\mathrm{TeV}$					
$M_* = 1\mathrm{TeV}$	2.64×10^{-1}	1.66×10^{2}	2.23×10^{2}	2.85×10^{2}	8.19
$M_* = 3\mathrm{TeV}$	3.51×10^{-5}	2.45×10^{-2}	3.30×10^{-2}	4.22×10^{-2}	1.17×10^{-3}
$M_* = 5\mathrm{TeV}$	7.37×10^{-9}	5.14×10^{-6}	6.94×10^{-6}	8.87×10^{-6}	2.47×10^{-7}
CoM energy of $\sqrt{\mathrm{s}} = 14\mathrm{TeV}$					
$M_* = 1\mathrm{TeV}$	2.14	1.08×10^{3}	1.44×10^{3}	1.84×10^{3}	5.65×10^{1}
$M_* = 3\mathrm{TeV}$	1.98×10^{-3}	1.36	1.84	2.35	6.56×10^{-2}
$M_* = 5\mathrm{TeV}$	1.79×10^{-5}	1.25×10^{-2}	1.68×10^{-2}	2.15×10^{-2}	5.99×10^{-4}

Table 6.11: *Cross sections for discrete QBHs decaying into an electron and positron , or alternatively into an electron and anti-muon, with lepton as well as quark flavor violated, but B-L and Lorentz invariance conserved (model 4). The center of mass energies* $\sqrt{s} = 7, 8,$ *and* 14TeV *are considered with a Planck mass of* $M_* = 1, 3,$ *and* 5TeV*, respectively. The following five low-scale gravity models are adopted: the four-dimensional case,* $n = 5, 6, 7$ *large extra dimensions, and the warped dimension model. Suitable initial states for such a process are a quark and antiquark as well as two gluons. The decay into an electron and anti-muon is forbidden in model 1 and 3. Due to the symmetry restrictions in models 2, 4 and 5 the cross sections of both cases are identical.*

cross section in fb	model for low scale quantum gravity				
$\sigma\,(\mathrm{QBH} \to \mathrm{e}^+ + \mathrm{e}^-)$ or $\sigma\,(\mathrm{QBH} \to \mu^+ + \mathrm{e}^-)$	4 dim[4]	ADD n = 5	ADD n = 6	ADD n = 7	RS
center of mass energy of $\sqrt{\mathrm{s}} = 7\,\mathrm{TeV}$					
CoM energy of $\sqrt{\mathrm{s}} = 7\mathrm{TeV}$					
$M_* = 1\mathrm{TeV}$	1.44×10^{-1}	9.31×10^{1}	1.26×10^{2}	1.60×10^{2}	4.56
$M_* = 3\mathrm{TeV}$	8.31×10^{-6}	5.79×10^{-3}	7.82×10^{-3}	9.99×10^{-3}	2.78×10^{-4}
$M_* = 5\mathrm{TeV}$	2.33×10^{-10}	1.63×10^{-7}	2.20×10^{-7}	2.81×10^{-7}	7.82×10^{-9}
CoM energy of $\sqrt{\mathrm{s}} = 8\mathrm{TeV}$					
$M_* = 1\mathrm{TeV}$	2.52×10^{-1}	1.58×10^{2}	2.13×10^{2}	2.71×10^{2}	7.80
$M_* = 3\mathrm{TeV}$	3.33×10^{-5}	2.32×10^{-2}	3.14×10^{-2}	4.01×10^{-2}	1.12×10^{-3}
$M_* = 5\mathrm{TeV}$	7.00×10^{-9}	4.88×10^{-6}	6.59×10^{-6}	8.42×10^{-6}	2.35×10^{-7}
CoM energy of $\sqrt{\mathrm{s}} = 14\mathrm{TeV}$					
$M_* = 1\mathrm{TeV}$	2.04	1.02×10^{3}	1.38×10^{3}	1.75×10^{3}	5.38×10^{1}
$M_* = 3\mathrm{TeV}$	1.88×10^{-3}	1.29	1.75	2.23	6.24×10^{-2}
$M_* = 5\mathrm{TeV}$	1.70×10^{-5}	1.18×10^{-2}	1.60×10^{-2}	2.04×10^{-2}	5.69×10^{-4}

Table 6.12: *Cross sections for discrete QBHs decaying into an electron and positron, or alternatively into an electron and anti-muon, with lepton as well as quark flavor, B-L violated, and only Lorentz invariance conserved (model 5). The center of mass energies* $\sqrt{s} = 7, 8,$ *and* 14TeV *are considered with a Planck mass of* $M_* = 1, 3,$ *and* 5TeV*, respectively. The following five low-scale gravity models are adopted: the four-dimensional case,* $n = 5, 6, 7$ *large extra dimensions, and the warped dimension model. Suitable initial states for such a process are a quark and antiquark as well as two gluons. The decay into an electron and anti-muon is forbidden in model 1 and 3. Due to the symmetry restrictions in models 2, 4 and 5 the cross sections of both cases are identical.*

cross section in fb	model for low scale quantum gravity				
$\sigma\,(\mathrm{QBH} \to \mathrm{u} + \mathrm{e}^-)$	4 dim[4]	ADD n = 5	ADD n = 6	ADD n = 7	RS
center of mass energy of $\sqrt{s} = 7\,\mathrm{TeV}$					
$M_* = 1\,\mathrm{TeV}$	3.47×10^{-2}	2.35×10^{1}	3.17×10^{1}	4.05×10^{1}	1.14
$M_* = 3\,\mathrm{TeV}$	4.22×10^{-7}	2.94×10^{-4}	3.98×10^{-4}	5.08×10^{-4}	1.41×10^{-5}
$M_* = 5\,\mathrm{TeV}$	5.34×10^{-12}	3.72×10^{-9}	5.03×10^{-9}	6.42×10^{-9}	1.79×10^{-10}
center of mass energy of $\sqrt{s} = 8\,\mathrm{TeV}$					
$M_* = 1\,\mathrm{TeV}$	6.71×10^{-2}	4.46×10^{1}	6.02×10^{1}	7.68×10^{1}	2.17
$M_* = 3\,\mathrm{TeV}$	2.20×10^{-6}	1.54×10^{-3}	2.07×10^{-3}	2.65×10^{-3}	7.38×10^{-5}
$M_* = 5\,\mathrm{TeV}$	1.88×10^{-10}	1.31×10^{-7}	1.77×10^{-7}	2.26×10^{-7}	6.30×10^{-9}
center of mass energy of $\sqrt{s} = 14\,\mathrm{TeV}$					
$M_* = 1\,\mathrm{TeV}$	7.28×10^{-1}	4.22×10^{2}	5.69×10^{2}	7.25×10^{2}	2.13×10^{1}
$M_* = 3\,\mathrm{TeV}$	3.09×10^{-4}	2.14×10^{-1}	2.90×10^{-1}	3.70×10^{-1}	1.03×10^{-2}
$M_* = 5\,\mathrm{TeV}$	1.24×10^{-6}	8.65×10^{-4}	1.17×10^{-3}	1.49×10^{-3}	4.15×10^{-5}

Table 6.13: *Cross sections for discrete QBHs decaying into an electron and up-quark with lepton as well as quark flavor violated, but B-L and Lorentz invariance conserved (model 4). The suitable initial state for such a process is an antiup-quark and an antidown-quark.*

cross section in fb	model for low scale quantum gravity				
$\sigma\,(\mathrm{QBH} \to \mathrm{u} + \mathrm{e}^-)$	4 dim[4]	ADD n = 5	ADD n = 6	ADD n = 7	RS
center of mass energy of $\sqrt{s} = 7\,\mathrm{TeV}$					
$M_* = 1\,\mathrm{TeV}$	2.89×10^{-2}	1.96×10^{1}	2.64×10^{1}	3.37×10^{1}	9.48×10^{-1}
$M_* = 3\,\mathrm{TeV}$	3.52×10^{-7}	2.45×10^{-4}	3.31×10^{-4}	4.23×10^{-4}	1.18×10^{-5}
$M_* = 5\,\mathrm{TeV}$	4.45×10^{-12}	3.10×10^{-9}	4.19×10^{-9}	5.35×10^{-9}	1.49×10^{-10}
center of mass energy of $\sqrt{s} = 8\,\mathrm{TeV}$					
$M_* = 1\,\mathrm{TeV}$	5.59×10^{-2}	3.72×10^{1}	5.02×10^{1}	6.40×10^{1}	1.81
$M_* = 3\,\mathrm{TeV}$	1.83×10^{-6}	1.28×10^{-3}	1.73×10^{-3}	2.21×10^{-3}	6.15×10^{-5}
$M_* = 5\,\mathrm{TeV}$	1.57×10^{-10}	1.09×10^{-7}	1.48×10^{-7}	1.89×10^{-7}	5.25×10^{-9}
center of mass energy of $\sqrt{s} = 14\,\mathrm{TeV}$					
$M_* = 1\,\mathrm{TeV}$	6.07×10^{-1}	3.52×10^{2}	4.74×10^{2}	6.04×10^{2}	1.78×10^{1}
$M_* = 3\,\mathrm{TeV}$	2.57×10^{-4}	1.79×10^{-1}	2.41×10^{-1}	3.08×10^{-1}	8.60×10^{-3}
$M_* = 5\,\mathrm{TeV}$	1.03×10^{-6}	7.21×10^{-4}	9.73×10^{-4}	1.24×10^{-3}	3.46×10^{-5}

Table 6.14: *Cross sections for discrete QBHs decaying into an electron and up-quark with lepton and quark flavor, as well as B-L violated and only Lorentz invariance conserved (model 5). The suitable initial state consists of an antiup-quark and an antidown-quark.*

cross section in fb	model for low scale quantum gravity				
$\sigma\,(\mathrm{QBH} \to \mathrm{d} + \mu^+)$	4 dim[4]	ADD n = 5	ADD n = 6	ADD n = 7	RS
center of mass energy of $\sqrt{s} = 7\,\mathrm{TeV}$					
$M_* = 1\,\mathrm{TeV}$	4.57×10^{-2}	3.12×10^{1}	4.21×10^{1}	5.37×10^{1}	1.51
$M_* = 3\,\mathrm{TeV}$	3.61×10^{-7}	2.51×10^{-4}	3.40×10^{-4}	4.34×10^{-4}	1.21×10^{-5}
$M_* = 5\,\mathrm{TeV}$	5.48×10^{-12}	3.82×10^{-9}	5.16×10^{-9}	6.59×10^{-9}	1.84×10^{-10}
center of mass energy of $\sqrt{s} = 8\,\mathrm{TeV}$					
$M_* = 1\,\mathrm{TeV}$	8.98×10^{-2}	6.03×10^{1}	8.13×10^{1}	1.04×10^{2}	2.93
$M_* = 3\,\mathrm{TeV}$	1.94×10^{-6}	1.36×10^{-3}	1.83×10^{-3}	2.34×10^{-3}	6.52×10^{-5}
$M_* = 5\,\mathrm{TeV}$	1.79×10^{-10}	1.25×10^{-7}	1.68×10^{-7}	2.15×10^{-7}	5.99×10^{-9}
center of mass energy of $\sqrt{s} = 14\,\mathrm{TeV}$					
$M_* = 1\,\mathrm{TeV}$	9.79×10^{-1}	5.74×10^{2}	7.73×10^{2}	9.85×10^{2}	2.89×10^{1}
$M_* = 3\,\mathrm{TeV}$	3.57×10^{-4}	2.48×10^{-1}	3.35×10^{-1}	4.28×10^{-1}	1.19×10^{-2}
$M_* = 5\,\mathrm{TeV}$	1.12×10^{-6}	7.79×10^{-4}	1.05×10^{-3}	1.34×10^{-3}	3.74×10^{-5}

Table 6.15: *Cross sections for discrete QBHs decaying into an anti-muon and down quark with lepton as well as quark flavor violated, but B-L and Lorentz invariance conserved (model 4). The suitable initial state for such a process consists of two antidown-quarks.*

cross section in fb	model for low scale quantum gravity				
$\sigma\,(\mathrm{QBH} \to \mathrm{d} + \mu^+)$	4 dim[4]	ADD n = 5	ADD n = 6	ADD n = 7	RS
center of mass energy of $\sqrt{s} = 7\,\mathrm{TeV}$					
$M_* = 1\,\mathrm{TeV}$	3.66×10^{-2}	2.49×10^{1}	3.37×10^{1}	4.30×10^{1}	1.21
$M_* = 3\,\mathrm{TeV}$	2.88×10^{-7}	2.01×10^{-4}	2.72×10^{-4}	3.47×10^{-4}	9.66×10^{-6}
$M_* = 5\,\mathrm{TeV}$	4.38×10^{-12}	3.06×10^{-9}	4.13×10^{-9}	5.27×10^{-9}	1.47×10^{-10}
center of mass energy of $\sqrt{s} = 8\,\mathrm{TeV}$					
$M_* = 1\,\mathrm{TeV}$	7.18×10^{-2}	4.82×10^{1}	6.51×10^{1}	8.31×10^{1}	2.34
$M_* = 3\,\mathrm{TeV}$	1.56×10^{-6}	1.08×10^{-3}	1.47×10^{-3}	1.87×10^{-3}	5.21×10^{-5}
$M_* = 5\,\mathrm{TeV}$	1.43×10^{-10}	9.97×10^{-8}	1.35×10^{-7}	1.72×10^{-7}	4.79×10^{-9}
center of mass energy of $\sqrt{s} = 14\,\mathrm{TeV}$					
$M_* = 1\,\mathrm{TeV}$	7.83×10^{-1}	4.59×10^{2}	6.18×10^{2}	7.88×10^{2}	2.31×10^{1}
$M_* = 3\,\mathrm{TeV}$	2.86×10^{-4}	1.99×10^{-1}	2.68×10^{-1}	3.43×10^{-1}	9.55×10^{-3}
$M_* = 5\,\mathrm{TeV}$	8.93×10^{-7}	6.23×10^{-4}	8.41×10^{-4}	1.07×10^{-3}	2.99×10^{-5}

Table 6.16: *Cross sections for discrete QBHs decaying into an anti-muon and down quark with lepton as well as quark flavor, and B-L violated and only Lorentz invariance conserved (model 5). The suitable initial state for such a process consists of two antidown-quarks.*

Chapter 7

Enhancement of supersymmetric particle production via quantum black holes

Despite the LHC accumulating data at an impressive pace, there is so far no indication of physics beyond the Standard Model. On the contrary, the discovery of a Higgs boson with a mass of 125 GeV would fit very nicely with the minimal Standard Model. Additionally, this may be an indication that the hierarchy problem was not the correct principle to guide us towards physics beyond the Standard Model but simply a fine tuning problem. As long as no further physics beyond the Standard Model is detected, the lack of observation of new particles beyond the Standard Model ones proves to be a blow to models designed to stabilize the value of the Higgs mass at the weak scale. Thus, it is particularly serious for supersymmetric models which justification lies precisely in stabilizing the Higgs potential which comes at the expense of introducing a plethora of new particles and some tedious model building to break supersymmetry.

One could argue that supersymmetry is useful to unify the gauge couplings of the Standard Model and give up the hierarchy problem as suggested in [92, 93] but it has been demonstrated recently that threshold corrections, whether they are due to quantum gravitational physics or strong dynamics above the unification scale, can account very nicely for the numerical unification of these couplings without having to introduce new particles below the grand unification scale [94–97]. While supersymmetry may not be relevant at the weak scale, it has been recently emphasized that this symmetry is important for quantum gravity [98]. However, below the Planck scale, this symmetry could be broken as jokingly suggested in the supersplit supersymmetry April fools' day paper [99].

In this paper we advocate that if supersymmetry is broken at a very high energy scale and even in a supersplit scenario, the particles of that sector must interact gravitationally with the particles of the Standard Model. In particular, quantum black holes must be able to mediate transitions from our sector, i.e. the Standard Model, to the hidden supersector. In order to illustrate our point, we shall consider the Minimal Supersymmetric Standard Model (MSSM) with all supersymmetric particles, including an extra Higgs boson, to have masses of the order of the Planck scale. Actually, quantum black holes could be a gateway to any hidden sector that interacts only gravitationally with the particles of the Standard Model. If supersymmetry is restored at the Planck scale, it is apparent that besides being produced via quantum black holes, superpartners of the Standard Model particles will obviously also be produced via the well studied processes. Quantum black holes would thus lead to an enhancement of the cross sections and allow to expand the search for superpartners beyond the expected reach of the LHC in traditional supersymmetric searches. The black hole production cross section is given, by the geometric cross section introduced in the previous chapters and is for high center of mass energies much larger than any usual particle physics cross section.

While models with low scale quantum gravity [1–4, 78] have been introduced to address the hierarchy problem, the real value in these ideas was to show that we do not know from first principles the energy scale at which quantum gravitational effects become strong. Indeed, the Planck scale could be anywhere between a few TeV and the traditional 10^{19} GeV. If the Planck scale is low, and accessible to the LHC, supersymmetric particles must be produced in quantum black hole processes as well. Due to their masses close to the Planck scale and their resulting non-thermal character, QBHs are expected to decay to only a couple of particles immediately after their creation. The interaction with matter is fixed with regard to the classification of the QBHs presented in Section 5.2, i.e. they are classified according to their Lorentz, $U(1)_{em}$ and $SU(3)_c$ groups. This leads to most of the QBHs carrying a $SU(3)_c$ charge as well as QED charges. We will use their classification to predict their decay, including supersymmetric particles, by means of their production process. We will consider the enhancement of supersymmetric particles through QBH processes for a continuous as well as a discrete mass spectrum. In both cases, we extrapolate the production cross section from the semi-classical case, see Chapters 5 and 6,

respectively. For a continuous mass spectrum, the cross section is given by

$$\sigma^{(pp)}(s, x_{min}, n, M_*) = \int_0^1 2zdz \int_{\frac{(x_{min}M_*)^2}{y(z)^2 s}}^1 du \int_u^1 \frac{dv}{v} \times F(n)\pi r_s^2(us, n, M_*) \sum_{i,j} f_i(v, Q) f_j(u/v, Q) \tag{7.1}$$

where the $(n+4)$-dimensional Schwarzschild radius takes the form

$$r_s(us, n, M_*) = \left[2^n \sqrt{\pi}^{n-3} \frac{\Gamma((3+n)/2)}{2+n}\right]^{1/(1+n)} M_*^{-1} [\frac{\sqrt{us}}{M_*}]^{1/(1+n)} \quad . \tag{7.2}$$

For QBHs with discrete masses, on the other hand, one assumes the total cross section to be the sum of the individual ones:

$$\sigma_{tot}^{(pp)}(s, n, M_*) = \sum_i \sigma_{QBH}^{(pp)}(s, M_{QBH}^i, n, M_*) \quad , \tag{7.3}$$

with

$$\sigma_{QBH}^{pp}(s, M_{QBH}, n, M_*) = \pi r_s^2(M_{QBH}, n, M_*) \int_0^1 2zdz \int_{\frac{(M_{QBH})^2}{y(z)^2 s}}^1 du \int_u^1 \frac{dv}{v} \times F(n) \sum_{i,j} f_i(v, Q) f_j(u/v, Q) \quad . \tag{7.4}$$

The Schwarzschild radius, now being constant, is expressed by

$$r_s(M_{QBH}^2, n, M_*) = \left[2^n \sqrt{\pi}^{n-3} \frac{\Gamma((3+n)/2)}{2+n}\right]^{1/(1+n)} M_*^{-1} [\sqrt{M_{QBH}^2}/M_*]^{1/(1+n)} \quad . \tag{7.5}$$

This obviously yields to the total cross sections given in Chapters 5 and 6.

For reasons of clarity and since it serves to illustrate the purpose of this work, we will present the cross sections for all possible final states for a Planck mass of 3 TeV and a 14 TeV LHC. We thus assume that the first quantum black hole has a mass of 3 TeV. The total cross sections for this scenario are given in Table 7.1. Since the particle

	4 dim	ADD $n=5$	ADD $n=6$	ADD $n=7$	RS
continuous	6.56×10^2	3.12×10^5	4.17×10^5	5.29×10^5	1.73×10^4
discrete	4.40×10^2	2.97×10^5	4.00×10^5	5.12×10^5	1.44×10^4

Table 7.1: *Total cross sections for discrete and continuous QBHs at* $M_* = 3$ TeV *and* $\sqrt{s} = 14$ TeV *in fb, considering that all symmetries are conserved.*

spectrum of supersymmetric theories is much richer than in the Standard Model, the branching ratios calculated and used in [15, 16] have to be revisited. This was done by D.Fragkakis, assuming that the particle spectrum at the Planck scale is that of the

MSSM, and the branching ratios can be viewed in Section D, Tables D.1 to D.5. It should again be noted that the term branching ratio is not used in its usual sense but to describe the decomposition of a collection of black holes created by the same initial states particles. Obviously, the branching ratios are strongly dependent on the symmetries which are preserved by quantum gravity. Here we are as conservative as possible and assume that gauge symmetries, flavor symmetries, B-L number and Lorentz invariance are conserved. Following the procedure in Chapters 5 and 6, the cross section for a specific final state in the continuous case is obtained by summing over the production cross sections of the contributing QBHs which have been multiplied with the desired branching ratio (cf. Tables D.1 to D.5):

$$\sigma_{\text{QBH}\to\text{final state}} = \sum_{\substack{\text{average}\\ \text{initial states}}} \sigma_{\text{initial state}\to\text{QBH}} \times \text{BR}_{\text{final state}} \,.$$

Each cross section for a specific initial state was calculated using the Monte Carlo integration algorithm developed for Chapter 5. We then multiply the result with the suitable branching ratios. The desired cross section for the chosen final state is given by taking the average over all initial state contributions. We considered an ADD brane world model with 5, 6 and 7 extra dimensions [1, 2], the Randall Sundrum model [3] with one warped extra dimension and a four-dimensional model with TeV quantum gravity presented in [4].

Assuming that space-time is quantized at short distances and that there is a minimal length [86, 88–91], the mass distribution is expected to be partitioned in terms of the Planck mass. As before, the cross section for a specific final state is obtained by summing over the production cross sections of the contributing QBHs which have been multiplied with the desired branching ratio Tables (2) to (9):

$$\sigma_{\text{QBH}\to\text{final state}} = \sum_{\substack{\text{average}\\ \text{initial states}}} \sum_{\text{masses}} \sigma_{\text{initial state}\to\text{QBH}_{\text{mass}}} \times \text{BR}_{\text{final state,model}} \,.$$

For the sake of illustration we take a Planck mass of 3 TeV and a center of mass energy of 14 TeV. The minimal quantum black hole mass is 3 TeV and we set all the Yoshino and Nambu functions to one. We find that if the reduced Planck scale is in the TeV region, the cross section for the production of superpartners could be quite large even in a supersplit scenario, indeed they are typically large at least for the continuous black mass scenario. The production cross section for each decay mode is obtained by multiplying the production cross section for quantum black holes in a given model and multiplying it by the appropriate branching ratio. Note that the conservation laws we have chosen allow

transitions of the type $uu \to \tilde{u}\tilde{u}$ which look like a baryon number violating operator. One should, however, keep in mind that these operators are only relevant for energies $\sqrt{s} \sim M_P$ since there is a threshold energy for the production of quantum black holes. These effective operators could, become problematic if inserted into loops. Since very little is known about quantum gravity and the physics of these quantum black holes, we choose not to worry about it. It could be that these holes do not couple to long wavelength and highly off-shell perturbative modes are suppressed or that B is conserved in these processes. In the latter case, quantum black holes formed by two quarks would always decay back to two quarks, while quantum black holes formed by a gluon and a (anti-) quark, two gluons or a quark and anti-quark would still be allowed to decay into the superpartners of Standard Model particles. The numerical cross sections for the different final states allowed in our model can be found in the following tables; the continuous mass case cross sections in Tables 7.2 to 7.5 are obviously larger than the one obtained for a discrete mass spectrum (Tables 7.6 to 7.9). Note that if the supersymmetric particles all have masses equal to the Planck scale, i.e. 3 TeV in the value we took to illustrate our framework, the signature for supersymmetric particles would be quite different from usual ones. While they will be produced via the well studied typical supersymmetric production mechanism, they will principally be produced via quantum black hole processes. Note that quantum black holes with masses smaller than twice the Planck scale would not decay into the supersymmetric sector as there is no phase space available. For heavier black holes, in our example heavier than 6 TeV, they would be able to decay to two supersymmetric objects which would decay quickly to two standard model particles and an extra supersymmetric one via the usual supersymmetric decay channels. This production mechanism is very different from the standard ones and dedicated searches should be considered.

Particle 1	Particle 2	4 dim	ADD n=5	ADD n=6	ADD n=7	RS
u	u	6.69	3.02×10^{3}	4.03×10^{3}	5.11×10^{3}	1.70×10^{2}
u	$\bar{u}$	1.68×10^{-1}	8.50×10^{1}	1.14×10^{2}	1.45×10^{2}	4.60
u	d	2.65	1.25×10^{3}	1.68×10^{3}	2.13×10^{3}	6.96×10^{1}
u	$\bar{d}$	4.69×10^{-1}	2.41×10^{2}	3.23×10^{2}	4.10×10^{2}	1.30×10^{1}
$\bar{u}$	d	1.11×10^{-1}	5.75×10^{1}	7.70×10^{1}	9.78×10^{1}	3.09
$\bar{u}$	$\bar{d}$	1.49×10^{-2}	8.06	1.08×10^{1}	1.37×10^{1}	4.26×10^{-1}
d	d	9.20×10^{-1}	4.50×10^{2}	6.02×10^{2}	7.64×10^{2}	2.47×10^{1}
d	$\bar{d}$	1.46×10^{-1}	7.53×10^{1}	1.01×10^{2}	1.28×10^{2}	4.05
$\bar{u}$	$\bar{u}$	8.90×10^{-3}	4.75	6.37	8.09	2.52×10^{-1}
$\bar{d}$	$\bar{d}$	1.35×10^{-2}	7.45	1.00×10^{1}	1.27×10^{1}	3.91×10^{-1}
u	g	4.82×10^{-1}	2.42×10^{2}	3.24×10^{2}	4.11×10^{2}	1.31×10^{1}
u	γ	6.02×10^{-2}	3.02×10^{1}	4.05×10^{1}	5.14×10^{1}	1.64
u	Z^0	6.02×10^{-2}	3.02×10^{1}	4.05×10^{1}	5.14×10^{1}	1.64
u	H	2.01×10^{-2}	1.01×10^{1}	1.35×10^{1}	1.71×10^{1}	5.47×10^{-1}
u	G	4.01×10^{-2}	2.01×10^{1}	2.70×10^{1}	3.42×10^{1}	1.09
d	g	1.66×10^{-1}	8.53×10^{1}	1.14×10^{2}	1.45×10^{2}	4.59
d	γ	2.07×10^{-2}	1.07×10^{1}	1.43×10^{1}	1.81×10^{1}	5.74×10^{-1}
d	Z^0	2.07×10^{-2}	1.07×10^{1}	1.43×10^{1}	1.81×10^{1}	5.74×10^{-1}
d	H	6.90×10^{-3}	3.55	4.76	6.05	1.91×10^{-1}
d	G	1.38×10^{-2}	7.11	9.52	1.21×10^{1}	3.82×10^{-1}
$\bar{u}$	g	1.67×10^{-2}	8.90	1.19×10^{1}	1.52×10^{1}	4.74×10^{-1}
$\bar{u}$	γ	2.09×10^{-3}	1.11	1.49	1.90	5.92×10^{-2}
$\bar{u}$	Z^0	2.09×10^{-3}	1.11	1.49	1.90	5.92×10^{-2}
$\bar{u}$	H	6.97×10^{-4}	3.71×10^{-1}	4.97×10^{-1}	6.32×10^{-1}	1.97×10^{-2}
$\bar{u}$	G	1.39×10^{-3}	7.42×10^{-1}	9.95×10^{-1}	1.26	3.95×10^{-2}
$\bar{d}$	g	2.23×10^{-2}	1.21×10^{1}	1.62×10^{1}	2.06×10^{1}	6.38×10^{-1}
$\bar{d}$	γ	2.79×10^{-3}	1.51	2.02	2.57	7.97×10^{-2}
$\bar{d}$	Z^0	2.79×10^{-3}	1.51	2.02	2.57	7.97×10^{-2}
$\bar{d}$	H	9.30×10^{-4}	5.02×10^{-1}	6.74×10^{-1}	8.56×10^{-1}	2.66×10^{-2}
$\bar{d}$	G	1.86×10^{-3}	1.00	1.35	1.71	5.31×10^{-2}

Table 7.2: *Continuous mass spectrum black holes. Particle 1 and Particle 2 refer to the particles produced in the decomposition of the black hole. For illustration, we considered a center of mass energy of 14 TeV with a Planck scale of 3 TeV and a minimal black hole mass of 3 TeV. All cross sections are in fb.*

Particle 1	Particle 2	4 dim	ADD n=5	ADD n=6	ADD n=7	RS
l^-	l^+	7.78×10^{-3}	3.96	5.31	6.74	2.14×10^{-1}
ν	$\bar{\nu}$	7.78×10^{-3}	3.96	5.31	6.74	2.14×10^{-1}
g	g	3.24×10^{-2}	1.71×10^{1}	2.29×10^{1}	2.91×10^{1}	9.12×10^{-1}
g	γ	1.17×10^{-2}	6.10	8.18	1.04×10^{1}	3.27×10^{-1}
g	Z^0	2.67×10^{-2}	1.37×10^{1}	1.84×10^{1}	2.34×10^{1}	7.39×10^{-1}
g	H	1.50×10^{-2}	7.63	1.02×10^{1}	1.30×10^{1}	4.12×10^{-1}
g	G	1.50×10^{-2}	7.63	1.02×10^{1}	1.30×10^{1}	4.12×10^{-1}
γ	γ	1.04×10^{-3}	5.40×10^{-1}	7.24×10^{-1}	9.20×10^{-1}	2.90×10^{-2}
γ	Z^0	2.92×10^{-3}	1.49	2.00	2.54	8.06×10^{-2}
γ	H	1.87×10^{-3}	9.54×10^{-1}	1.28	1.62	5.16×10^{-2}
γ	G	1.87×10^{-3}	9.54×10^{-1}	1.28	1.62	5.16×10^{-2}
Z^0	Z^0	2.92×10^{-3}	1.49	2.00	2.54	8.06×10^{-2}
Z^0	H	1.87×10^{-3}	9.54×10^{-1}	1.28	1.62	5.16×10^{-2}
Z^0	G	2.20×10^{-3}	1.13	1.51	1.92	6.08×10^{-2}
W^-	W^+	2.92×10^{-3}	1.49	2.00	2.54	8.06×10^{-2}
H	H	7.18×10^{-4}	3.67×10^{-1}	4.92×10^{-1}	6.25×10^{-1}	1.98×10^{-2}
H	G	3.26×10^{-4}	1.73×10^{-1}	2.32×10^{-1}	2.95×10^{-1}	9.21×10^{-3}
G	G	2.82×10^{-3}	1.44	1.94	2.46	7.79×10^{-2}

Table 7.3: *Continuous mass spectrum black holes. Particle 1 and Particle 2 refer to the particles produced in the decomposition of the black hole. For illustration, we considered a center of mass energy of 14 TeV with a Planck scale of 3 TeV and a minimal black hole mass of 3 TeV. All cross sections are in fb.*

Particle 1	Particle 2	4 dim	ADD n=5	ADD n=6	ADD n=7	RS
$\tilde{u}$	$\tilde{u}$	1.67	7.54×10^{2}	1.01×10^{3}	1.28×10^{3}	4.26×10^{1}
$\tilde{u}$	$\tilde{\bar{u}}$	4.55×10^{-2}	2.31×10^{1}	3.10×10^{1}	3.94×10^{1}	1.25
$\tilde{u}$	$\tilde{d}$	6.63×10^{-1}	3.14×10^{2}	4.19×10^{2}	5.32×10^{2}	1.74×10^{1}
$\tilde{u}$	$\tilde{\bar{d}}$	1.17×10^{-1}	6.02×10^{1}	8.07×10^{1}	1.02×10^{2}	3.24
$\tilde{\bar{u}}$	$\tilde{d}$	2.79×10^{-2}	1.44×10^{1}	1.93×10^{1}	2.45×10^{1}	7.73×10^{-1}
$\tilde{\bar{u}}$	$\tilde{\bar{d}}$	3.72×10^{-3}	2.02	2.70	3.44	1.06×10^{-1}
$\tilde{d}$	$\tilde{d}$	2.30×10^{-1}	1.12×10^{2}	1.50×10^{2}	1.91×10^{2}	6.17
$\tilde{d}$	$\tilde{\bar{d}}$	4.00×10^{-2}	2.07×10^{1}	2.77×10^{1}	3.52×10^{1}	1.11
$\tilde{\bar{u}}$	$\tilde{\bar{u}}$	2.23×10^{-3}	1.19	1.59	2.02	6.31×10^{-2}
$\tilde{\bar{d}}$	$\tilde{\bar{d}}$	3.38×10^{-3}	1.86	2.50	3.18	9.79×10^{-2}
$\tilde{u}$	$\tilde{g}$	1.61×10^{-1}	8.06×10^{1}	1.08×10^{2}	1.37×10^{2}	4.38
$\tilde{u}$	$\tilde{\gamma}$	2.01×10^{-2}	1.01×10^{1}	1.35×10^{1}	1.71×10^{1}	5.47×10^{-1}
$\tilde{u}$	$\tilde{Z}^0$	2.01×10^{-2}	1.01×10^{1}	1.35×10^{1}	1.71×10^{1}	5.47×10^{-1}
$\tilde{u}$	$\tilde{H}$	2.01×10^{-2}	1.01×10^{1}	1.35×10^{1}	1.71×10^{1}	5.47×10^{-1}
$\tilde{u}$	$\tilde{G}$	4.01×10^{-2}	2.01×10^{1}	2.70×10^{1}	3.42×10^{1}	1.09
$\tilde{d}$	$\tilde{g}$	5.52×10^{-2}	2.84×10^{1}	3.81×10^{1}	4.84×10^{1}	1.53
$\tilde{d}$	$\tilde{\gamma}$	6.90×10^{-3}	3.55	4.76	6.05	1.91×10^{-1}
$\tilde{d}$	$\tilde{Z}^0$	6.90×10^{-3}	3.55	4.76	6.05	1.91×10^{-1}
$\tilde{d}$	$\tilde{H}$	6.90×10^{-3}	3.55	4.76	6.05	1.91×10^{-1}
$\tilde{d}$	$\tilde{G}$	1.38×10^{-2}	7.11	9.52	1.21×10^{1}	3.82×10^{-1}
$\tilde{\bar{u}}$	$\tilde{g}$	5.58×10^{-3}	2.97	3.98	5.06	1.58×10^{-1}
$\tilde{\bar{u}}$	$\tilde{\gamma}$	6.97×10^{-4}	3.71×10^{-1}	4.97×10^{-1}	6.32×10^{-1}	1.97×10^{-2}
$\tilde{\bar{u}}$	$\tilde{Z}^0$	6.97×10^{-4}	3.71×10^{-1}	4.97×10^{-1}	6.32×10^{-1}	1.97×10^{-2}
$\tilde{\bar{u}}$	$\tilde{H}$	6.97×10^{-4}	3.71×10^{-1}	4.97×10^{-1}	6.32×10^{-1}	1.97×10^{-2}
$\tilde{\bar{u}}$	$\tilde{G}$	1.39×10^{-3}	7.42×10^{-1}	9.95×10^{-1}	1.26	3.95×10^{-2}
$\tilde{\bar{d}}$	$\tilde{g}$	7.44×10^{-3}	4.02	5.39	6.85	2.13×10^{-1}
$\tilde{\bar{d}}$	$\tilde{\gamma}$	9.30×10^{-4}	5.02×10^{-1}	6.74×10^{-1}	8.56×10^{-1}	2.66×10^{-2}
$\tilde{\bar{d}}$	$\tilde{Z}^0$	9.30×10^{-4}	5.02×10^{-1}	6.74×10^{-1}	8.56×10^{-1}	2.66×10^{-2}
$\tilde{\bar{d}}$	$\tilde{H}$	9.30×10^{-4}	5.02×10^{-1}	6.74×10^{-1}	8.56×10^{-1}	2.66×10^{-2}
$\tilde{\bar{d}}$	$\tilde{G}$	1.86×10^{-3}	1.00	1.35	1.71	5.31×10^{-2}

Table 7.4: *Continuous mass spectrum black holes. Particle 1 and Particle 2 refer to the particles produced in the decomposition of the black hole. For illustration, we considered a center of mass energy of 14 TeV with a Planck scale of 3 TeV and a minimal black hole mass of 3 TeV. All cross sections are in fb.*

Particle 1	Particle 2	4 dim	ADD n=5	ADD n=6	ADD n=7	RS
$\tilde{l^-}$	$\tilde{l^+}$	2.15×10^{-3}	1.10	1.48	1.88	5.94×10^{-2}
$\tilde{\nu}$	$\tilde{\bar{\nu}}$	2.15×10^{-3}	1.10	1.48	1.88	5.94×10^{-2}
$\tilde{g}$	$\tilde{g}$	2.85×10^{-2}	1.46×10^{1}	1.96×10^{1}	2.49×10^{1}	7.87×10^{-1}
$\tilde{g}$	$\tilde{\gamma}$	2.15×10^{-2}	1.10×10^{1}	1.47×10^{1}	1.87×10^{1}	5.92×10^{-1}
$\tilde{g}$	$\tilde{Z^0}$	2.15×10^{-2}	1.10×10^{1}	1.47×10^{1}	1.87×10^{1}	5.92×10^{-1}
$\tilde{g}$	$\tilde{H}$	2.00×10^{-2}	1.02×10^{1}	1.36×10^{1}	1.73×10^{1}	5.50×10^{-1}
$\tilde{g}$	$\tilde{G}$	1.50×10^{-2}	7.63	1.02×10^{1}	1.30×10^{1}	4.12×10^{-1}
$\tilde{\gamma}$	$\tilde{\gamma}$	2.59×10^{-3}	1.32	1.77	2.25	7.14×10^{-2}
$\tilde{\gamma}$	$\tilde{Z^0}$	2.59×10^{-3}	1.32	1.77	2.25	7.14×10^{-2}
$\tilde{\gamma}$	$\tilde{H}$	2.50×10^{-3}	1.27	1.70	2.16	6.87×10^{-2}
$\tilde{\gamma}$	$\tilde{G}$	1.87×10^{-3}	9.54×10^{-1}	1.28	1.62	5.16×10^{-2}
$\tilde{Z^0}$	$\tilde{Z^0}$	2.59×10^{-3}	1.32	1.77	2.25	7.14×10^{-2}
$\tilde{Z^0}$	$\tilde{H}$	2.59×10^{-3}	1.32	1.77	2.25	7.14×10^{-2}
$\tilde{Z^0}$	$\tilde{G}$	2.20×10^{-3}	1.13	1.51	1.92	6.08×10^{-2}
$\tilde{W^-}$	$\tilde{W^+}$	2.59×10^{-3}	1.32	1.77	2.25	7.14×10^{-2}
$\tilde{H}$	$\tilde{H}$	2.59×10^{-3}	1.32	1.77	2.25	7.14×10^{-2}
$\tilde{H}$	$\tilde{G}$	2.20×10^{-3}	1.13	1.51	1.92	6.08×10^{-2}
$\tilde{G}$	$\tilde{G}$	2.82×10^{-3}	1.44	1.94	2.46	7.79×10^{-2}

Table 7.5: *Continuous mass spectrum black holes. Particle 1 and Particle 2 refer to the particles produced in the decomposition of the black hole. For illustration, we considered a center of mass energy of 14 TeV with a Planck scale of 3 TeV and a minimal black hole mass of 3 TeV. All cross sections are in fb.*

Particle 1	Particle 2	4 dim	ADD n=5	ADD n=6	ADD n=7	RS
u	u	4.33	2.87×10^{3}	3.87×10^{3}	4.94×10^{3}	1.40×10^{2}
u	$\bar{u}$	1.18×10^{-1}	8.10×10^{1}	1.09×10^{2}	1.40×10^{2}	3.90
u	d	1.76	1.19×10^{3}	1.61×10^{3}	2.05×10^{3}	5.77×10^{1}
u	$\bar{d}$	3.32×10^{-1}	2.29×10^{2}	3.10×10^{2}	3.95×10^{2}	1.10×10^{1}
$\bar{u}$	d	7.93×10^{-2}	5.48×10^{1}	7.39×10^{1}	9.44×10^{1}	2.64
$\bar{u}$	$\bar{d}$	1.11×10^{-2}	7.72	1.04×10^{1}	1.33×10^{1}	3.71×10^{-1}
d	d	6.25×10^{-1}	4.27×10^{2}	5.76×10^{2}	7.36×10^{2}	2.06×10^{1}
d	$\bar{d}$	1.04×10^{-1}	7.17×10^{1}	9.68×10^{1}	1.24×10^{2}	3.46
$\bar{u}$	$\bar{u}$	6.54×10^{-3}	4.54	6.13	7.83	2.18×10^{-1}
$\bar{d}$	$\bar{d}$	1.03×10^{-2}	7.15	9.66	1.23×10^{1}	3.44×10^{-1}
u	g	3.35×10^{-1}	2.30×10^{2}	3.11×10^{2}	3.97×10^{2}	1.11×10^{1}
u	γ	4.19×10^{-2}	2.88×10^{1}	3.88×10^{1}	4.96×10^{1}	1.39
u	Z^0	4.19×10^{-2}	2.88×10^{1}	3.88×10^{1}	4.96×10^{1}	1.39
u	H	1.40×10^{-2}	9.59	1.29×10^{1}	1.65×10^{1}	4.63×10^{-1}
u	G	2.80×10^{-2}	1.92×10^{1}	2.59×10^{1}	3.31×10^{1}	9.25×10^{-1}
d	g	1.18×10^{-1}	8.13×10^{1}	1.10×10^{2}	1.40×10^{2}	3.92
d	γ	1.47×10^{-2}	1.02×10^{1}	1.37×10^{1}	1.75×10^{1}	4.89×10^{-1}
d	Z^0	1.47×10^{-2}	1.02×10^{1}	1.37×10^{1}	1.75×10^{1}	4.89×10^{-1}
d	H	4.91×10^{-3}	3.39	4.57	5.84	1.63×10^{-1}
d	G	9.81×10^{-3}	6.77	9.14	1.17×10^{1}	3.26×10^{-1}
$\bar{u}$	g	1.23×10^{-2}	8.51	1.15×10^{1}	1.47×10^{1}	4.10×10^{-1}
$\bar{u}$	γ	1.53×10^{-3}	1.06	1.44	1.83	5.12×10^{-2}
$\bar{u}$	Z^0	1.53×10^{-3}	1.06	1.44	1.83	5.12×10^{-2}
$\bar{u}$	H	5.11×10^{-4}	3.55×10^{-1}	4.79×10^{-1}	6.12×10^{-1}	1.71×10^{-2}
$\bar{u}$	G	1.02×10^{-3}	7.09×10^{-1}	9.58×10^{-1}	1.22	3.41×10^{-2}
$\bar{d}$	g	1.66×10^{-2}	1.15×10^{1}	1.56×10^{1}	1.99×10^{1}	5.55×10^{-1}
$\bar{d}$	γ	2.08×10^{-3}	1.44	1.95	2.49	6.94×10^{-2}
$\bar{d}$	Z^0	2.08×10^{-3}	1.44	1.95	2.49	6.94×10^{-2}
$\bar{d}$	H	6.92×10^{-4}	4.81×10^{-1}	6.49×10^{-1}	8.29×10^{-1}	2.31×10^{-2}
$\bar{d}$	G	1.38×10^{-3}	9.62×10^{-1}	1.30	1.66	4.63×10^{-2}

Table 7.6: *Discrete mass spectrum quantum black holes. Particle 1 and Particle 2 refer to the particles produced in the decomposition of the black hole. For illustration, we considered a center of mass energy of 14 TeV with a Planck scale of 3 TeV and a minimal black hole mass of 3 TeV. All cross sections are in fb.*

Particle 1	Particle 2	4 dim	ADD n=5	ADD n=6	ADD n=7	RS
l^-	l^+	5.48×10^{-3}	3.77	5.10	6.51	1.82×10^{-1}
ν	$\bar{\nu}$	5.48×10^{-3}	3.77	5.10	6.51	1.82×10^{-1}
g	g	2.36×10^{-2}	1.63×10^{1}	2.20×10^{1}	2.82×10^{1}	7.86×10^{-1}
g	γ	8.43×10^{-3}	5.82	7.86	1.00×10^{1}	2.80×10^{-1}
g	Z^0	1.90×10^{-2}	1.31×10^{1}	1.77×10^{1}	2.26×10^{1}	6.31×10^{-1}
g	H	1.05×10^{-2}	7.26	9.81	1.25×10^{1}	3.50×10^{-1}
g	G	1.05×10^{-2}	7.26	9.81	1.25×10^{1}	3.50×10^{-1}
γ	γ	7.46×10^{-4}	5.15×10^{-1}	6.96×10^{-1}	8.89×10^{-1}	2.48×10^{-2}
γ	Z^0	2.06×10^{-3}	1.42	1.92	2.45	6.86×10^{-2}
γ	H	1.32×10^{-3}	9.08×10^{-1}	1.23	1.57	4.38×10^{-2}
γ	G	1.32×10^{-3}	9.08×10^{-1}	1.23	1.57	4.38×10^{-2}
Z^0	Z^0	2.06×10^{-3}	1.42	1.92	2.45	6.86×10^{-2}
Z^0	H	1.32×10^{-3}	9.08×10^{-1}	1.23	1.57	4.38×10^{-2}
Z^0	G	1.56×10^{-3}	1.07	1.45	1.85	5.17×10^{-2}
W^-	W^+	2.06×10^{-3}	1.42	1.92	2.45	6.86×10^{-2}
H	H	5.08×10^{-4}	3.50×10^{-1}	4.72×10^{-1}	6.03×10^{-1}	1.69×10^{-2}
H	G	2.39×10^{-4}	1.65×10^{-1}	2.23×10^{-1}	2.85×10^{-1}	7.96×10^{-3}
G	G	2.00×10^{-3}	1.38	1.86	2.37	6.63×10^{-2}

Table 7.7: *Discrete mass spectrum quantum black holes. Particle 1 and Particle 2 refer to the particles produced in the decomposition of the black hole. For illustration, we considered a center of mass energy of 14 TeV with a Planck scale of 3 TeV and a minimal black hole mass of 3 TeV. All cross sections are in fb.*

Particle 1	Particle 2	4 dim	ADD n=5	ADD n=6	ADD n=7	RS
$\tilde{u}$	$\tilde{u}$	1.08	7.17×10^{2}	9.68×10^{2}	1.24×10^{3}	3.49×10^{1}
$\tilde{u}$	$\tilde{\bar{u}}$	3.20×10^{-2}	2.20×10^{1}	2.98×10^{1}	3.80×10^{1}	1.06
$\tilde{u}$	$\tilde{d}$	4.41×10^{-1}	2.98×10^{2}	4.02×10^{2}	5.13×10^{2}	1.44×10^{1}
$\tilde{u}$	$\tilde{\bar{d}}$	8.31×10^{-2}	5.73×10^{1}	7.74×10^{1}	9.88×10^{1}	2.76
$\tilde{\bar{u}}$	$\tilde{d}$	1.98×10^{-2}	1.37×10^{1}	1.85×10^{1}	2.36×10^{1}	6.59×10^{-1}
$\tilde{\bar{u}}$	$\tilde{\bar{d}}$	2.78×10^{-3}	1.93	2.61	3.33	9.28×10^{-2}
$\tilde{d}$	$\tilde{d}$	1.56×10^{-1}	1.07×10^{2}	1.44×10^{2}	1.84×10^{2}	5.16
$\tilde{d}$	$\tilde{\bar{d}}$	2.86×10^{-2}	1.97×10^{1}	2.67×10^{1}	3.40×10^{1}	9.51×10^{-1}
$\tilde{\bar{u}}$	$\tilde{\bar{u}}$	1.64×10^{-3}	1.13	1.53	1.96	5.46×10^{-2}
$\tilde{\bar{d}}$	$\tilde{\bar{d}}$	2.57×10^{-3}	1.79	2.41	3.08	8.60×10^{-2}
$\tilde{u}$	$\tilde{g}$	1.12×10^{-1}	7.67×10^{1}	1.04×10^{2}	1.32×10^{2}	3.70
$\tilde{u}$	$\tilde{\gamma}$	1.40×10^{-2}	9.59	1.29×10^{1}	1.65×10^{1}	4.63×10^{-1}
$\tilde{u}$	$\tilde{Z}^0$	1.40×10^{-2}	9.59	1.29×10^{1}	1.65×10^{1}	4.63×10^{-1}
$\tilde{u}$	$\tilde{H}$	1.40×10^{-2}	9.59	1.29×10^{1}	1.65×10^{1}	4.63×10^{-1}
$\tilde{u}$	$\tilde{G}$	2.80×10^{-2}	1.92×10^{1}	2.59×10^{1}	3.31×10^{1}	9.25×10^{-1}
$\tilde{d}$	$\tilde{g}$	3.93×10^{-2}	2.71×10^{1}	3.66×10^{1}	4.67×10^{1}	1.31
$\tilde{d}$	$\tilde{\gamma}$	4.91×10^{-3}	3.39	4.57	5.84	1.63×10^{-1}
$\tilde{d}$	$\tilde{Z}^0$	4.91×10^{-3}	3.39	4.57	5.84	1.63×10^{-1}
$\tilde{d}$	$\tilde{H}$	4.91×10^{-3}	3.39	4.57	5.84	1.63×10^{-1}
$\tilde{d}$	$\tilde{G}$	9.81×10^{-3}	6.77	9.14	1.17×10^{1}	3.26×10^{-1}
$\tilde{\bar{u}}$	$\tilde{g}$	4.09×10^{-3}	2.84	3.83	4.89	1.37×10^{-1}
$\tilde{\bar{u}}$	$\tilde{\gamma}$	5.11×10^{-4}	3.55×10^{-1}	4.79×10^{-1}	6.12×10^{-1}	1.71×10^{-2}
$\tilde{\bar{u}}$	$\tilde{Z}^0$	5.11×10^{-4}	3.55×10^{-1}	4.79×10^{-1}	6.12×10^{-1}	1.71×10^{-2}
$\tilde{\bar{u}}$	$\tilde{H}$	5.11×10^{-4}	3.55×10^{-1}	4.79×10^{-1}	6.12×10^{-1}	1.71×10^{-2}
$\tilde{\bar{u}}$	$\tilde{G}$	1.02×10^{-3}	7.09×10^{-1}	9.58×10^{-1}	1.22	3.41×10^{-2}
$\tilde{\bar{d}}$	$\tilde{g}$	5.54×10^{-3}	3.85	5.19	6.63	1.85×10^{-1}
$\tilde{\bar{d}}$	$\tilde{\gamma}$	6.92×10^{-4}	4.81×10^{-1}	6.49×10^{-1}	8.29×10^{-1}	2.31×10^{-2}
$\tilde{\bar{d}}$	$\tilde{Z}^0$	6.92×10^{-4}	4.81×10^{-1}	6.49×10^{-1}	8.29×10^{-1}	2.31×10^{-2}
$\tilde{\bar{d}}$	$\tilde{H}$	6.92×10^{-4}	4.81×10^{-1}	6.49×10^{-1}	8.29×10^{-1}	2.31×10^{-2}
$\tilde{\bar{d}}$	$\tilde{G}$	1.38×10^{-3}	9.62×10^{-1}	1.30	1.66	4.63×10^{-2}

Table 7.8: *Discrete mass spectrum quantum black holes. Particle 1 and Particle 2 refer to the particles produced in the decomposition of the black hole. For illustration, we considered a center of mass energy of 14 TeV with a Planck scale of 3 TeV and a minimal black hole mass of 3 TeV. All cross sections are in fb.*

Particle 1	Particle 2	4 dim	ADD n=5	ADD n=6	ADD n=7	RS
$\tilde{l^-}$	$\tilde{l^+}$	1.52×10^{-3}	1.05	1.42	1.81	5.06×10^{-2}
$\tilde{\nu}$	$\tilde{\bar{\nu}}$	1.52×10^{-3}	1.05	1.42	1.81	5.06×10^{-2}
$\tilde{g}$	$\tilde{g}$	2.02×10^{-2}	1.39×10^{1}	1.88×10^{1}	2.40×10^{1}	6.71×10^{-1}
$\tilde{g}$	$\tilde{\gamma}$	1.52×10^{-2}	1.04×10^{1}	1.41×10^{1}	1.80×10^{1}	5.03×10^{-1}
$\tilde{g}$	$\tilde{Z^0}$	1.52×10^{-2}	1.04×10^{1}	1.41×10^{1}	1.80×10^{1}	5.03×10^{-1}
$\tilde{g}$	$\tilde{H}$	1.41×10^{-2}	9.69	1.31×10^{1}	1.67×10^{1}	4.67×10^{-1}
$\tilde{g}$	$\tilde{G}$	1.05×10^{-2}	7.26	9.81	1.25×10^{1}	3.50×10^{-1}
$\tilde{\gamma}$	$\tilde{\gamma}$	1.83×10^{-3}	1.26	1.70	2.17	6.06×10^{-2}
$\tilde{\gamma}$	$\tilde{Z^0}$	1.83×10^{-3}	1.26	1.70	2.17	6.06×10^{-2}
$\tilde{\gamma}$	$\tilde{H}$	1.76×10^{-3}	1.21	1.63	2.09	5.84×10^{-2}
$\tilde{\gamma}$	$\tilde{G}$	1.32×10^{-3}	9.08×10^{-1}	1.23	1.57	4.38×10^{-2}
$\tilde{Z^0}$	$\tilde{Z^0}$	1.83×10^{-3}	1.26	1.70	2.17	6.06×10^{-2}
$\tilde{Z^0}$	$\tilde{H}$	1.83×10^{-3}	1.26	1.70	2.17	6.06×10^{-2}
$\tilde{Z^0}$	$\tilde{G}$	1.56×10^{-3}	1.07	1.45	1.85	5.17×10^{-2}
$\tilde{W^-}$	$\tilde{W^+}$	1.83×10^{-3}	1.26	1.70	2.17	6.06×10^{-2}
$\tilde{H}$	$\tilde{H}$	1.83×10^{-3}	1.26	1.70	2.17	6.06×10^{-2}
$\tilde{H}$	$\tilde{G}$	1.56×10^{-3}	1.07	1.45	1.85	5.17×10^{-2}
$\tilde{G}$	$\tilde{G}$	2.00×10^{-3}	1.38	1.86	2.37	6.63×10^{-2}

Table 7.9: *Discrete mass spectrum quantum black holes. Particle 1 and Particle 2 refer to the particles produced in the decomposition of the black hole. For illustration, we considered a center of mass energy of 14 TeV with a Planck scale of 3 TeV and a minimal black hole mass of 3 TeV. All cross sections are in fb.*

Chapter 8

Conclusion

Models of low scale gravity and their consequences have been studied in many publications, not only because they predict quantum gravity to be accessible at low energies and thus in the reach of ongoing colliders such as the LHC, but also because they provide approaches to resolve the seemingly unnatural hierarchy problem. The current lack of observation of any indications of physics beyond the Standard Model (SM) has been a setback for the excitement of these models. Nonetheless, the continuing studies and recent experiments prove to give essential insights into the quantum theory of gravitational effects. The search of extra dimensions yielded to fruitful combined studies in both fields of particle and astrophysics. They undoubtedly give limits, e.g. on the fundamental Planck mass, which bring us closer to a better understanding of processes in such an energy regime.

In this thesis we reviewed the leading models suggesting a low scale quantum gravity, see Chapter 2. This includes the proposed large volume of extra dimensions, which was followed shortly after by the suggestion of the existence of one warped extra dimensions. In addition, we review the four-dimensional model that proposes a large hidden sector due to the running of the gravitational constant. Motivated by these models, the concept of black hole creation in high energy collisions was put forward and has been extensively studied up to the semi-classical regime. A review of black holes created in particle collisions is given in Chapter 3. A theoretical approach of Quantum Black Holes (QBHs), gravitational objects with masses close to the Planck scale, followed. In pursuit of the proposition of these non-thermal objects, the work presented in this thesis extends the theory regarding these objects.

In Chapter 4, we establish an effective way of describing the production mechanism of QBHs using SM quantum fields. Remaining in a model independent description, we were able to match the amplitude to the extrapolated geometrical cross section by applying

the necessary Feynman rules. Using an effective Lagrangian formulation for non-thermal QBHs, we derived bounds on the fundamental Planck mass. The reasonably good agreement between the experimental value of the anomalous magnetic moment of the muon and the theoretical predictions leads to a bound on the Planck mass of the order of 266 GeV, which only assumes that QBHs can be treated as virtual objects and couple to low energy modes. Additionally, we considered processes in which discrete symmetries, such as lepton number or CP, are violated by quantum gravitational physics. One obtains tighter limits on the energy scale at which quantum gravity effects become sizable, respectively 10^4 GeV and 10^3 GeV. These bounds are surprisingly weak. Again, we want to stress here that these limits are determined in a model independent way. On the other hand, we find that the limit coming from the lack of observation of proton decay is much tighter and unless this decomposition is forbidden by some mechanism, it represents the tightest limit to date on the reduced Planck mass. Note that cosmic rays allow one to set a limit on the four-dimensional Planck mass of about 500 GeV [40], but there are several theoretical uncertainties in that bound. In contrast, the limits presented in this paper are rather model independent. A consequence of our result is that the assumption made in [17] concerning the coupling of QBHs to long wave modes or their lack of virtuality can be relaxed. Unless quantum gravity violates CP, QBHs could well be within the reach of the LHC.

Chapter 5 deals with the production and decay of QBHs with a continuous mass spectrum at the LHC within several frameworks for low scale quantum gravity. We investigated the processes in ADD with $n = 5, 6$, and 7 extra dimensions, Randall and Sundrum's brane world and a 4-dimensional construction proposed in [4]. The collisions are assumed to take place at the different center of mass energies and we present the total production cross sections for 7 TeV to 14 TeV. Several models corresponding to different symmetry conservation laws are studied and the cross sections for the following specific final states are given: A QBH decaying into two photons, an electron-positron pair and accordingly an electron-antimuon pair, an electron and up-quark, and an antimuon and down-quark. The Planck scale is taken to be 1 TeV, 3 TeV, and 5 TeV. We find that the cross sections can be sizable, depending on the value of the Planck scale. For the LHC operating at a center of mass energy of 7 TeV and 8 TeV, the cross sections are, generally speaking, only able to probe a Planck mass in the 1 TeV region. We observe the expected increase in the total cross section with center of mass energy of the process and for models with a higher number of extra dimensions. For higher Planck masses, the cross sections decrease rapidly due to the momentum dependence of the parton distribution functions. It shall be noted

that all cross sections calculated in this thesis have been determined using LHAPDF[1] [85] with the CTEQ6 parton distribution functions [84] and could be calculated for any other set of parton distribution functions (PDFs). The different PDFs do not change the order of magnitude of the results, we observed only a slight discrepancy compared to using the CTEQ5M [100]. For the choice of momentum scale, we found that it results in a difference between choosing the fundamental Planck mass and the inverse Schwarzschild radius of maximal 20%, so not affecting the order of magnitude either. The discrepancy is actually smaller for most cases, increasing with the size of the Planck scale.

With regard to specific final states, we anticipate that the SM background for these center of mass energies is likely to be too large to probe a Planck scale higher than 2 TeV. For a 14 TeV LHC, we expect to be able probe the Planck scale up to 3 TeV. For rare events, such as final states with a muon and a positron or an electron and up-quark back to back, one could potentially test a larger Planck scale due to absent background of SM processes. To quantify an exact reach of the LHC, a dedicated background study and detector simulation is required which goes beyond the scope of this thesis. The implementation of this model into the black hole generator BlackMax will, however, allows the user to make assumptions about the quantum gravitational regime. We emphasize that the limits found in the literature on the production of small, semi-classical, black holes do not apply to those considered here.

Acknowledging models proposing the existence of a minimal length in quantum gravity [86–91], we considered a discrete mass spectrum for QBHs in Chapter 6. As expected, due to the underlying phenomenology in quantizing the discrete states, we find lower total cross sections than in Chapter 5. Although the nature of the discrete QBHs is more particle-like than in the continuous case, where the QBHs rather correspond to gravitational scattering, the discussed objects resemble plateau shaped signatures. The considered spacing in terms of the examined Planck scale yields clearly to smaller cross section. It shall be noted that in case of a fixed quantization, e.g. 1 TeV, and higher Planck masses, i.e. 3 TeV or 5 TeV, this characteristic is not given. How the mass spectrum is quantized cannot be known without a complete understanding of quantum gravity and it would be interesting to compare our proposed discretization to different ones in future projects. Since we do not restrict ourselves to a certain symmetry model for quantum gravity, the same branching ratios as portrayed for the continuous case apply to the final states of discrete QBHs. This is reasonable if one assumes that the same quantum numbers, i.e. $SU(3)_c$, U(1) and

[1] For more information refer to Section C.

spin are conserved. As for the continuous case, we assume a large SM background for most of the final states, which resemble two jets back to back, whereas final states with two photons or two leptons should be easy to identify at the Large Hadron Collider and should be the focus of searches. It shall be highlighted that in case of a quantum theory of gravity that violates lepton, quark flavor, or even B-L, we find more exotic signatures, such as a high transverse momentum muon and a high transverse momentum positron back to back or a muon-down-quark pair final state, which cross sections are shown in this chapter. These final states would undoubtedly be smoking guns for non-thermal quantum black holes and could enable one to probe considerably higher Planck scales.

In Chapter 7 we argued that even if supersymmetry is broken at the Planck scale, the superpartners of the Standard Model particles must couple gravitationally to their Standard Model partners. We extend the decay mechanism to include all supersymmetric cases and present all possible final state cross sections for a center of mass energy of 14 TeV and a Planck scale of 3 TeV. Quantum black holes could thus be a portal into the supersymmetric world and we estimated the enhancement of the production cross sections of supersymmetric particles. Under the considered assumptions about supersymmetry, we have shown that in models with low scale quantum gravity, supersymmetric particles could be produced with large cross sections at the studied center of mass energy. The signatures for these transitions are rather different from standard supersymmetric ones and a discovery of supersymmetry in this scenario would require dedicated searches. It shall be noted that the branching ratios in this case consider quantum gravity to conserve all quantum numbers. Since the understanding of a quantum theory of gravity is still far from complete, it would be sensible to direct future research into less conservative symmetry restrictions, such as quark and lepton flavor violating processes.

It is important to note that for the production of QBHs, we assumed that the cross section can be extrapolated from the semi-classical case. This has been done by using an effective way of describing the physics of QBHs by matching the cross sections to each other. One can thus not picture the description as a full effective field theory in the usual sense, i.e. higher-dimensional operators will only change the procedure of the matching but not the cross section or its precision. With this extrapolation in mind, QBHs have much smaller masses and entropies than semi-classical black holes and their decay cannot be described thermally. They are so to speak particle-like and couple only to a few particles, allowing for a description using SM fields. We do, however, expect them to couple only to low energy modes and assume that processes involving QBHs conserve QCD and U(1) charges.

In other words, quantum gravity does not violate local gauge symmetries but we make no such assumption about global charges, for which we provide a number of different applicable symmetry restrictions.

With searches for physics beyond the Standard Model at current experiments in energy regions which have never been reached in collider experiments before, we are closer to probing the quantum gravity regime than we have ever been before. If the Planck scale is indeed lower than traditionally expected, one of the most interesting signatures would definitely be the production of quantum black holes. With experimental bounds starting to appear [71–73] and theoretical predictions, we cannot only learn about the theory of quantum black holes but also set limits on the scale at which quantum gravitational effects become relevant.

Bibliography

[1] N. Arkani-Hamed, S. Dimopoulos, and G. Dvali. "The hierarchy problem and new dimensions at a millimeter". *Phys.Lett. B*, 429:263–272, 1998. [arXiv:hep-ph/9803315]. 1, 5, 6, 31, 82, 84

[2] N. Arkani-Hamed, S. Dimopoulos, and G. Dvali. "Phenomenology, astrophysics, and cosmology of theories with submillimeter dimensions and TeV scale quantum gravity". *Phys.Rev. D*, 59(086004), 1999. [arXiv:hep-ph/9807344]. 5, 6, 84

[3] L. Randall and R. Sundrum. "Large Mass Hierarchy from a Small Extra Dimension". *Phys.Rev.Lett.*, 83(17):3370–3373, 1999. [arXiv:hep-ph/9905221]. 5, 9, 31, 84

[4] X. Calmet, S.D.H. Hsu, and D. Reeb. "Quantum gravity at a TeV and the renormalization of Newton's constant". *Phys.Rev. D*, 77(125015), 2008. [arXiv:0803.1836 [hep-th]]. 1, 5, 12, 31, 53, 54, 56, 57, 58, 59, 60, 61, 62, 63, 64, 69, 70, 71, 72, 73, 74, 75, 76, 77, 78, 79, 80, 82, 84, 95

[5] http://home.web.cern.ch/about/accelerators/large-hadron-collider. 1

[6] S. Dimopoulos and G.L. Landsberg. "Black holes at the LHC". *Phys.Rev.Lett.*, 87(161602), 2001. [arXiv:hep-ph/0106295]. 2, 23, 27, 108, 109

[7] T. Banks and W. Fischler. "A Model for High Energy Scattering in Quantum Gravity". 1999. [arXiv:hep-th/9906038]. 16, 24, 27

[8] S.B. Giddings and S.D. Thomas. "High energy colliders as black hole factories: The end of short distance physics". *Phys.Rev. D*, 65(056010), 2002. [arXiv:hep-ph/0106219]. 23, 24, 26, 27, 108, 109

[9] J.L. Feng and A.D. Shapere. "Black hole production by cosmic rays". *Phys.Rev.Lett.*, 88(021303), 2002. [arXiv:hep-ph/0109106].

[10] L.A. Anchordoqui, J.L. Feng, H. Goldberg, and A.D. Shapere. "Black holes from cosmic rays: Probes of extra dimensions and new limits on TeV-scale gravity". *Phys.Rev. D*, 65(124027), 2002. [arXiv:hep-ph/0112247].

[11] L.A. Anchordoqui, J.L. Feng, H. Goldberg, and A.D. Shapere. "Updated limits on TeV-scale gravity from absence of neutrino cosmic ray showers mediated by black holes". *Phys.Rev. D*, 68(104025), 2003. [arXiv:hep-ph/0307228]. 23, 25

[12] L.A. Anchordoqui, J.L. Feng, H. Goldberg, and A.D. Shapere. "Inelastic black hole production and large extra dimensions". *Phys.Lett. B*, 594(363), 2004. [arXiv:hep-ph/0311365]. 27, 40

[13] D.C. Dai, G. Starkman, D. Stojkovic, C. Issever, E. Rizvi, and J. Tseng. "BlackMax: A black-hole event generator with rotation, recoil, split branes, and brane tension". *Phys.Rev. D*, 77(076007), 2008. [arXiv:0711.3012 [hep-ph]]. 2, 39

[14] X. Calmet, D. Fragkakis, and N. Gausmann. "The flavor of quantum gravity". *Eur.Phys.J. C*, 71(1781), 2011. [arXiv:1105.1779 [hep-ph]]. 2, 31

[15] X. Calmet, D. Fragkakis, and N. Gausmann. *"Non thermal small black holes"*, pages 165–170. Nova Science Publishers, 2012. [arXiv:1201.4463 [hep-ph]]. 2, 3, 39, 65, 66, 83

[16] X. Calmet and N. Gausmann. "Non-thermal quantum black holes with quantized masses". *Int. J. Mod. Phys. A*, 28:1350045, 2013. [arXiv:1209.4618 [hep-ph]]. 2, 3, 39, 65, 83

[17] X. Calmet, W. Gong, and S.D.H. Hsu. "Colorful quantum black holes at the LHC". *Phys.Lett. B*, 668(20), 2008. [arXiv:0806.4605 [hep-ph]]. 2, 28, 31, 34, 40, 52, 95

[18] D.J. Kapner et al. "Tests of the Gravitational Inverse-Square Law below the Dark-Energy Length Scale". *Phys.Rev.Lett.*, 98(021101), 2007. [arXiv:hep-ph/0611184]. 4

[19] J. Beringer et al. (Particle Data Group). *Phys.Rev. D*, 86:010001, 2012. [http://pdg.lbl.gov]. 5, 31, 35, 36, 118

[20] I. Antoniadis, N. Arkani-Hamed, S. Dimopoulos, and G. Dvali. "New dimensions at a millimeter to a fermi and superstrings at a TeV". *Phys.Lett. B*, 436:257–263, 1998. [arXiv:hep-ph/9804398]. 5, 6

[21] L. Randall and R. Sundrum. "An Alternative to Compactification". *Phys.Rev.Lett.*, 83:4690–4693, 1999. [arXiv:hep-th/9906064]. 5, 9, 10

[22] T. Kaluza. "On the Problem of Unity in Physics". *Sitzungsber.Preuss.Akad.Wiss.Berlin*, (Math.Phys.):966–972, 1921. 5

[23] O. Klein. "Quantum Theory and Five-Dimensional Theory of Relativity (In German and English)". *Z.Phys.*, 37:895–906, 1926. 5

[24] A. Perez-Lorenzana. "An Introduction to Extra Dimensions". *J.Phys.Conf.Ser.*, 18:224–269, 2005. [arXiv:hep-ph/0503177]. 6

[25] P. Kanti. "Black Holes at the LHC". *Lect. Notes Phys.*, 769:387–423, 2009. [arXiv:0802.2218 [hep-th]]. 16, 21

[26] H.-C. Cheng. "2009 TASI Lecture, Introduction to Extra Dimensions". 2009. [arXiv:1003.1162 [hep-ph]].

[27] M. Gabella. "The Randall-Sundrum Model". [www-thphys.physics.ox.ac.uk/people/MaximeGabella/rs.pdf]. 6, 9

[28] I. Antoniadis. "A possible new dimension at a few TeV". *Phys.Lett. B*, 246:377–384, 1990. 6

[29] V.A. Rubakov and M.E. Shaposhnikov. "Do we live inside a domain wall?". *Phys.Lett. B*, 125(2-3):136–138, 1983. 9

[30] D. Reeb. "Running of Newton's Constant and Quantum Gravitational Effects". 2009. Proceedings of the International School of Subnuclear Physics, 46th course: "Predicted and totally unexpected in the energy frontier opened by LHC" (Ed. A. Zichichi), World Scientific (2011), [arXiv:0901.2963 [hep-th]]. 12

[31] X. Calmet. "Primordial Black Holes and a Large Hidden Sector". *Phys.Rev. D*, 82(087501), 2010. [arXiv:1007.2919 [hep-ph]].

[32] X. Calmet. "Renormalization of Newton's constant and Particle Physics". to appear in the proceedings of the 12th Marcel Grossman Meeting, [arXiv:1002.0473 [hep-ph]]. 12

[33] F. Larsen and F. Wilczek. "Renormalization of Black Hole Entropy and of the Gravitational Coupling Constant". *Nucl. Phys. B*, 458:249–266, 1996. [arXiv:hep-th/9506066]. 14, 15

[34] B.S. DeWitt. *"Dynamical theory of groups and fields"*. Gordon and Breach, 1965. 14

[35] B.S. DeWitt. "Quantum field theory in curved spacetime". *Phys. Rept.*, 19(6):295–357, 1975.

[36] N.D. Birrell and P.C.W. Davies. "Quantum fields in curved space". 1982. [with corrections 1984]. 14

[37] R. Balian and C. Bloch. "Distribution of eigenfrequencies for the wave equation in a finite domain. II. Electromagnetic field. Riemannian spaces". *Annals of Phys.*, 64(1):271–307, 1971. 14

[38] G. Dvali, G. Gabadadze, M. Kolanovic, and F. Nitti. "Scales of Gravity". *Phys.Rev. D*, 65(024031), 2001. [arXiv:hep-th/0106058]. 15

[39] G. Dvali and M. Redi. "Black Hole Bound on the Number of Species and Quantum Gravity at LHC". *Phys.Rev. D*, 77(045027), 2008. [arXiv:0710.4344 [hep-th]]. 15

[40] X. Calmet and M. Feliciangeli. "Bound on four-dimensional Planck mass". *Phys.Rev. D*, 78(067702), 2008. [arXiv:0806.4304 [hep-ph]]. 15, 95

[41] K.S. Thorne. *"Nonspherical gravitational collapse: A short review"*, pages 231–258. 1972. 17, 23

[42] D. Ida and K.-i. Nakao. "Isoperimetric inequality for higher-dimensional black holes". *Phys.Rev. D*, 66(064026), 2002. 17

[43] R. Emparan, G.T. Horowitz, and R.C. Myers. "Black holes Radiate Mainly on the Brane". *Phys.Rev.Lett.*, 85:499–502, 2000. [arXiv:hep-th/0003118]. 17, 27

[44] R. Emparan. "Black Hole Radiation On and Off the Brane". volume Proceeding style, 2000. Contribution to the Proceedings of the TMR Conference "Non-Perturbative Quantum Effects 2000", [arXiv:hep-th/0009136]. 17, 27

[45] F. R. Tangherlini. "Schwarzschild field in n dimensions and the dimensionality of space problem". *Nuovo Cimento*, 27:636–651, 1963. 17

[46] R.C. Myers and M.J. Perry. "Black holes in higher dimensional space-times". *Annals of Phys.*, 172(2):304–347, 1986. 17, 26

[47] G.F. Giudice, R. Rattazzi, and J.D. Wells. "Quantum Gravity and Extra Dimensions at High-Energy Colliders". *Nucl. Phys. B*, 544:3–38, 1999. [arXiv:hep-ph/9811291]. 17, 109

[48] P. Meade and L. Randall. "Black holes and Quantum Gravity at the LHC". *JHEP*, 0805(003), 2008. [arXiv:0708.3017 [hep-ph]]. 18, 27, 28, 31, 32, 37, 40

[49] P.C. Aichelburg and R.U. Sexl. "On the gravitational field of a massless particle". *Gen. Rel. & Grav.*, 2(4):303–312, 1971. 18, 19

[50] K.A. Khan and R. Penrose. "Scattering of Two Impulsive Gravitational Plane Waves". *Nature*, 229:185–186, 1971.

[51] P.D. D'Eath and P.N. Payne. "Gravitational Radiation In High Speed Black Hole Collisions. 1. Perturbation Treatment Of The Axisymmetric Speed Of Light Collision". *Phys.Rev. D*, 46(658), 1992. 21

[52] P.D. D'Eath and P.N. Payne. "Gravitational Radiation In High Speed Black Hole Collisions. 2. Reduction To Two Independent Variables And Calculation Of The Second Order News Function". *Phys.Rev. D*, 46(675), 1992.

[53] P.D. D'Eath and P.N. Payne. "Gravitational radiation in high speed black hole collisions. 3. Results and conclusions". *Phys.Rev. D*, 46(694), 1992. 18, 21

[54] B. Schutz. *"A First Course in GENERAL RELATIVITY"*. Cambridge University Press, 2 edition, 2009. 18

[55] C.W. Misner, K.S. Thorne, and J.A. Wheeler. *"GRAVITATION"*. W. H. Freeman and Company, 1970. 18

[56] R. Penrose. unpublished. presented at a seminar at Cambridge University, 1974. 21

[57] D.M. Eardley and S.B. Giddings. "Classical black hole production in high-energy collisions". *Phys.Rev. D*, 66(044011):1–7, 2002. [arXiv:gr-qc/0201034]. 21, 22, 23, 24, 25, 27, 67

[58] H. Yoshino and Y. Nambu. "High-energy head-on collisions of particles and hoop conjecture". *Phys.Rev. D*, 66:065004, 2003. [arXiv:gr-qc/0204060]. 22

[59] H. Yoshino and Y. Nambu. "Black hole formation in the grazing collision of high-energy particles". *Phys.Rev. D*, 67:024009, 2003. [arXiv:gr-qc/0209003]. 22, 24, 40, 66

[60] E. Kohlprath and G. Veneziano. "Black holes from high-energy beam-beam collisions". *JHEP*, 0206:057, 2002. [arXiv:gr-qc/0203093]. 24

[61] H. Yoshino and V.S. Rychkov. "Improved analysis of black hole formation in high-energy particle collisions". *Phys.Rev. D*, 71(104028), 2005. [arXiv:hep-th/0503171], [Erratum-ibid. Phys.Rev. D **77**, 089905 (2008)]. 24, 40, 51, 66, 117

[62] S.D.H. Hsu. "Quantum production of black holes". *Phys.Lett. B*, 555(92), 2003. [arXiv:hep-ph/0203154]. 24, 26, 67

[63] L.A. Anchordoqui, J.L. Feng, H. Goldberg, and A.D. Shapere. "Neutrino Bounds on Astrophysical Sources and New Physics". *Phys.Rev.D*, 66:103002, 2002. [arXiv:hep-ph/0207139]. 25

[64] T.M. Gould, S.D.H. Hsu, and E.R. Poppitz. "Quantum Scattering from Classical Field Theory". *Nucl. Phys. B*, 437:83–106, 1995. [arXiv:hep-ph/94033539]. 26

[65] S.D.H. Hsu. "Quantum Scattering and Classical Solutions". 1994. in Sintra '94 NATO Workshop on Electroweak Physics and the Early Universe, [arXiv:hep-ph/9406234]. 26

[66] S.W. Hawking. "Particle creation by black holes". *Commun. Math. Phys.*, 43:199–220, 1975. [Eratum-ibid. **46**, 206 (1976)]. 26

[67] M. Cavaglia. "Black Hole and Brane Production in TeV Gravity: A Review". *Int. J. Mod. Phys. A*, 18:1843–1882, 2003. [arXiv:hep-ph/0210296]. 26

[68] P. Argyres, S. Dimopoulos, and J. March-Russel. "Black Holes and Sub-millimeter Dimensions". *Phys.Lett. B*, 441:96–104, 1998. [arXiv:hep-th/9808138]. 27

[69] M. Bleicher, P. Nicolini, M. Spencer, and E. Winstanley. "Micro black holes in the laboratory". *Int. J. Mod. Phys. E*, 20:7–14, 2011. [arXiv:1111.0657 [hep-th]]. 27

[70] G. Aad et al. "Search for New Physics in Dijet Mass and Angular Distributions in pp Collisions at sqrt(s) = 7 TeV Measured with the ATLAS Detector". 2011. (ATLAS Collaboration) [arXiv:1103.3864 [hep-ex]]. 28, 31

[71] CMS Colaboration. "Search for microscopic black holes in pp collisions at sqrt(s) = 8 TeV". 2013. Submitted to JHEP, [arXiv:1303.5338 [hep-ex]]. 98

[72] ATLAS Collaboration. "Search for microscopic black holes in a like-sign dimuon final state using large track multiplicity with the ATLAS detector". 2013. Submitted to Phys. Rev. D, [arXiv:1308.4075 [hep-ex]].

[73] ATLAS Collaboration. "Search for new phenomena in photon+jet events collected in proton–proton collisions at sqrt(s) = 8 TeV with the ATLAS detector". 2013. Submitted to PLB, [arXiv:1309.3230 [hep-ex]]. 28, 31, 98

[74] B. Koch, M. Bleicher, and S. Hossenfelder. "Black Hole Remnants at the LHC". *JHEP*, 0510:053, 2005. [arXiv:hep-ph/0507138]. 29

[75] S. Hossenfelder. "News about TeV-scale Black Holes". *Nucl.Phys.A*, 774:865–868, 2006. [arXiv:hep-ph/0510236].

[76] G.L. Alberghi, L. Bellagamba, X. Calmet, R. Casadio, and O. Micu. "Charged Black Hole Remnants at the LHC". *Eur.Phys.J. C*, 73:2448, 2013. [arXiv:1303.3150 [hep-ph]]. 29

[77] G. Dvali, C. Gomez, and S. Mukhanov. "Black Hole Masses are Quantized". 2011. arXiv:1106.5894 [hep-ph]. 29, 40, 65

[78] X. Calmet. "A Review of Quantum Gravity at the Large Hadron Collider". *Mod.Phys.Lett. A*, 25(1553), 2010. [arXiv:1005.1805 [hep-ph]]. 31, 39, 82

[79] V.A. Kostelecky and S. Samuel. "Spontaneous Breaking of Lorentz Symmetry in String Theory". *Phys.Rev. D*, 39(683), 1989. 32

[80] P. Nakamura et al. (Particle Data Group). *J.Phy. G*, 37(075021), 2010. [http://pdg.lbl.gov]. 35, 36, 37, 43, 44

[81] D.M. Gingrich. "Quantum black holes with charge, colour, and spin at the LHC". *J.Phy. G*, 37(105108), 2010. [arXiv:0912.0826 [hep-ph]]. 45

[82] N. Gausmann. "QBH.cc". to be published as part of BlackMax 3.0, standalone version available as "QBH.cc". 51, 67, 114

[83] T. Hahn. "Cuba—a library for multidimensional numerical integration". *Comput. Phys. Commun.*, 168(2):78–95, 2005. [arXiv:hep-ph/0404043, sourcecode available at www.feynarts.de/cuba/]. 51, 114, 115

[84] J. Pumplin, D.R. Stump, J. Huston, H.L. Lai, P. Nadolsky, and W.K. Tung. "New Generation of Parton Distributions with Uncertainties from Global QCD Analysis". *JHEP*, 0207:012, 2002. [arXiv:hep-ph/0201195]. 51, 96

[85] M.R. Whalley, D. Bourilkov, and R.C. Group. "The Les Houches Accord PDFs (LHAPDF) and Lhaglue". 2005. Contribution to the HERALHC workshop, [arXiv:hep-ph/0508110 , http://hepforge.cedar.ac.uk/lhapdf/]. 51, 96

[86] L.J. Garay. "Quantum gravity and minimum length". *Int.J.Mod.Phys. A*, 10(145), 1995. [arXiv:gr-qc/9403008]. 65, 66, 84, 96

[87] C.A. Mead. "Possible Connection Between Gravitation and Fundamental Length". *Phys.Rev.*, 135(3B):B849–B862, 1964.

[88] X. Calmet, M. Graesser, and S.D.H. Hsu. "Minimum length from quantum mechanics and general relativity". *Phys.Rev.Lett.*, 93(211101), 2004. [arXiv:hep-th/0405033]. 84

[89] X. Calmet, M. Graesser, and S.D.H. Hsu. "Minimum length from first principles". *Int.J.Mod.Phys. D*, 14(2195), 2005. [arXiv:hep-th/0505144]. 65

[90] T. Padmanabhan. "Limitations On The Operational Definition Of Space-Time Events And Quantum Gravity". *Class.Quant.Grav.*, 4(L107), 1987.

[91] X. Calmet. "On the Precision of a Length Measurement". *Eur.Phys.J. C*, 54(501), 2008. [hep-th/0701073]. 66, 84, 96

[92] G.F. Giudice and A. Romanino. "Split Supersymmetry". *Nucl. Phys. B*, 699:65–89, 2004. Erratum-ibid.B706:65-89,2005, [arXiv:hep-ph/0406088]. 81

[93] N. Arkani-Hamed and S. Dimopoulos. "Supersymmetric Unification Without Low Energy Supersymmetry And Signatures for Fine-Tuning at the LHC". *JHEP*, 0506:073, 2005. [arXiv:hep-th/0405159]. 81

[94] X. Calmet, S.D.H. Hsu, and D. Reeb. "Grand unification and enhanced quantum gravitational effects". *Phys.Rev.Lett.*, 101:171802, 2008. [arXiv:0805.0145 [hep-ph]]. 81

[95] X. Calmet, S.D.H. Hsu, and D. Reeb. "Quantum Gravitational Effects and Grand Unification". volume 1078, pages 432–434, 2009. [arXiv:0809.3953 [hep-ph]].

[96] X. Calmet, S.D.H. Hsu, and D. Reeb. "Grand unification through gravitational effects". *Phys.Rev. D*, 81:035007, 2010. [arXiv:0911.0415 [hep-ph]].

[97] X. Calmet and T.C. Yang. "Gravitational Corrections to Fermion Masses in Grand Unified Theories". *Phys.Rev. D*, 84:037701, 2011. [arXiv:1105.0424 [hep-ph]]. 81

[98] S. Ferrara and A. Marrani. "Quantum Gravity Needs Supersymmetry". page 2012. Contribution to the Proceedings of the International School of Subnuclear Physics, 49th Course: "Searching for the Unexpected at LHC and Status of Our Knowledge", Erice, Italy, June 24 - July 3, 2011, [arXiv:1201.4328 [hep-th]]. 81

[99] P.J. Fox, D.E. Kaplan, E. Katz, E. Poppitz, V. Sanz, N. Weiner, M. Schmaltz, and M.D. Schwartz. "Supersplit supersymmetry". 2005. [arXiv:hep-th/0503249]. 81

[100] H.L. Lai, J. Huston, S. Kuhlmann, J. Morfin, F. Olness, J. F. Owens, J. Pumplin, and W. K. Tung. "Global QCD Analysis of Parton Structure of the Nucleon: CTEQ5 Parton Distributions". *Eur.Phys.J.*, C12:375–392, 1999. [arXiv:hep-ph/9903282]. 96

[101] S.B. Giddings. "Black hole production in TeV-scale gravity, and the future of high energy physics". *eConf*, C010630:P328, 2001. [arXiv:hep-ph/0110127]. 108

[102] "The Durham HepData Project - PDF plotter". [http://hepdata.cedar.ac.uk/pdf/pdf3.html]. 111, 112, 113

Appendix A

Dimensional analysis and Planck mass conventions

A.1 Dimensional analysis

In case of an dimensionless metric for higher dimensional space-times and considering natural units, we find for the following parameters:

- length: $[\text{length}] = [\text{mass}]^{-1}$
- compactification radius: $[R] = [\text{mass}]^{2}$
- Newton constant: $[G_N] = [\text{mass}]^{-2}$
- higher dimensional gravity coupling: $[G_*] = [\text{mass}]^{-(2+n)}$
- higher dimensional scalar field: $[\phi] = [\text{mass}]^{(1+n)/2}$

A.2 Planck mass conventions

In the literature, one finds different conventions for the relation of the higher-dimensional Planck mass M_* and Newton's fundamental gravitational constant G_*. Dimopoulos and Landsberg [6] define the Planck mass to be

$$M_{*_{DL}}^{n+2} = \frac{1}{G_*} \tag{A.1}$$

where n is the number of extra dimensions. On the other hand, Giddings and Thomas [8] (see also [101]) proposed the following convention

$$M_{*_{GT}}^{n+2} = \frac{(2\pi)^n}{4\pi\, G_*} \quad . \tag{A.2}$$

For the determination of the production cross section of QBHs, we use the PDG convention [47] which defines the ratio to be

$$M_{*_{PDG}}^{n+2} = \frac{(2\pi)^n}{8\pi\, G_*} \quad . \tag{A.3}$$

This yields to a relation of the different conventions of

$$M_{*_{PDG}}^{n+2} = \frac{(2\pi)^n}{8\pi} M_{*_{DL}}^{n+2} = \frac{1}{2} M_{*_{GT}}^{n+2} \quad . \tag{A.4}$$

Whereas there is a small relative correction between the convention used by Giddings and Thomas and the PDG convention, the factor between the convention proposed by Dimopoulos and Landsberg and the PDG convention becomes substantial for higher dimensions, see table A.1.

n	0	1	2	3	4	5	6	7
$M_{*_{PDG}}/M_{*_{DL}}$	0.20	0.63	1.12	1.58	1.99	2.34	2.65	2.92
$M_{*_{PDG}}/M_{*_{GT}}$	0.71	0.79	0.84	0.87	0.89	0.91	0.92	0.93

Table A.1: Relation between different conventions for the fundamental Planck mass depending on the number of extra dimensions n, where $M_{*_{PDG}}$ stands for the PDG convention [47], $M_{*_{DL}}$ for the convention introduced by Dimopoulos and Landsberg [6], and $M_{*_{GT}}$ for the convention by Giddings and Thomas [8].

Appendix B

Plots

B.1 Parton distribution functions

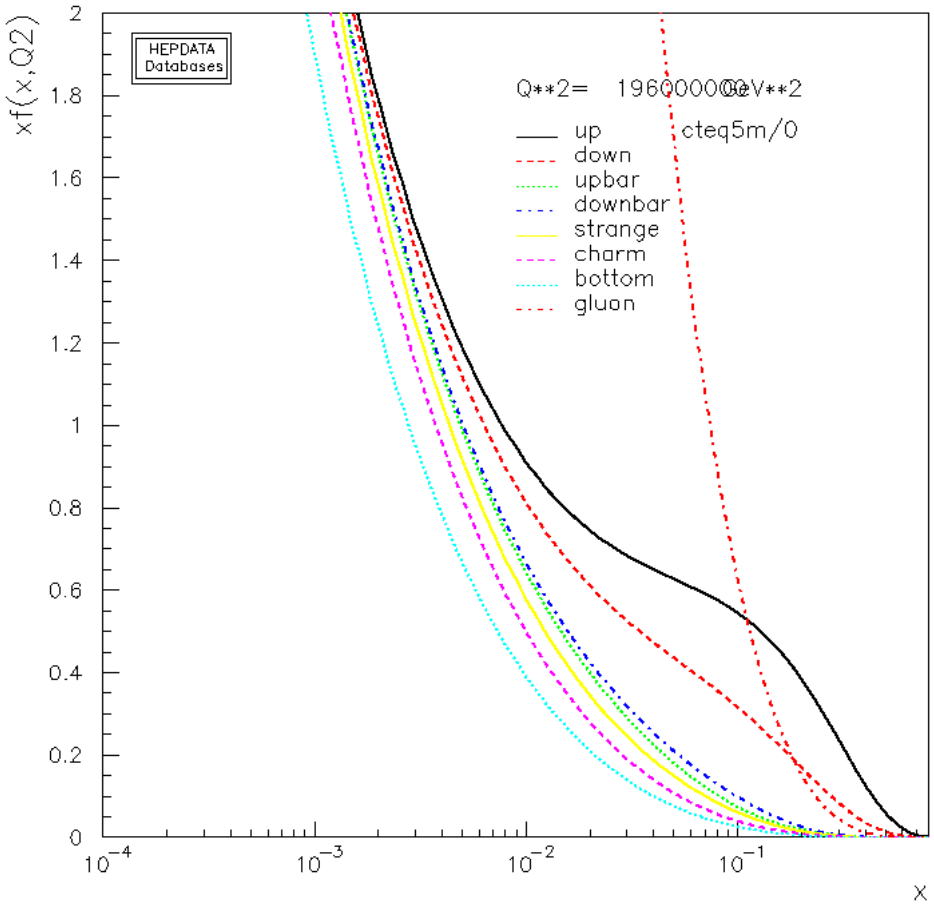

Figure B.1: Plot of the parton distribution function with the momentum scale Q chosen to be the center of mass energy $\sqrt{s} = 14\,\text{TeV}$. The parton distribution function $f(x, Q^2)$ multiplied by the momentum x for a variety of quarks and antiquarks is plotted against the momentum x. The plot was generated using the HepData PDF plotter [102].

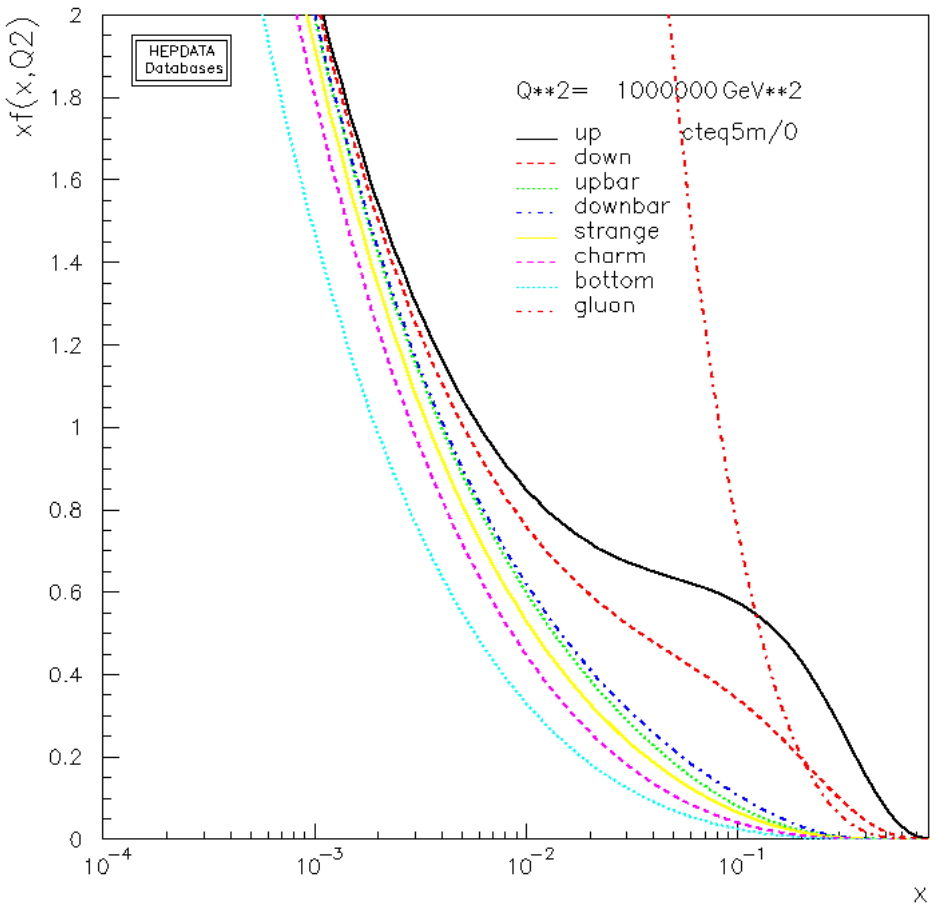

Figure B.2: Plot of the parton distribution function with the momentum scale Q chosen to be the fundamental Planck scale $M_* = 1\,\text{TeV}$. The parton distribution function $f(x, Q^2)$ multiplied by the momentum x for a variety of quarks and antiquarks is plotted against the momentum x. The plot was generated using the HepData PDF plotter [102].

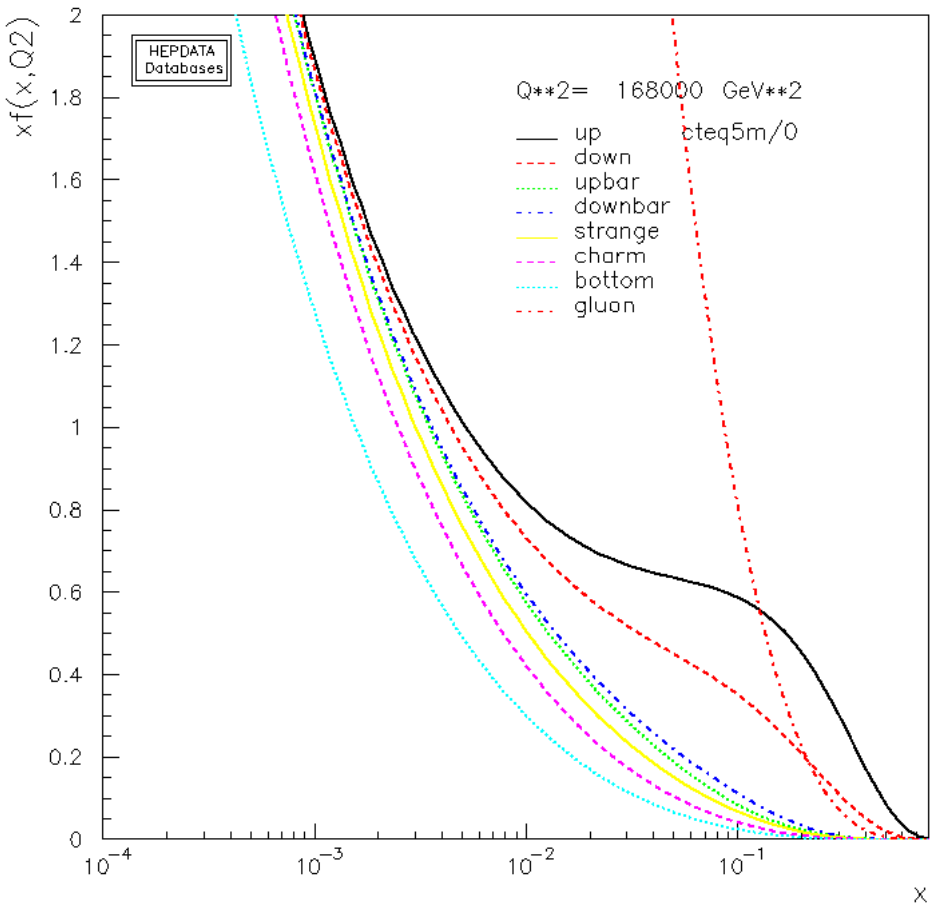

Figure B.3: Plot of the parton distribution function with the momentum scale Q chosen to be the fundamental Planck scale $r_s^{-1}(\sqrt{us} = 14\,\text{TeV}, n = 1, M_* = 1\,\text{TeV}) \approx 0.41\,\text{TeV}$. For purposes of illustration, we consider the ADD model with one extra dimension, a fundamental Planck scale of $M_* = 1\,\text{TeV}$, and a center of mass energy of $\sqrt{us} = 14\,\text{TeV}$. The parton distribution function $f(x, Q^2)$ multiplied by the momentum x for a variety of quarks and antiquarks is plotted against the momentum x. The plot was generated using the HepData PDF plotter [102].

Appendix C

Code Manual

This part of the thesis covers a manual for the C++ code "QBH.cc" [82] which is used to determine the cross sections of quantum black holes (QBHs) described in Chapter 5, 6 and 7. We will outline the installation process, including the necessary libraries and interfaces to compile and run the program, as well as the input and output.

C.1 Installation

The compilation of QBH.cc requires the GNU Compiler Collection (`GCC`). The program uses the Les Houches accord PDFs (LHAPDF) an interface that provides access to sets of parton distribution functions (PDFs). Since it is of essential use for the successful compilation of the program, the installation process is described in the following section. In addition, we cover the installation of `CUBA` [83] which is the library used for the multidimensional numerical integration.

C.1.1 LHAPDF interface

To download the most recent source code and find a detailed description of the interface, visit `lhapdf.hepforge.org`. After unpacking the tar file, change into the LHAPDF directory

```
cd lhapdf-"version"
```

of the downloaded version of LHAPDF. Choosing the low memory version and assuming that the user has root privileges, now configure with

```
./configure --enable-low-memory ,
```

whereas you would create an alternative directory and use

```
./configure --prefix=/path/to/directory --enable-low-memory
```

if you do not possess root privileges. To avoid causing issues with the configuration, the newly created directory has to be named differently from the LHAPDF directory. Now run

```
make
(sudo) make install
```

which should have created the static and dynamic library, respectively:

```
/usr/local/lib/libLHAPDF.a
/usr/local/lib/libLHAPDF.so .
```

To download a specific PDF set, use the command

```
lhapdf-getdata cteq6.LHpdf
```

where "cteq6.LHpdf" could be replaced by any other available PDF set, a comma separated list of PDF sets, a group of sets defined by the group name, e.g. "cteq", or the command "all" to download all available sets.

C.1.2 CUBA library

The stand-alone versions of QBH.cc use the Vegas algorithm of the CUBA library [83] for the numerical Monte Carlo integration. The source code can be downloaded at

```
www.feynarts.de/cuba/ .
```

After unzipping the directory, the user has to run the commands

```
.\configure
make
```

to finalize the installation of the library. This should have created the static library

```
libcuba.a
```

in the CUBA directory. The current version of QBH.cc uses the version CUBA-3.1.

C.2 Compilation and execution of QBH.cc

There are different models of QBH.cc depending on the considered theoretical background. The user has the opportunity to determine the cross sections for

- QBHs with a continuous mass spectrum (`QBH_continuous.cc`),
- QBHs with a discrete mass spectrum (`QBH_discrete.cc`),
- QBHs with a continuous mass spectrum including supersymmetric particles in the final state (`QBH_continuous_SUSY.cc`),
- QBHs with a discrete mass spectrum including supersymmetric particles in the final state (`QBH_discrete_SUSY.cc`).

Each model allows the user to produce cross sections for a range of fundamental Planck masses and center of mass energies. Additionally, we provide "`_single.cc`" versions which let the user check a certain set of parameters. The parameters for each version can be modified in the headerfile, respectively, which is described in more detail in the following section. To compile the desired version of QBH.cc use the command

```
make QBH_continuous
```

where `QBH_continuous` can be replaced by any of the versions:
`QBH_continuous.cc, QBH_discrete.cc, QBH_continuous_SUSY.cc,`
`QBH_discrete_SUSY.cc, QBH_continuous_single.cc, QBH_discrete_single.cc,`
`QBH_continuous_SUSY_single.cc, QBH_discrete_SUSY_single.cc`.
The user then needs to run it by using

```
./QBH_continuous
```

or accordingly. If the user wants to run the code with another version of `CUBA` or LHAPDF, the program will have to be modified at the indicated parts in source and makefile.

C.3 Input for QBH.cc

There are various parameters which can be chosen by the user. The input parameters for QBH.cc can be found and changed in the according headerfile. For the continuous case, for only SM particles as well as including supersymmetric particle production, one can change the parameters in

`input/inputParameter.h` ,

or alternatively in the single case

`input/inputParameter_single.h` .

For the discrete case, one needs to modify `input/inputParameterDiscrete.h` and `input/inputParameterDiscrete_single.h`, respectively. There are a number of variable input parameters.

1. `NUM_EXTRA_DIM` sets the number of the extra dimensions.
2. `THEORY_TYPE` sets the underlying model of the extra dimensions.
   - `TheoryType::ADD`: Model proposed by Nima Arkani-Hamed, Savas Dimopoulos, and Gia Dvali with the choice of extra dimensions from $n = 0, \ldots, 7$.
   - `TheoryType::RS1`: Model constructed by Randall and Sundrum with the number of extra dimensions fixed to be equal to 1.
3. `CONSIDER_INELASTICITY` sets the constraints from inelasticity.
   - `CONSIDER_INELASTICITY = false`: All center-of-mass energy is trapped behind the event horizon and no elasticity effects are considered.
   - `CONSIDER_INELASTICITY = true`: Only a fraction of center-of-mass energy is behind the event horizon and the inelasticity effects by Yoshino and Rychkov [61] are considered.
4. `SCALE_PDF` sets the scale of the parton distribution functions.
   - `ScalePDF::MD`: reduced Planck mass.
   - `ScalePDF::RS`: inverse Schwarzschild radius.
5. `COM_ENERGY`: sets the center of mass energy of the initial proton system in GeV. In the `_single.cc` case this is fixed to one value, in the case for various center of mass energies the minimal (`COM_ENERGY_MIN`) and maximal (`COM_ENERGY_MAX`) considered value has to be specified.
6. `REDUCED_PLANCK_MASS`: sets the value of the fundamental quantum gravity scale in GeV. In the `_single.cc` case this is fixed to one value, in the case for various fundamental Planck masses the minimal (`REDUCED_PLANCK_MASS_MIN`) and maximal (`REDUCED_PLANCK_MASS_MAX`) considered value has to be specified.

7. `X_MIN`: sets (only for a continuous mass spectrum) the ratio of the minimal QBH mass over the Planck scale.

The user can also change the Monte Carlo variables in the headerfile to change the integration parameters, such as the relative accuracy.
The branching ratios can be found in

```
input/BranchingRatios/BranchingRatios.csv
```

for only SM particles in the final state, as described in Section 5.3.1, and in

```
input/BranchingRatios/BranchingRatiosSusy.csv
```

for including supersymmetric particles in the final state, see Chapter D. We use the Monte Carlo particle numbering scheme [19] to specify the incoming and outgoing particles. The necessary numbers can be found in Table C.1.

1	d	11	e	21	g
2	u	12	ν_e	22	γ
3	s	13	μ	23	Z^0
4	c	14	ν_μ	24	W^+
5	b	15	τ	25	H
6	t	16	ν_τ	39	G

Table C.1: **Particle numbering scheme**; antiparticles: negative numbers

C.4 Output for QBH.cc

QBH.cc prints the basic information about the input settings to the terminal screen and produces a comma-separated text file of the form[1]

```
crossSection_ADD_n7_M3TeV_s14TeV.txt .
```

This output file includes information about all possible QBHs. The filename indicates the underlying model of extra dimensions, the number of extra dimensions, the chosen fundamental Planck mass and the center of mass energy. The output file will be organized in blocks, the line beginning with `QBH` classifies the incoming particles creating the QBH. The following lines give the cross sections for the possible final states, indicated by the first two entries in each line, for the considered symmetry restrictions. In the above mentioned case, one would e.g. find for two anti-up-quarks creating a QBH:

```
QBH ,-2,-2,,,,
-2,-2,233.118,233.118,38.8529,25.902,25.902
-2,-4,0,0,38.8529,25.902,25.902
-2,-6,0,0,38.8529,25.902,25.902
-4,-4,0,0,38.8529,25.902,25.902
-4,-6,0,0,38.8529,25.902,25.902
-6,-6,0,0,38.8529,25.902,25.902
11,1,0,0,0,8.63398,8.63398
11,3,0,0,0,8.63398,8.63398
11,5,0,0,0,8.63398,8.63398
13,1,0,0,0,8.63398,8.63398
13,3,0,0,0,8.63398,8.63398
13,5,0,0,0,8.63398,8.63398
15,1,0,0,0,8.63398,8.63398
15,3,0,0,0,8.63398,8.63398
15,5,0,0,0,8.63398,8.63398
```

For the supersymmetric case, we considered only one symmetry model, thus one would only find one value for the cross section of each final state.

[1] depending on the chosen version, the name of the output file can slightly vary.

Appendix D

Branching ratios including supersymmetric particles

This chapter lists the branching ratios used to determine the cross sections for quantum black hole (QBH) processes with supersymmetric particles in the final state. Based on the branching ratios determined for QBHs which only decay into SM particles, the branching ratios were determined for a model in which we assume quark and lepton flavor as well as Lorentz invariance to be conserved. Using the classifications of the QBH according to its SU(3) color charge and spin, the branching ratios for SM and supersymmetric particles take the values shown in Table D.1 to D.5.

If one considers a black hole created by two up-quarks, the QBH carries an incidental $\mathrm{U}(1)_{\mathrm{em}}$ charge of 4/3. One finds $\mathbf{3} \times \mathbf{3} = \mathbf{6} + \overline{\mathbf{3}}$ for the color states when decaying into two up quarks. This has to be weighed by the spin factors; both spin states, spin-0 as well as spin-1, are possible, we thus multiply the amount of states with the sum of both spin factors:

$$\mathbf{QBH}(\mathbf{u}, \mathbf{u}, \mathbf{4/3}) \to \mathbf{u} + \mathbf{u}: \quad (6+3) \times (1+3) = 36 \quad . \tag{D.1}$$

The up-squark particles on the other hand carry an integer spin charge of one and therefore only apply to the spin-0 state. We find

$$\mathbf{QBH}(\mathbf{u}, \mathbf{u}, \mathbf{4/3}) \to \tilde{\mathbf{u}} + \tilde{\mathbf{u}}: \quad (6+3) \times (1) = 9 \tag{D.2}$$

and thus the ratio displayed in Table D.1. The other branching ratios are determined accordingly.

QBH (u, u, 4/3)			**QBH** (d, d, -2/3)		
Particle 1	Particle 2	Branching Ratios	Particle 1	Particle 2	Branching Ratios
u	u	80%	d	d	80%
$\tilde{u}$	$\tilde{u}$	20%	$\tilde{d}$	$\tilde{d}$	20%
QBH (u, d, 1/3)			**QBH** (u, $\bar{d}$, 1)		
Particle 1	Particle 2	Branching Ratios	Particle 1	Particle 2	Branching Ratios
u	d	80%	u	$\bar{d}$	80%
$\tilde{u}$	$\tilde{d}$	20%	$\tilde{u}$	$\tilde{\bar{d}}$	20%

Table D.1: Branching ratios for QBHs with electric charge created by up and down-type quarks (u, d) decaying into standard model and supersymmetric particles (denoted by tilde). All symmetries, including i.e. quark flavor, are assumed to be conserved.

QBH (u, g, 2/3)		
Particle 1	Particle 2	Branching Ratios
u	g	54.55%
u	γ	6.82%
u	Z^0	6.82%
u	H	1.52%
u	G	3.03%
$\tilde{u}$	$\tilde{g}$	18.18%
$\tilde{u}$	$\tilde{\gamma}$	2.27%
$\tilde{u}$	$\tilde{Z^0}$	2.27%
$\tilde{u}$	$\tilde{H}$	1.52%
$\tilde{u}$	$\tilde{G}$	3.03%

Table D.2: Branching ratios for QBHs created by up-type quark (u) and gluon (g) decaying into standard model and supersymmetric particles (denoted by tilde). The QBHs carry a QED charge of 2/3. All symmetries, including i.e. quark flavor, are assumed to be conserved.

QBH (q_i, $\bar{q_j}$, 0)		
Particle 1	Particle 2	Branching Ratios
q_i	$\bar{q_j}$	80%
$\tilde{q_i}$	$\tilde{\bar{q}_j}$	20%

Table D.3: Branching ratios for QBHs created by quark-antiquark pair with different quark flavor decaying into standard model and supersymmetric particles (denoted by tilde). The QBHs carry no QED charge. All symmetries, including i.e. quark flavor, are assumed to be conserved.

QBH (q_i, $\bar{q_i}$, 0)					
Particle 1	Particle 2	Branching Ratio	Particle 1	Particle 2	Branching Ratios
u	$\bar{u}$	20.52%	$\tilde{u}$	$\tilde{\bar{u}}$	5.13%
d	$\bar{d}$	20.52%	$\tilde{d}$	$\tilde{\bar{d}}$	5.13%
l^-	l^+	2.28%	$\tilde{l^-}$	$\tilde{l^+}$	0.57%
ν	$\bar{\nu}$	2.28%	$\tilde{\nu}$	$\tilde{\bar{\nu}}$	0.57%
g	g	4.28%	$\tilde{g}$	$\tilde{g}$	4.28
g	γ	3.8%	$\tilde{g}$	$\tilde{\gamma}$	3.8%
g	Z^0	3.8%	$\tilde{g}$	$\tilde{Z^0}$	3.8%
g	H	2.85%	$\tilde{g}$	$\tilde{H}$	2.85%
g	G	3.26%	$\tilde{g}$	$\tilde{G}$	2.44%
γ	γ	0.48%	$\tilde{\gamma}$	$\tilde{\gamma}$	0.48%
γ	Z^0	0.48%	$\tilde{\gamma}$	$\tilde{Z^0}$	0.48%
γ	H	0.36%	$\tilde{\gamma}$	$\tilde{H}$	0.36%
γ	G	0.4%	$\tilde{\gamma}$	$\tilde{G}$	0.3%
Z^0	Z^0	0.43%	$\tilde{Z^0}$	$\tilde{Z^0}$	0.48%
Z^0	H	0.36%	$\tilde{Z^0}$	$\tilde{H}$	0.36%
Z^0	G	0.4%	$\tilde{Z^0}$	$\tilde{G}$	0.3%
H	H	0.12%	$\tilde{H}$	$\tilde{H}$	0.12%
G	G	0.76%	$\tilde{G}$	$\tilde{G}$	0.19%
W^-	W^+	0.48%	$\tilde{W^-}$	$\tilde{W^+}$	0.48%

Table D.4: Branching ratios for QBHs created by quark-antiquark pair with the same quark flavor decaying into standard model and supersymmetric particles (denoted by tilde). The QBHs carry no QED charge. All symmetries, including i.e. quark flavor, are assumed to be conserved.

QBH (g, g, 0)					
Particle 1	Particle 2	Branching Ratio	Particle 1	Particle 2	Branching Ratios
q_i	$\bar{q_i}$	17.32%	$\tilde{q_i}$	$\tilde{\bar{q}_i}$	11.54%
l^-	l^+	0.51%	$\tilde{l^-}$	$\tilde{l^+}$	0.34%
ν	$\bar{\nu}$	0.51%	$\tilde{\nu}$	$\tilde{\bar{\nu}}$	0.34%
g	g	25.35%	$\tilde{g}$	$\tilde{g}$	18.11%
g	γ	6.34%	$\tilde{g}$	$\tilde{\gamma}$	4.53%
g	Z^0	6.34%	$\tilde{g}$	$\tilde{Z^0}$	4.53%
γ	γ	0.4%	$\tilde{\gamma}$	$\tilde{\gamma}$	0.28%
γ	Z^0	0.4%	$\tilde{\gamma}$	$\tilde{Z^0}$	0.28%
Z^0	Z^0	0.4%	$\tilde{Z^0}$	$\tilde{Z^0}$	0.28%
Z^0	H	0.1%	$\tilde{Z^0}$	$\tilde{H}$	0.07%
Z^0	G	0.09%	$\tilde{Z^0}$	$\tilde{G}$	0.48%
H	H	0.06%	$\tilde{H}$	$\tilde{H}$	0.05%
G	G	0.57%	$\tilde{G}$	$\tilde{G}$	0.11%
W^-	W^+	0.4%	$\tilde{W^-}$	$\tilde{W^+}$	0.28%

Table D.5: Branching ratios for QBHs created by two gluons decaying into standard model and supersymmetric particles (denoted by tilde). The QBHs carry no QED charge. All symmetries, including i.e. B-L, are assumed to be conserved.